Dear Prof. Luterbacher,

We would like to thank you and the referees for the comments and suggestions made on the manuscript. The manuscript has been modified quite a lot since the first submission and it is true that several figures were no longer consistent with each other. Therefore, and to be consistent, we revised Fig. 2, Fig. 5, designed a new Fig. 3 and double-checked Fig. S1.

Initially we measured and analyzed all the proxies over longer periods: CE 520-560, 1242-1286, 1625-1660, 1790-1835, 1950-2000 and all calculations performed were based on these time spans. However, in our first submission to the journal, we tried to simplify Fig. 2 and therefore presented only 10 years before and 10 years after the eruptions. However, in the supplementary material (Fig. S1), we still considered the full available time series over the periods (n=219). Therefore, there are differences between Fig 2 and Supplementary material Fig. S1. This discrepancy also led to value discrepancies in the text. Then in the process of controlling all data and calculation procedures, we also found a mistake in our script, which introduced a shift in 1816 and 1993.

We are happy that, thanks to the persistent and constructive comments of the reviewer, our latest thorough revision of the manuscript and figures has allowed us to removed all incongruences. We apologize for the inconveniences that were caused by these Figure discrepancies. Below, you can find the detailed point-by-point answers to the Reviewer's comments. To facilitate your assessment, we marked our responses in bold and highlighted the changes in the manuscript. We are providing both clean and track-mode changes versions.

Response to the Reviewer

Reviewer:

1. The new SEA fig. 3 means we can at last begin to see the behaviour of the five tree-ring parameters after eruptions. A minor comment on its interpretation: L369 "The behavior of isotope chronologies is rather more complex, with a distinct decrease in δ13C at the high-latitude sites (YAK, TAY), whereas δ18O series are impacted mainly at the high-latitude YAK and high-altitude ALT sites." The largest decrease in d18O (in terms of z-score) is in eruption+2years at the high---altitude site (ALT). So why do you highlight the high---latitude sites and not this one?

Answer 1: We re-plotted Fig. 3 by selecting 15 years before and 20 years after the eruptions (CE 535, 540, 1257, 1640, 1815) to better visualize deviation and duration of negative effects after the volcanic eruptions on Siberian trees (see below). For CE 1991, we considered 15 years prior to the event as well. After the event, the shortest series only has 9 years, however. We agree, that z-scores of $\delta^{18}O$ values from ALT in the first year after the eruptions decreased strongly compared to YAK and TAY sites. However, in terms of duration negative values in tree-ring parameters from the high-latitude sites (YAK and TAY) prevailed compared to high-altitude ALT site (revised Fig. 3 below).

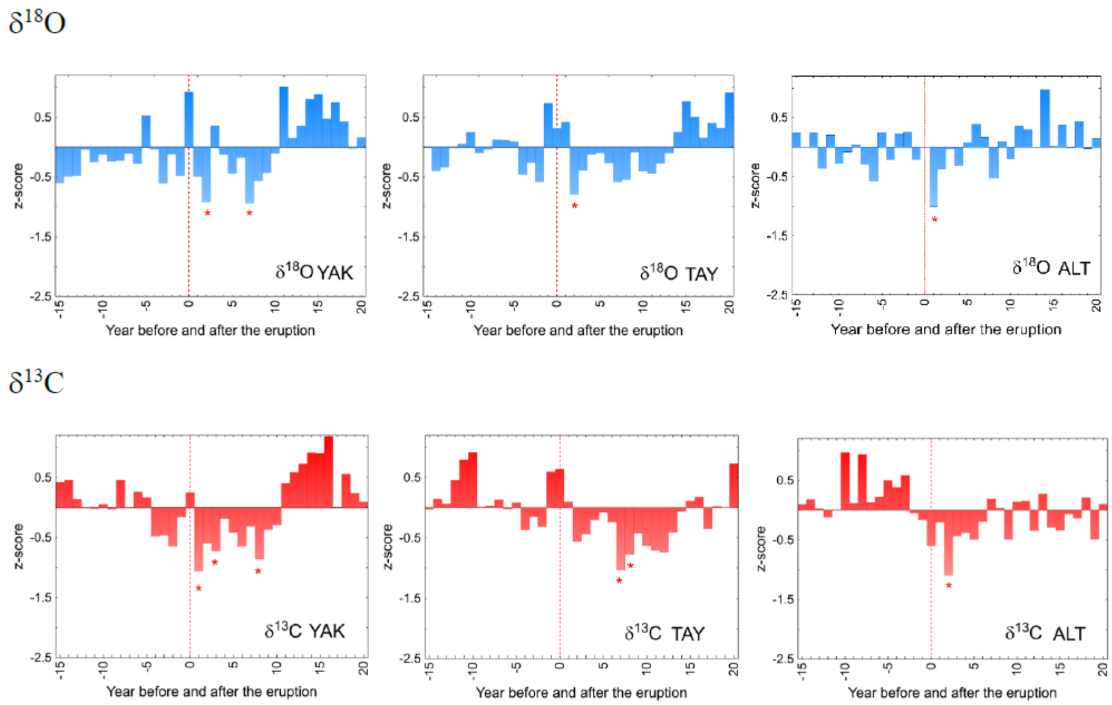

At the ALT site, δ^{18}O become positive 4 years after the eruptions, while at the TAY site, δ^{18}O values remained negative for 12 years with a response delay of 2 years after the eruption. At the YAK site, positive δ^{18}O value was revealed on the third year after the eruptions, followed by 7 years of negative values afterwards (in total longer, compared to ALT). For clarification we rephrased the sentences as follows:

"The δ^{18}O isotope chronologies (z-score) show a distinct decrease the year after the eruptions. At ALT, however, the duration of negative anomalies were shorter (5 years) than at the high-latitude TAY (12 years) and YAK (9 years) sites. At the YAK site, two negative years followed the events, intermitted with one positive value, to remain negative during the following 7 years. The duration of negative anomalies recorded in δ^{13}C values (z-score) lasts also longer at the high-latitude YAK site - 10 years after the eruptions and 13 years at TAY compared to 7 years at ALT (Fig. 3)." P.20, L. 373-379.

Reviewer:

2. L459 "1816 was cold only in YAK (based on the CWT chronology), but not at the other sites". This is in agreement with Fig. 5 but is not agreement with Fig. 2 or Fig. S1 (see page 14 of the supplement), nor are Figs. 2 and S1 in agreement with each other! I already highlighted the disagreements between Fig. 2 and Fig. S1 for YAK in 1816 in my previous review (see my previous comment on L347---348) and yet the authors just responded "We carefully checked and corrected figures accordingly" and added in the comment above about 1816 YAK CWT indicating cold.

<u>Answer 2:</u> There was indeed an error in the calculation of the pdfs for the Fig. S1 in the previous submission. We apologize for the inconvenience and thank the referee for spotting our mistake. We

double-checked all the values and figures and revised them. The revised figures are shown below (the old figures have been added as comparison):

REVISED Fig. 2:

YAK 1815

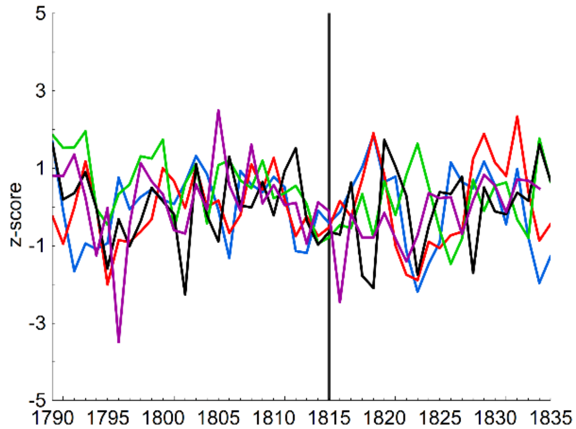

OLD Fig. 2:

YAK 1815

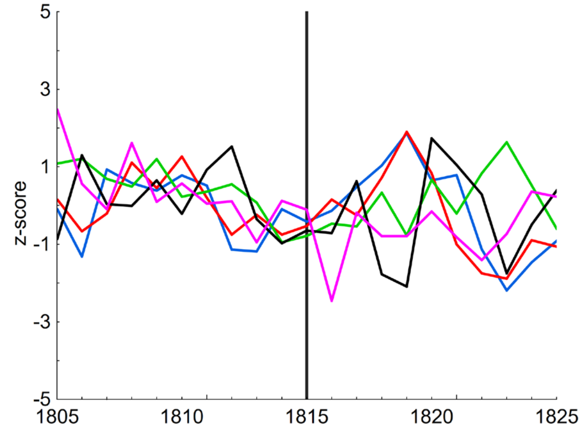

From revised Fig. 2: Normalized (z-score) individual tree-ring index chronologies (TRW, black), maximum latewood density (MXD, purple), cell wall thickness (CWT, green), δ^{13}C (red) and δ^{18}O (blue) in tree-ring cellulose chronologies from northeastern Yakutia (YAK) for the specific period CE 1790-1835 before and after the eruption (CE 1815) are presented. Vertical lines show year of the eruptions.

REVISED Fig. S1 YAK 1815

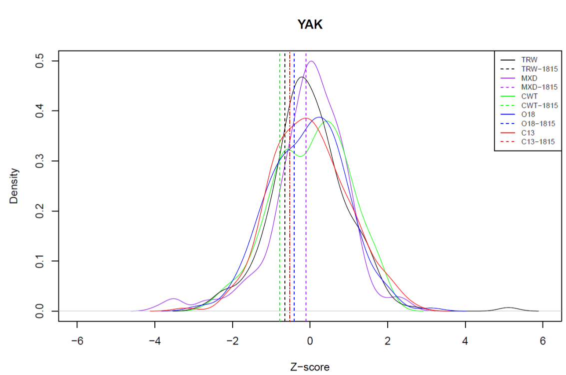

OLD: Fig. S1 YAK 1816

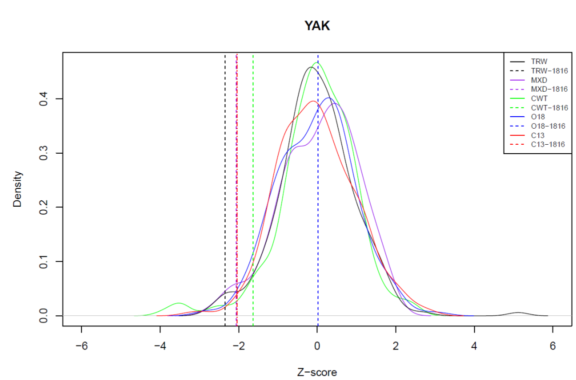

From Fig. S1. Probability density function (Pdf) computed for each of the tree-ring parameter for northeastern Yakutia. Tree-ring parameters (TRWi - black, MXD – purple, CWT – green, δ^{18}O - blue and δ^{13}C - red) in bold lines represent the probability density function. Dotted lines represent the anomalies (z-score) observed for the first and second years following the Tambora volcanic eruption (CE 1815) for each tree-ring parameter.

Reviewer: Fig. S1 shows YAK anomalies around ---2 (z-score) in 1816 (vertical dashed lines) for four out of the five parameters (TRW, MXD, C13 and CWT), only O18 (vertical dashed blue line is at zero). This is not compatible with Fig. 2 in the main text which shows only notably negative values in 1816 for YAK are for MXD (pink/purple) and the TRW (black), C13 (red) and CWT (green) do not show z-scores near -2. Which is correct, Fig. 2 or Fig. S1? And why does Fig. 5 show only notable cooling for YAK CWT in 1816 when Fig. 2 shows YAK CWT is not anomalous in 1816 (see above)?

Answer: In Fig. 2 we changed the pink line to purple and extended the periods to match those of Fig.S1. The data have been carefully double-checked and differences corrected. In Fig. 5 it is correct that YAK shows an anomalous 1816 –MXD (and not CWT).

Reviewer:

3. There appear to be other inconsistencies between Figs. 2, 5 and S1. Take ALT 1816 for instance. Fig. 2 shows no notable excursions for any parameter in 1816 at ALT (all lie between +/---1 for the z---scores). Fig. 5 shows notable d13C anomaly (orange rhomb and orange circle, indicating dry (high summer VPD or low July precip). Fig. S1 (p. 14 of supplement) shows d13C anomaly in 1816 (vertical dashed red line) is almost exactly zero! So why does Fig. 5 indicate notably dry?

Answer 3: Correct, there is no notable excursion for any parameter in 1816 at ALT. We corrected this mistake. The colors of Fig.5 have been revised, now using dark blue, light blue and white. The $\delta^{13}C$ anomaly for the humid year 1817 has been corrected to light blue.

Reviewer:

4. Since there have been similar inconsistencies between text and figures, or between figs. 2, 5 and S1, in previous versions of the manuscript that have not been corrected, I now have less faith in the accuracy of what is presented and I can only encourage the authors to print out large versions of these three figures and their text and go through them site-by-site, eruption-by-eruption and parameter-by-parameter and check/correct everything. Either that or explain what the vertical dashed lines in Fig. S1 mean because the caption says they represent the anomalies in the depicted years, but they are clearly different to the anomaly timeseries in Fig. 2 for the same years.

Answer 4: We now have revisited all figures and the text as suggested by the referee. Specifically, we revised and corrected Figures 2, 5, S1 and double-checked all values mentioned in the text.

The dotted, vertical lines represent the anomalies (z-score) observed for the first and second years following the CE 535, 540, 1257, 1640, 1815 and 1991 volcanic eruptions for each tree-ring parameter. We agree with the referee that there were inconsistencies between Fig. 2 and Fig S1. These have now been corrected and removed.

Reviewer:

5. In fact, I've just found another inconsistency. TAY 1817 MXD is -2.5 in Fig. S1, about -0.5 in Fig. 2 and white (indicating not notable) in Fig. 5. So is Fig. S1 wrong in this instance?

Answer 5: We thank the referee for the careful review. However, no anomalies occurred at TAY in 1816 or 1817 (Fig. 2, 5). MXD 1816 is correct for YAK.

Reviewer:

6. L461-2: You added this text in the latest version: "CE 1993 was an extremely cold year for ALT based on CWT and δ18O, while also sunny, which is confirmed by local weather station data". Really? Fig. 2 for ALT shows 1993 as having CWT (green) about +1.5, and the other parameters between -1 and -1.5. So how can you conclude that high CWT implies extremely cold when CWT is positively correlated with summer temperatures (Fig. 4)?

<u>Answer 6:</u> **Correct, CWT is positively correlated with summer temperatures. CE 1993 was not an extremely cold year at ALT based on CWT and $\delta^{18}O$. Negative value in CWT was recorded at YAK site, not ALT. We corrected the sentence as follows:**

Finally, the Pinatubo eruption is mainly captured by the MXD (-2.8σ) and CWT (-2.2σ) chronologies from YAK in CE 1992. Simultaneous decreases of all tree-ring proxies from ALT are observed in 1993 (Fig. 2), which, however, cannot be classified as extreme (Fig. S1). P.20, L. 366-368.

Siberian tree-ring and stable isotope proxies as indicators of temperature and moisture changes after major stratospheric volcanic eruptions

Olga V. Churakova (Sidorova)[1,2*], Marina V. Fonti[2], Matthias Saurer[3,4], Sébastien Guillet[1], Christophe Corona[5], Patrick Fonti[3], Vladimir S. Myglan[6], Alexander V. Kirdyanov[2,7,8], Oksana V. Naumova[6], Dmitriy V. Ovchinnikov[7], Alexander V. Shashkin[2,7], Irina P. Panyushkina[9], Ulf Büntgen[3,8], Malcolm K. Hughes[9], Eugene A. Vaganov[2,7,10], Rolf T.W. Siegwolf[3,4], Markus Stoffel[1,11,12]

[1]*Institute for Environmental Sciences, University of Geneva, CH-1205 Geneva, 66 Bvd Carl Vogt, Switzerland*

[2]*Institute of Ecology and Geography, Siberian Federal University RU-660049 Krasnoyarsk, Svobodniy pr 79/10, Russian Federation*

[3]*Swiss Federal Institute for Forest, Snow and Landscape Research WSL, Zürcherstrasse 111, CH-8903 Birmensdorf, Switzerland*

[4]*Paul Scherrer Institute, CH- 5232 Villigen - PSI, Switzerland*

[5]*Université Blaise Pascal, Geolab, UMR 6042 CNRS, 4 rue Ledru, F-63057 Clermont-Ferrand, France*

[6]*Institute of Humanities, Siberian Federal University RU-660049 Krasnoyarsk, Svobodniy pr 82, Russian Federation*

[7]*V.N. Sukachev Institute of Forest SB RAS, Federal Research Center "Krasnoyarsk Science Center SB RAS" RU-660036 Krasnoyarsk, Akademgorodok 50, bld. 28, Russian Federation*

[8]*Department of Geography, University of Cambridge, Downing Place, Cambridge CB2 3EN*

[9]*Laboratory of Tree-Ring Research, University of Arizona, 1215 E. Lowell St., Tucson, 85721, USA*

[10]*Siberian Federal University, Rectorate, RU-660049 Krasnoyarsk, Svobodniy pr 79/10, Russian Federation*

[11]*dendrolab.ch, Department of Earth Sciences, University of Geneva, 13 rue des Maraîchers, CH-1205 Geneva, Switzerland*

[12]*Department F.A. Forel for Environmental and Aquatic Sciences, University of Geneva, 66 Boulevard Carl-Vogt, CH-1205 Geneva, Switzerland*

Corresponding author: Olga V. Churakova (Sidorova)*

E-Mail: olga.churakova@hotmail.com

Abstract

Stratospheric volcanic eruptions have far-reaching impacts on global climate and society. Tree rings can provide valuable climatic information on these impacts across different spatial and temporal scales. To detect temperature and hydro-climatic changes after strong stratospheric Common Era (CE) volcanic eruptions for the last 1500 years (CE 535 Unknown, CE 540 Unknown, CE 1257 Samalas, CE 1640 Parker, CE 1815 Tambora, and CE 1991 Pinatubo), we measured and analyzed tree-ring width (TRW), maximum latewood density (MXD), cell wall thickness (CWT), and $\delta^{13}C$ and $\delta^{18}O$ in tree-ring cellulose chronologies of climate-sensitive larch trees from three different Siberian regions (Northeastern Yakutia - YAK, Eastern Taimyr – TAY, and Russian Altai – ALT).

All tree-ring proxies proved to encode a significant and specific climatic signal of the growing season. Our findings suggest that TRW, MXD, and CWT show strong negative summer air temperature anomalies in 536, 541-542, and 1258-1259 at all studied regions. Based on $\delta^{13}C$, 536 was extremely humid in YAK, 537-538 in TAY. No extreme hydro-climatic anomalies occurred in Siberia after the volcanic eruptions in 1640, 1815 and 1991, except for 1817 in ALT. The signal stored in $\delta^{18}O$ indicated significantly lower summer sunshine duration in 542, 1258-1259 in YAK, and 536 in ALT. Our results show that trees growing at YAK and ALT mainly responded the first year after the eruptions, whereas at TAY, the growth response occurred after two years.

The fact that differences exist in climate responses to volcanic eruptions – both in space and time – underlines the added value of a multiple tree-ring proxy assessment. As such, the various indicators used clearly help to provide a more realistic picture of the impact of volcanic eruption to past climate dynamics, which is fundamental for an improved understanding of climate dynamics, but also for the validation of global climate models.

Key words: Dendrochronology, $\delta^{13}C$ and $\delta^{18}O$ in tree-ring cellulose, tree-ring width, maximum latewood density, cell wall thickness, temperature, precipitation, sunshine duration, vapor pressure deficit

1. Introduction

Major stratospheric volcanic eruptions can modify the Earth's radiative balance and substantially cool the troposphere. This is due to the massive injection of sulphate aerosols, which reduce surface temperatures on timescales ranging from months to years (Robock, 2000). Volcanic aerosols significantly absorb terrestrial radiation and scatter incoming solar radiation, resulting in a cooling that has been estimated to about 0.5°C during the two years following the Mount Pinatubo eruption in June 1991 (Hansen et al., 1996).

Since trees – as living organisms – are impacted in their metabolism by environmental changes, their responses to these changes are recorded in the biomass, as it is found in tree-ring parameters (Schweingruber, 1996). The decoding of tree-ring archives is used to reconstruct past climates. A summer cooling of the Northern Hemisphere ranging from 0.6°C to 1.3°C has been reported after the strongest known volcanic eruptions of the past 1500 years (CE 1257 Samalas, 1815 Tambora and 1991 Pinatubo) based on temperature reconstructions using tree-ring width (TRW) and maximum latewood density (MXD) records (Briffa et al., 1998; Schneider et al., 2015; Stoffel et al., 2015; Wilson et al., 2016; Esper et al., 2017, 2018; Guillet et al., 2017; Barinov et al., 2018).

Climate simulations show significant changes in the precipitation regime after large volcanic eruptions. These include, among others, rainfall deficit in monsoon prone regions and in Southern Europe (Joseph and Zeng, 2011), and wetter than normal conditions in Northern Europe (Robock and Liu 1994; Gillet et al., 2004; Peng et al., 2009; Meronen et al., 2012; Iles et al., 2013; Wegmann et al., 2014). However, despite recent advances in the field, the impacts of stratospheric volcanic eruptions on hydro-climatic variability at regional scales remain largely unknown. Therefore, further knowledge about moisture anomalies is critically needed, especially at high-latitude sites where tree growth is mainly limited by summer temperatures.

As dust and aerosol particles of large volcanic eruptions affect primarily the radiation regime, three major drivers of plant growth (i.e. photosynthetic active radiation (PaR), temperature and vapor pressure deficit (VPD)) will be affected by volcanic activity. This reflects in low TRW as a result of reduced photosynthesis but even more so due to low temperature. As cell division is temperature dependent, its rate (tree-ring growth) will exponentially decrease with decreasing temperature below +3°C (Körner, 2015), outweighing the "low light / low-photo-synthesis" effect by far.

Furthermore, over the last years some studies using mainly carbon isotopic signals ($\delta^{13}C$) in tree rings showed eco-physiological responses of trees to volcanic eruptions at the mid- (Battipaglia et al., 2007) or high- (Gennaretti et al., 2017) latitudes. By contrast, a combination of both carbon ($\delta^{13}C$) and oxygen ($\delta^{18}O$) isotopes in tree rings has been employed only rarely to trace volcanic eruptions in high-latitude or high-altitude proxy records (Churakova (Sidorova) et al., 2014).

Application of TRW, MXD, and cell wall thickness (CWT) as well as $\delta^{13}C$ and $\delta^{18}O$ in tree cellulose chronologies is a promising tool to disentangle hydro-climatic variability as well as winter and early spring temperatures at high-latitude and high-altitude sites (Kirdyanov et al., 2008; Sidorova et al., 2008, 2010, 2011; Churakova (Sidorova) et al., 2014; Castagneri et al., 2017). In that sense, recent CWT measurements allowed generating high-resolution, seasonal information of water and carbon limitations on growth during springs and summers (Panyushkina et al., 2003; Sidorova et al., 2011; Fonti et al., 2013; Bryukhanova et al., 2015).

Depending on site conditions, $\delta^{13}C$ variations reflect light (stand density) (Loader et al., 2013), water availability (soil properties) and air humidity (proximity to open waters, i.e. rivers, lakes, swamps and orography) as these parameters have been recognized to modulate stomatal conductance (g_l) controlling carbon isotopic discrimination.

Depending on the study site, a decrease in the carbon isotope ratio can be expected after stratospheric volcanic eruptions due to limited photosynthetic activity and higher stomatal conductance, which in turn would be the result of decreased temperatures, VPD, and a reduction in light intensity. By contrast, volcanic eruptions have also been credited for an increase in photosynthesis as dust and aerosol particles cause an increased light scattering, compensating for the light reduction (Gu et al., 2003). A significant increase in $\delta^{13}C$ values in tree-ring cellulose should be interpreted as an indicator of drought (stomatal closure) or high photosynthesis (Farquhar et al., 1982). In the past, very little attention has been paid to the elemental and isotopic composition of tree rings for years during which they may have been subjected to the climatic influence of powerful, but remote, and often tropical, volcanic eruptions.

In this study, we aim to fill this gap by investigating the response of different components of the Siberian climate system (i.e. temperature, precipitations, VPD, and sunshine duration) to stratospheric volcanic events of the last 1500 years. By doing so, we seek to extend our understanding of the effects of volcanic eruptions on climate by combining multiple climate-sensitive variables measured in tree rings that were clustered around the time of the major volcanic eruptions (Table 1). We focus our investigation on remote tree-ring sites in Siberia, two at high latitudes (northeastern Yakutia - YAK and eastern Taimyr - TAY), and one at high altitude (Russian Altai - ALT), for which long tree-ring chronologies were developed previously with highly climate sensitive trees. We assemble a dataset from five tree-ring proxies: TRW, MXD, CWT, $\delta^{13}C$ and $\delta^{18}O$ in larch tree-ring cellulose chronologies in order to: (1) determine the major climatic drivers of the tree-ring proxies and to evaluate their individual and integrative response to climate change, and to (2) reconstruct the climatic impacts of volcanic eruptions over specific periods of the past (Table 1).

2. Material and methods

2.1. Study sites

The study sites are situated in Siberia (Russian Federation), far away from industrial centers (and 1500–3400 km apart from each other), in the zone of continuous permafrost in north-eastern Yakutia (YAK: 69°N, 148°E) and eastern Taimyr (TAY: 70°N, 103°E), and mountain permafrost in Altai (ALT: 50°N, 89°E) (Fig. 1a, Table 2). Tree-ring samples were collected during several field trips and included old relict wood and living larch trees: *Larix cajanderi* Mayr (up to 1216 years) in YAK, *Larix gmelinii* Rupr. (max. 640 years) in TAY and *Larix sibirica* Ldb. (max. 950 years) in ALT. TRW chronologies have been developed and published in the past (Fig. 1, Hughes et al., 1999; Sidorova and Naurzbaev, 2002; Sidorova, 2003 for YAK; Naurzbaev et al., 2002; Panyushkina et al., 2003 for TAY; Myglan et al., 2008 for ALT).

Due to the remote location of our study sites, we used meteorological data from monitored weather stations located at distances ranging from 50-200 km from the sampled sites. Temperature data from these weather stations are significantly correlated ($r>0.91$; $p<0.05$) with gridded data (http://climexp.knmi.nl). However, poor correlation is found with precipitation data ($r<0.45$; $p<0.05$), which most likely is the result of local topography (Churakova (Sidorova) et al., 2016).

Mean annual air temperature is lower at the high-latitude YAK and TAY sites than at the high-altitude ALT site (Table 2). Annual precipitation is low (153-269 mm yr^{-1}) at all sites. The growing season calculated with the tree growth threshold of +5ºC (Fritts, 1976; Schweingruber, 1996) is very short (50-120 days) at all locations (Table 2). Sunshine duration is higher at YAK and TAY (ca. 18-20 h/day in summer) compared to ALT (ca. 18 h/day in summer) (Sidorova et al., 2005; Myglan et al., 2008; Sidorova et al., 2011; Churakova (Sidorova) et al., 2014).

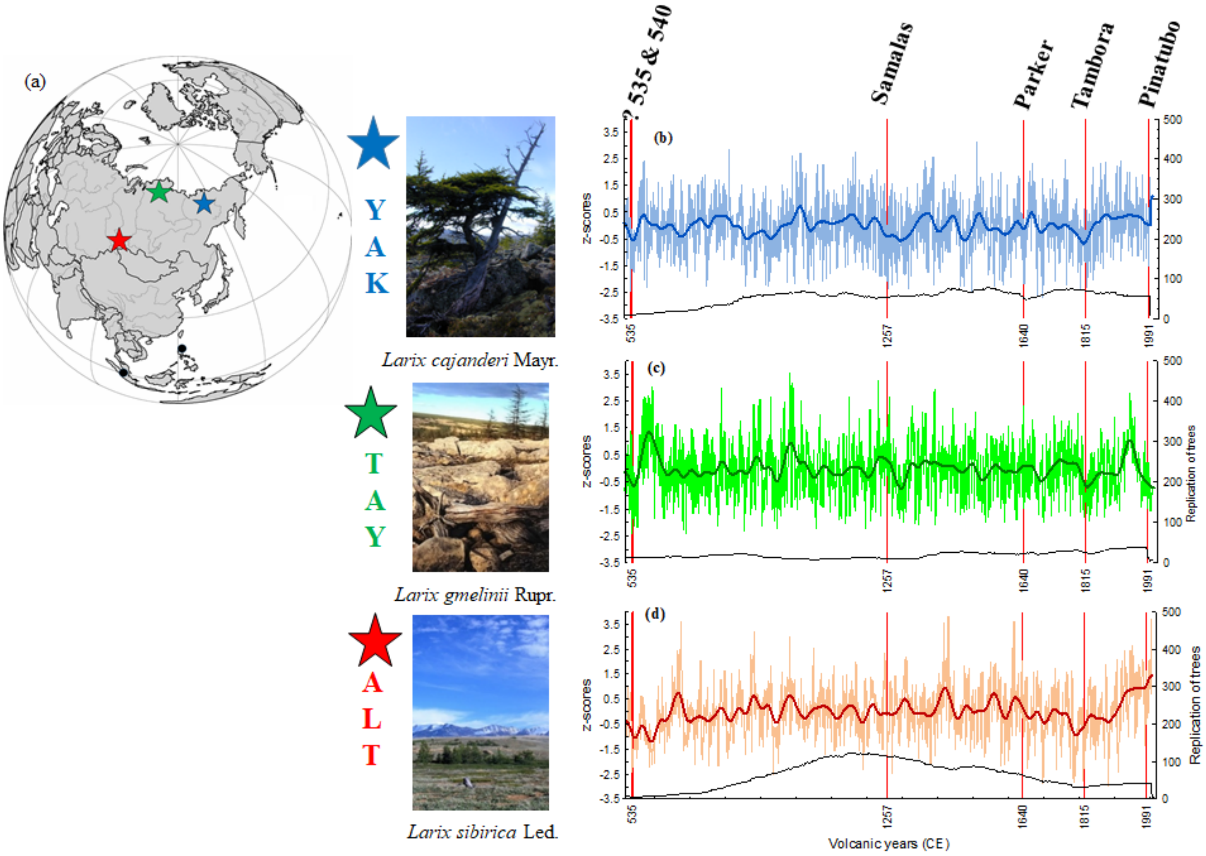

Fig. 1. Location of the study sites (stars) and known volcanos from the tropics (black dots) considered in this study (a). Annual tree-ring width index (light lines) and smoothed by 51-year Hamming window (bold lines) from the northeastern Yakutia (YAK - **blue**, b) (Hughes et al., 1999; Sidorova and Naurzbaev, 2002; Sidorova, 2003), eastern Taimyr (TAY - **green**, c) (Naurzbaev et al., 2002), and Russian Altai (ALT - **red**, d) (Myglan et al., 2009). Photos show the larch stnads at YAK, TAY (M.M. Naurzbaev) and ALT (V.S. Myglan) sites.

2.2. Selection of volcanic events and larch subsamples

Identification of the events used in this study was based on volcanic aerosols deposited in ice core records (Zielinski 1994; Robock 2000), and more precisely on Toohey and Sigl (2017), where the authors listed the top 20 eruptions over the past 2000 years, based on volcanic stratospheric sulfur injection (VSSI). From that list, we selected those reconstructed VSSI and events that are well recorded in tree-ring proxies and may thus have had a noticeable impact on the forest ecosystems in high-latitude and high-altitude regions (Briffa et al., 1998; D'Arrigo et al., 2001; Churakova (Sidorova) et al., 2014; Büntgen et al., 2016; Gennaretti et al., 2017; Helama et al., 2018). Therefore, based on our previously published TRW and developed MXD, CWT, $\delta^{13}C$ and $\delta^{18}O$ in tree-ring cellulose chronologies, we selected the periods CE 520-560, 1242-1286, 1625-1660, 1790-1835, and 1950-2000 with strong volcanic eruptions in CE 535, 540, 1257, 1640, 1815, and 1991, as they have had far-reaching climatic effects (Table 1). The recent period 1950-2000 is used to calibrate the tree-ring proxy against available climate data.

Tree-ring material was prepared from the 2000-year TRW chronologies available at each of site from the previous studies (Fig. 1 b-d). According to the level of conservation of the material, the largest possible number of samples was prepared for each of the proxies. Unlike TRW, which could be measured on virtually all samples, some of the material was not available with sufficient quality to allow for tree-ring anatomy and stable isotope analysis. We therefore use a smaller sample size for CWT (n=4) and stable isotopes (n=4) than for TRW (n=12) or MXD (n=12). Nonetheless, replications are still comparable with those used in reference papers on stable isotopes and CWT (Loader et al., 1997; Panyushkina et al., 2003).

Table 1. List of stratospheric volcanic eruptions used in the study.

Study period (CE)	Date of eruption Month/Day/Year	Volcano name	Volcanic Explosivity Index (VEI)	Location, coordinates	References
520-560	NA/NA/535	Unknown	?	Unknown	Stothers, 1984
	NA/NA/540	Unknown	?	Unknown	Sigl et al., 2015; Toohey, Sigl 2017
1242-1286	May-October/NA/ 1257	Samalas	7	Indonesia, 8.42°N, 116.47°E	Stothers, 2000; Lavigne et al., 2013; Sigl et al., 2015
1625-1660	December/26/1640	Parker	5	Philippines, 6°N, 124°E	Zielinski et al., 1994; 2000
1790-1835	April/10/1815	Tambora	7	Indonesia, 8°S, 118°E	Zielinski et al., 1994; 2000
1950 - 2000	June/15/1991	Pinatubo	6	Philippines, 15°N, 120°E	Zielinski et al., 1994; Sigl et al., 2015

NA – not available.

Table 2. Tree-ring sites in northeastern Yakutia (YAK), eastern Taimyr (TAY), and Altai (ALT) and weather stations used in the study. Monthly air temperature (T, °C), precipitation (P, mm), sunshine duration (S, h/month) and vapor pressure deficit (VPD, kPa) data were downloaded from the meteorological database: http://aisori.meteo.ru/ClimateR.

Site	Tree species	Location	Weather station	Meteorological parameters				Length of growing season (day)	Thawing permafrost depth (max, cm)	Annual air temperature (°C)	Annual precipitation (mm)
				T (°C)	P (mm)	S (h/month)	VPD (kPa)				
				Periods							
YAK	*Larix cajanderi* Mayr.	69°N, 148°E	Chokurdach 62°N, 147°E, 61 m. a.s.l.	1950-2000	1966-2000	1961-2000	1950-2000	50-70*	20-50*	-14.7	205
TAY	*Larix gmelinii* Rupr.	70°N, 103°E	Khatanga 71°N, 102°E, 33m. a.s.l.	1950-2000	1966-2000	1961-2000	1950-2000	90**	40-60**	-13.2	269
ALT	*Larix sibirica* Ledeb.	50°N, 89°E	Mugur Aksy 50°N, 90°E 1850 m. a.s.l.	1963-2000	1966-2000			90-120***	80-100***	-2.7	153
			Kosh-Agach 50°N, 88°E 1758 m.a.s.l.			1961-2000	1950-2000				

*Abaimov et al., 1996; Hughes et al., 1999; Churakova (Sidorova) et al., 2016

**Naurzbaev et al., 2002

***Sidorova et al., 2011

2.3. Tree-ring width analysis

Ring width of 12 trees was re-measured for each selected period. Cross-dating was checked by comparison with the existing full-length 2000-yr TRW chronologies (Fig. 1). The TRW series were standardized using the ARSTAN program (Cook and Krusic, 2008) with negative exponential curve (k>0) or a linear regression (any slope) prior to bi-weight robust averaging (Cook and Kairiukstis, 1990). Signal strength in the regional TRW chronologies was assessed with the Expressed Population Signal (EPS) statistics as it measures how well the finite sample chronology compares with a theoretical population chronology with an infinite number of trees (Wigley et al., 1984). Mean inter-series correlation (RBAR) and EPS values of stable isotope chronologies were calculated for the period 1950-2000, for which individual trees were analyzed separately. All series have RBAR ranges between 0.59 and 0.87, and the common signal exceeds the EPS threshold of 0.85. Before 1950, we used pooled cellulose only. For all other tree-ring parameters and studied periods, the EPS exceeds the threshold of 0.85, and RBAR values range from 0.63 to 0.94.

2.4. Image analysis of cell wall thickness (CWT)

Analysis of wood anatomy was performed for all studied periods with an AxioVision scanner (Carl Zeiss, Germany). Micro-sections were prepared using a sliding microtome and stained with methyl blue (Furst, 1979). Tracheids in each tree ring were measured along five radial files of cells (Munro et al., 1996; Vaganov et al., 2006) selected for their larger tangential cell diameter (T). For each tracheid, CWT was computed separately. In a second step, tracheid anatomical parameters were averaged for each tree ring. Site chronologies are presented for the complete annual ring chronology without standardization due to the lack of low-frequency trend. CWT data from ALT for the periods 1790-1835 and 1950-2000 were used from the past studies (Sidorova et al., 2011; Fonti et al., 2013) and for YAK for the period from 1600-1980 from Panyushkina et al. (2003). Unfortunately, the remaining sample material for the CE 536 ring at TAY was insufficient to produce a clear signal. As a result, CWT is missing for CE 536 at TAY (Fig. 2).

2.5. Maximum latewood density (MXD)

Maximum latewood density chronologies from ALT were available continuously for the period CE 600-2007 from Schneider et al. (2015) and Kirdyanov A.V. (personal communication), and from YAK and TAY for the period CE 1790-2004 from Sidorova et al. (2010). For any other periods, at least six cross-sections and for CE 520-560 four sections are used. The wood is subsampled with a double-bladed saw at 1.2 mm thickness with the angle to the fiber direction. The samples were exposed to X-rays for 35-60 min (Schweingruber, 1996). MXD measurements were obtained at 0.01 mm resolution and brightness variations calibrated to g/cm^3 (Lenz et al., 1976; Eschbach et al., 1995) using a Walesch X-ray densitometer 2003. All MXD series were detrended in the ARSTAN program by calculating deviation from straight-line function (Fritts, 1976). Site MXD chronologies were developed for each volcanic period using the bi-weight robust averaging.

2.6. Stable carbon ($\delta^{13}C$) and oxygen ($\delta^{18}O$) isotopes in tree-ring cellulose

During photosynthetic CO_2 assimilation $^{13}CO_2$ is discriminated against $^{12}CO_2$, leaving the newly produced assimilates depleted in ^{13}C. The carbon isotope discrimination ($^{13}\Delta$) is partitioned in the diffusional component with a = 4.4‰ and the biochemical fractionation with b = 27‰, for C3 plants, during carboxylation via Rubisco. The $^{13}\Delta$ is directly proportional to the c_i/c_a ratio, where c_i is the leaf intercellular, and c_a the ambient CO_2 concentration. This ratio reflects the balance between stomatal conductance (g_l) and photosynthetic rate (A_N). A decrease in g_l at a given A_N results in a decrease of $^{13}\Delta$, as c_i/c_a decreases and vice versa. The same is true when A_N increases or decreases at a given g_l. Since CO_2 and H_2O gas exchange are strongly interlinked with the C-isotope fractionation $^{13}\Delta$ is controlled by the same environmental variables i.e. PaR, CO_2, VPD and temperature (Farquhar et al., 1982, 1989; Cernusak et al., 2013). The oxygen isotopic compositions of tree-ring cellulose record the $\delta^{18}O$ of the source water derived from precipitation, which itself is related to temperature variations at middle and high latitudes (Craig, 1961; Dansgaard, 1964). It is modulated by evaporation at the soil surface and to a larger degree by evaporative and diffusion processes in leaves; the process is largely controlled by the vapor pressure deficit (Dongmann et al., 1972, Farquhar and Loyd, 1993, Cernusak et al., 2016). A further step of fractionation occurs as sugar molecules are transferred to the locations of growth (Roden et al., 2000). During the formation of organic compounds the biosynthetic fractionation leads to a positive shift of the $\delta^{18}O$ values by 27‰ relative to the leaf water (Sternberg, 2009). The oxygen isotope variation in tree-ring cellulose therefore reflects a mixed climate information, often dominated by a temperature, source water or sunshine duration modulated by the VPD influence. The cross-sections of relict wood and cores from living trees used for the TRW, MXD and CWT measurements were then selected for the isotope analyses. We analyzed four subsamples for each studied period according to the standards and criteria described in Loader et al. (2013). The first 50 yrs. of each sample were excluded to limit juvenile effects (McCarroll and Loader, 2004). After splitting annual rings with a scalpel, the whole wood samples were enclosed in filter bags. α-cellulose extraction was performed according to the method described by Boettger et al. (2007). For the analyses of $^{13}C/^{12}C$ and $^{18}O/^{16}O$ isotope ratios, 0.2-0.3 mg and 0.5-0.6 mg of cellulose were weighed for each annual ring, into tin and silver capsules, respectively. Carbon and oxygen isotopic ratios in cellulose were determined with an isotope ratio mass spectrometer (Delta-S, Finnigan MAT, Bremen, Germany) linked to two elemental analyzers (EA-1108, and EA-1110 Carlo Erba, Italy) via a variable open split interface (CONFLO-II, Finnigan MAT, Bremen, Germany). The $^{13}C/^{12}C$ ratio was determined separately by combustion under oxygen excess at a reactor temperature of 1020°C. Samples for $^{18}O/^{16}O$ ratio measurements were pyrolyzed to CO at 1080°C (Saurer et al., 1998). The instrument was operated in the continuous flow mode for both, the C and O isotopes. The isotopic values were expressed in the delta notation multiplied by 1000 relative to the international standards (Eq. 1):

$$\delta \text{ sample} = R_{sample}/R_{standard}-1 \qquad \text{(Eq. 1)}$$

where R_{sample} is the molar fraction of $^{13}C/^{12}C$ or $^{18}O/^{16}O$ ratio of the sample and $R_{standard}$ the molar fraction of the standards, Vienna Pee Dee Belemnite (VPDB) for carbon and Vienna Standard Mean Ocean Water (VSMOW) for oxygen. The precision is $\sigma \pm 0.1‰$ for carbon and $\sigma \pm 0.2‰$ for oxygen. To remove the atmospheric $\delta^{13}C$ trend after CE 1800 from the carbon isotope values in tree rings (i.e. Suess effect, due to fossil fuel combustion) we used atmospheric $\delta^{13}C$ data from Francey et al. (1999), http://www.cmdl.noaa.gov./info/ftpdata.html). These corrected series were used for all statistical analyses. The $\delta^{18}O$ cellulose series were not detrended.

2.7. Climatic data

Meteorological series were obtained from local weather stations close to the study sites and used for the computation of correlation functions between tree-ring proxies and monthly climatic parameters (Table 2, http://aisori.meteo.ru/ClimateR).

2.8. Statistical analysis

All chronologies for each period were normalized to z-scores (Fig. 2). To assess post-volcanic climate variability, we used Superposed Epoch Analysis (SEA, Panofsky and Brier, 1958) with the five proxy chronologies available at each of the three study sites. In this study, intervals of 15 years before and 20 years after a volcanic eruption were analyzed. SEA is applied to the six annually dated volcanic eruptions (Table 1).

To test the sensitivity of the studied tree-ring parameters to climate bootstrap correlation functions were computed between proxy chronologies and monthly climate predictors using the 'bootRes' package of R software (R Core Team 2016) for the period 1950 (1966)-2000.

To estimate whether volcanic years can be considered as extreme and how anomalous they are compared to non-volcanic years, we computed Probability Density Functions (PDFs, Stirzaker, 2003) for each study site and for each tree-ring parameter over a period of 219 years for which measurements are available (Fig. S1). A year is considered (very) extreme if the value of a given parameter is below the (5^{th}) 10^{th} percentile of the PDF.

3. Results

3.1. Anomalies in tree-ring proxy chronologies after stratospheric volcanic eruptions

Normalized TRW chronologies show negative deviations the year following the eruptions at all studied sites (Fig. 2). Regarding CWT, a strong decrease is observed in CE 537 at all study sites. Only two layers of cells were formed in CE 537 (-1.8σ) and 541 (-2.4σ) for YAK as compared to the 11-20 layers of cells formed on average during "normal" years. In addition, we also observe the formation of frost rings in ALT between CE 536 and 538, as well as in 1259. An abrupt CWT decrease is recorded in TAY in 537 (-3.1σ).

Furthermore, we found decreasing MXD values at ALT (-4.4 σ) in CE 537 and YAK (-2.8 σ) in CE 536. However, for TAY, data show a less pronounced pattern of MXD variation (Fig. 2). In this regard, the sharpest decrease was observed in the CWT chronologies from YAK in CE 540 (-1.9σ) and 541 (-2.4σ), whereas the response was smaller in TAY and ALT for the same years (Fig. 2). The ALT $\delta^{18}O$ chronology recorded a drastic decrease in 536 CE with - 4.8 σ (Fig. 2, Fig. S1). A $\delta^{18}O$ decrease for YAK was found after the CE 1257 Samalas eruption in CE 1258 (-1.5 σ) and in 1259 (-2.9σ), which is opposite to the increased $\delta^{18}O$ value found in CE 1259 at ALT (Fig. 2; Fig. S1).

Regarding the carbon isotope ratio, negative anomalies are observed in ALT already in 1258 (-2.3σ). The CE 540 eruption was less clearly recorded in tree-ring proxies from TAY, compared to YAK and ALT (Fig. 2). With respect to the CE 1257 Samalas eruption (Fig. 2), the year following the eruption was recorded as very extreme in the TRW, MXD, $\delta^{18}O$, while less extreme in CWT and $\delta^{13}C$ from YAK. ALT chronologies show a synchronous decrease for all proxies following two years after the eruption (Fig. 2, Fig. S1).

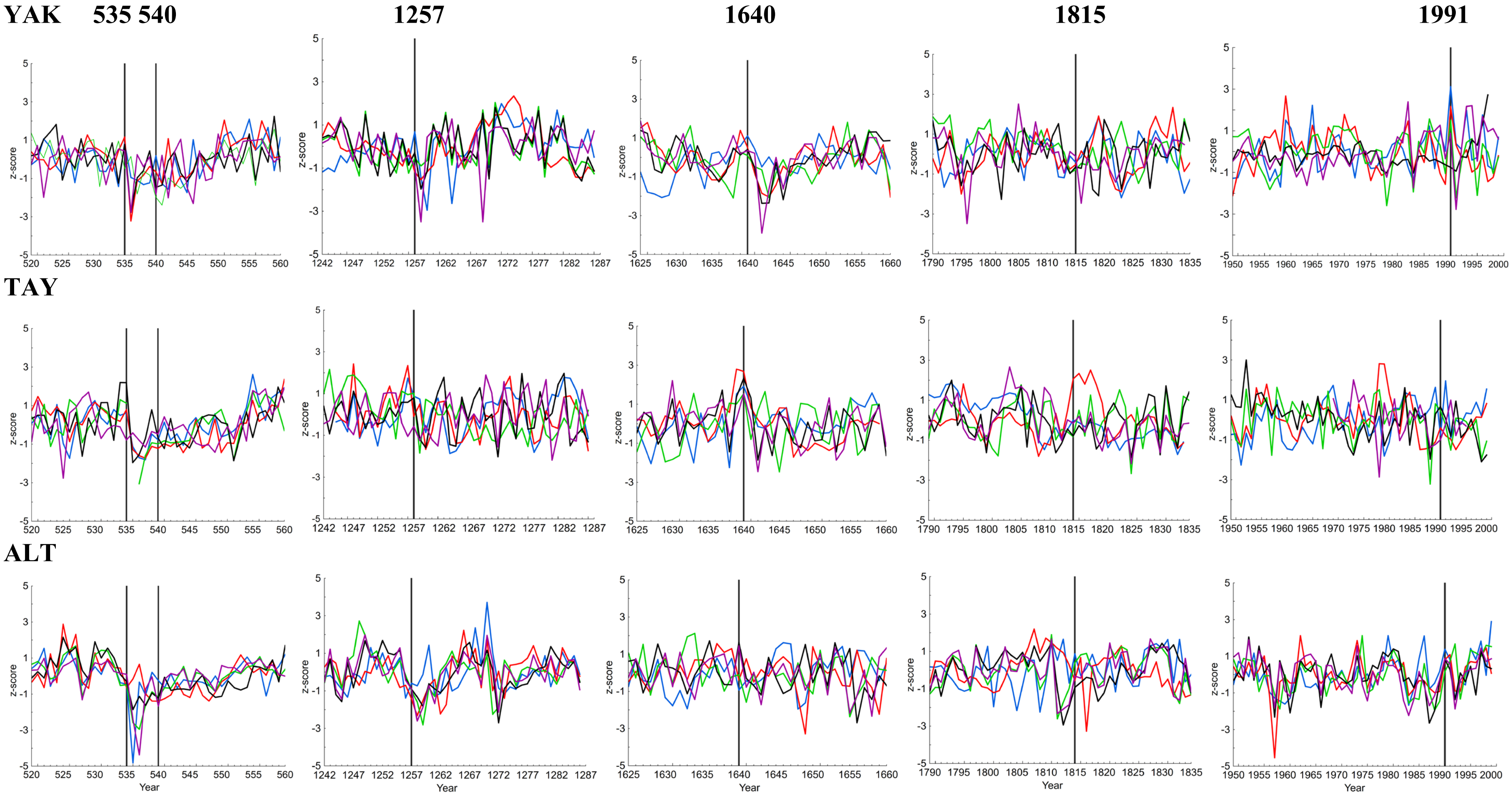

Fig. 2. Normalized (z-score) individual tree-ring index chronologies (TRW, **black**), maximum latewood density (MXD, **purple**), cell wall thickness (CWT, **green**), $\delta^{13}C$ (**red**) and $\delta^{18}O$ (**blue**) in tree-ring cellulose chronologies from northeastern Yakutia (YAK), eastern Taimyr (TAY) and Altai (ALT) for the specific periods CE 520-560, 1242-1286, 1625-1660, 1790-1835, 1950-2000 before and after the eruptions CE 535, 540, 1257, 1640, 1815 and 1991 are presented. Vertical lines show year of the eruptions.

The impacts of the more recent CE 1640 Parker, 1815 Tambora, and 1991 Pinatubo eruptions are, by contrast, far less obvious. In CE 1642, decreasing values are observed in all tree-ring proxies from the high-latitude sites YAK and TAY, whereas tree-ring proxies are not clearly affected at ALT (Fig. 2; Fig. S1).

Hardly any strong anomalies are observed in CE 1816 in Siberia regardless of the site and the tree-ring parameter analyzed. The ALT $\delta^{13}C$ value (-3.3σ) in CE 1817 and YAK MXD (-2.4σ) in 1816 can be seen as an exception to the rule here as they evidenced extreme values, respectively (Fig. S1).

Finally, the Pinatubo eruption is mainly captured by the MXD (-2.8σ) and CWT (-2.2σ) chronologies from YAK in CE 1992. Simultaneous decreases of all tree-ring proxies from ALT are observed in 1993 (Fig. 2), which, however, cannot be classified as extreme (Fig. S1).

Overall, the SEA (Fig. 3) shows that volcanic eruptions centered around CE 535, 540, 1257, 1640, 1815, and 1991 have led to decreasing values for all tree-ring proxies following next two years afterwards. A short-term response by two years after the eruptions is observed in the TRW and CWT proxies for TAY, while for YAK and ALT, the CWT decrease lasts longer (up to 5-6 years in ALT and YAK, respectively) (Fig. 3). The $\delta^{18}O$ isotope chronologies (z-score) show a distinct decrease the year after the eruptions. At ALT, however, the duration of negative anomalies were shorter (5 years) than at the high-latitude TAY (12 years) and YAK (9 years) sites. At the YAK site, two negative years followed the events, intermitted with one positive value, to remain negative during the following 7 years. The duration of negative anomalies recorded in $\delta^{13}C$ values (z-score) lasts also longer at the high-latitude YAK site - 10 years after the eruptions and 13 years at TAY compared to 7 years at ALT (Fig. 3).

The largest decrease in MXD values (in terms of z-score) is found at the high-latitude YAK site. The SEA for TRW, MXD, $\delta^{13}C$, and CWT from YAK as well as TRW and MXD from

ALT show a more drastic decrease of values during the first year when compared to other proxies and study sites (Fig. 3).

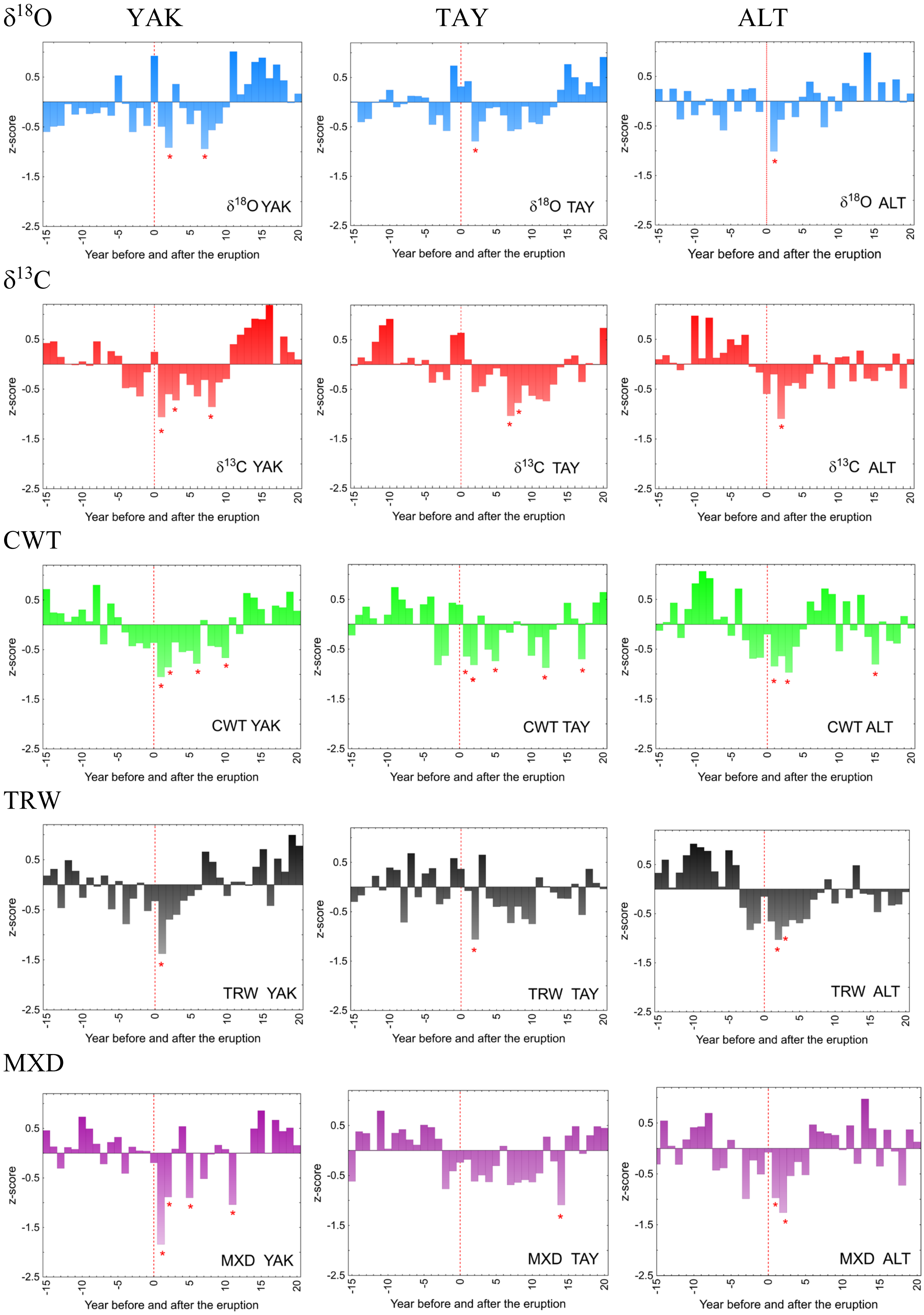

Fig. 3. Superposed epoch analysis (SEA) of $\delta^{18}O$, $\delta^{13}C$, CWT, TRW, and MXD chronologies for the Yakutia (YAK), Taimyr (TAY), and Altai (ALT) sites, summarizing negative anomalies 15 years before and 20 years after the volcanic eruptions in CE 535, 540, 1257, 1640, 1815, and 1991. Statistically negative anomalies are marked with a red star (**p<0.05*).

3.2. Tree-ring proxies versus meteorological series

3.2.1. Monthly air temperatures and sunshine duration

Bootstrapped functions calculated for the instrumental period (1950-2000) show significant positive correlations ($p<0.05$) between TRW and MXD chronologies and mean summer (June-July) temperatures at all sites. Temperatures at the beginning (June) and the end of the growing season (mid-August) influenced the MXD chronology in ALT ($r = 0.57$) and YAK ($r = 0.55$), respectively (Fig. 4). July temperatures appear as a key factor for determining tree growth as they significantly impact CWT, $\delta^{13}C$, and $\delta^{18}O$ (with the exception of TAY for the latter) chronologies ($r=0.28$-0.60) at YAK and ALT.

Correlation analysis between July temperature and July sunshine duration indicate significant ($p<0.05$) correlation for YAK ($r=0.56$) and ALT ($r=0.34$). July sunshine duration are strongly and positively correlated with $\delta^{18}O$ in larch tree-ring cellulose chronologies from YAK ($r=0.73$) and ALT ($r=0.51$) for the period 1961-2000 (available sunshine duration data set).

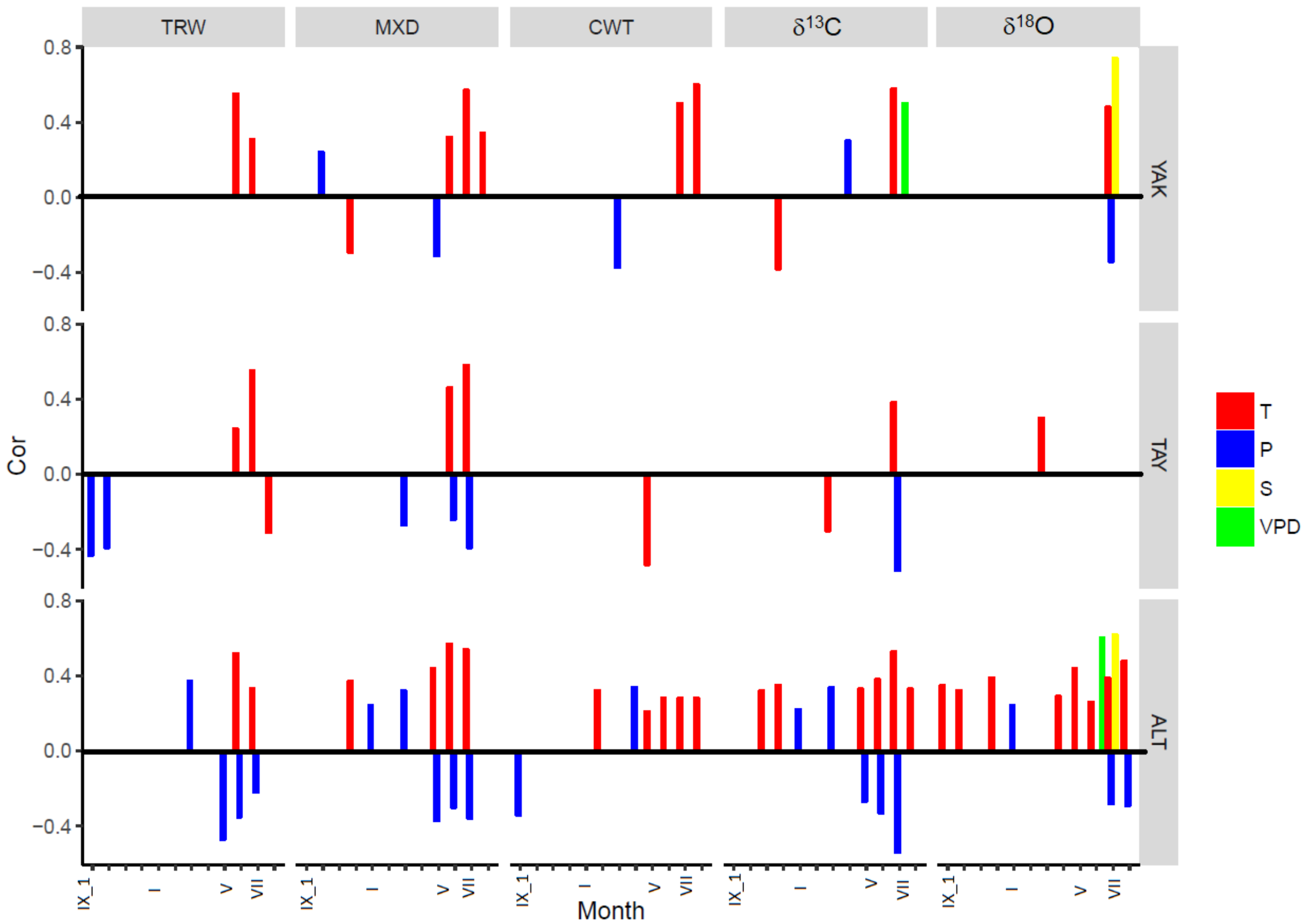

Fig. 4. Significant correlation coefficients between tree-ring parameters: TRW, MXD, CWT, $\delta^{13}C$ and $\delta^{18}O$ versus weather station data: temperature (T, red), precipitation (P, blue), vapor pressure deficit (VPD, green), and sunshine duration (S, yellow) from September of the previous year to August of the current year for three study sites were calculated. Table 2 lists stations and periods used in the analysis.

3.2.2. Monthly precipitation

The strongest July precipitation signal is observed at ALT (r=-0.54) and TAY (r=-0.51) with $\delta^{13}C$ chronologies (*$p<0.05$*). In addition, the ALT data shows a significant relationship (*$p<0.05$*) between March precipitation and TRW (r=0.37) and MXD (r=0.32), whereas April precipitation correlates positively with CWT (r=0.34). At YAK, July precipitation showed negative relationship with $\delta^{18}O$ in tree-ring cellulose (r=-0.34; *$p<0.05$*) only.

3.2.3. Vapor pressure deficit (VPD)

June VPD is significantly and positively correlated with the $\delta^{18}O$ chronology from ALT (r=0.67 *p<0.05*, respectively) for the period 1950-2000. The $\delta^{13}C$ in tree-ring cellulose from YAK correlate with July VPD only (r=0.69 *p<0.05*). We did not find significant influence of VPD in TAY tree-ring and stable isotope parameters.

3.2.4. Synthesis of the climate data analysis

In summary, during the instrumental period of weather station observations (Table 2) summer temperature impacts TRW, MXD and CWT at the high-latitude sites (YAK, TAY), while summer precipitation affects stable carbon and oxygen isotopes (YAK, TAY, ALT), sunshine duration (YAK, ALT), and vapor pressure deficit (YAK, ALT).

3.3. Response of Siberian larch trees to climatic changes after the major volcanic eruptions

Based on the statistical analysis above for the calibration period, we assumed that these relationships would not change over time and will provide information about climatic changes during the past volcanic periods (Fig. 5).

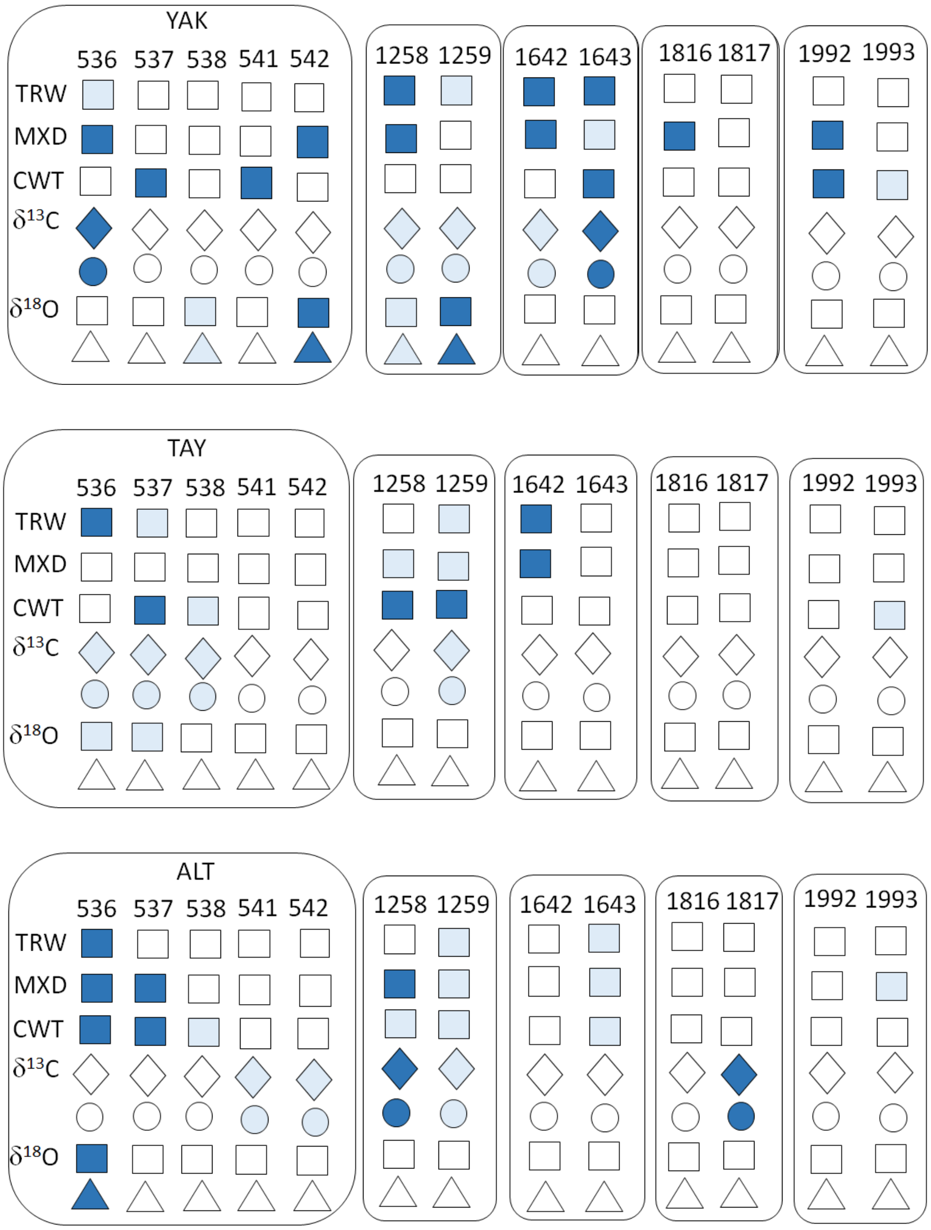

Fig. 5. Responses of larch trees from Yakutia (YAK), Taimyr (TAY) and Altai (ALT) to volcanic eruptions (Table 1). Squares, rhombs, circles, and triangles indicate the years following each eruption that can be considered as very extreme (negative values < 5th percentile of the PDFs, intensive color), extreme (negative values >5th, <10th percentile of the PDFs, light color) and non-extreme (>10th percentile of the PDFs, white color). July temperature changes are presented with squares. Summer vapor pressure deficit (VPD) variability is shown with circles. July precipitations are presented with rhombs, and July sunshine duration is shown as triangles.

3.3.1. Temperature proxies

We found strong negative summer air temperature anomalies at all sites after the CE 535 and 1257 volcanic eruptions. The temperature decrease was found in the TRW and CWT datasets at all sites, and also in the MXD datasets at YAK and ALT (Fig. 5). For the volcanic eruptions in later centuries, the evidence for a decrease in temperature was not as pronounced. Whereas no strong decline of summer temperature was found at ALT in CE 1642, we observe a slight decrease in TRW, MXD and CWT values in 1643. By contrast, a cold summer was recorded by most tree-ring parameters at YAK, except for $\delta^{18}O$. The absence of strong cooling is even more so striking during the years that followed the CE 1815 Tambora eruption. In CE 1816, only the MXD from YAK shows colder than normal conditions (Fig. 5). CE 1992 was recorded as a cold year in MXD and CWT from YAK, but again not at the other regions and by other proxies.

3.3.2. Moisture proxies: precipitation and VPD

Based on the climatological analysis with the local weather stations data (Table 2, Fig. 4) for all studied sites we considered $\delta^{13}C$ in tree-ring cellulose as a proxy for precipitation and vapor pressure deficit changes. Yet, CWT from ALT could be considered as a proxy with mixed temperature and precipitation signal (Fig. 4). Accordingly, the $\delta^{13}C$ values point to humid summers at YAK in 536, 1258, 1259, 1642, and 1643, at TAY in 536-538, and 1259, and at ALT the years of 541, 542, 1258, 1259 and 1817. Compared to other proxies and sites, the years 536-538 were neither extremely humid nor dry at ALT (Fig. 5). No negative hydrological anomalies were recorded after the Tambora and Pinatubo eruptions at the high-latitude sites (YAK, TAY). However, positive anomalies were recorded in $\delta^{13}C$ values, pointing to dry conditions at TAY in CE 1817 (Fig. 2). A rather wet summer was reconstructed for the high-altitude ALT site in CE 1817 compared to 1816 (Fig. 5). Overall, there were mostly humid anomalies after the eruptions at YAK.

3.3.3. Sunshine duration proxies

Instrumental measurements of sunshine duration (Table 2) at YAK and ALT during the recent period showed a significant link with $\delta^{18}O$ cellulose. The sunshine duration is decreased after various eruptions at YAK (538, 542, 1258, and 1259) and in 536 at ALT site.

4. Discussion

In this paper, we analyze climatic anomalies in years following selected large volcanic eruptions using long-term tree-ring multi-proxy chronologies for $\delta^{13}C$ and $\delta^{18}O$, TRW, MXD, CWT for the high-latitude (YAK, TAY) and high-altitude (ALT) sites. Since trees as living organisms respond to various climatic impacts, the carbon assimilation and growth patterns accordingly leave unique "finger prints" in the photosynthates, which is recorded in the wood in the tree rings specifically and individually for each proxy.

4.1. Evaluation of the applied proxies in Siberian tree-ring data

This study clearly shows that each proxy has to be analyzed and interpreted specifically for its validity at each studied site and evaluated for its suitability for the reconstruction of abrupt climatic changes.

The TRW in temperature-limited environments is an indirect proxy for summer temperature reconstructions, as growth is a temperature-controlled process. Temperature clearly determines the duration of the growing season and the rate of cell division (Cuny et al., 2014). Accordingly, low temperature of growing season is recorded by narrow tree rings. The upper limit of temperature is specific to tree species and biome. In most cases, tree growth is limited by drought rather than by high temperatures, since water shortage and VPD increase with increasing temperature. Still this does not make TRW a suitable proxy to determine the influence of water availability and air humidity, especially at the temperature-limited sites. MXD chronologies obtained for the Eurasian subarctic record mainly a July-August temperature signal (Vaganov et al., 1999; Sidorova et al., 2010; Büntgen et al., 2016) and add valuable information about climate conditions toward the end of the growth season. Similarly, CWT is an anatomical parameter, which contains information on carbon sink limitation of the cambium due to extreme cold conditions (Panyushkina et al., 2003; Fonti et al., 2013; Bryukhanova et al., 2015). There is a strong signal of low cell number within a growing season, for example, strong decreasing CWT in CE 537 at YAK or the formation of frost rings at ALT in (CE 536-538, and 1259) has been shown in our study.

Low $\delta^{13}C$ values can be explained by a reduction in photosynthesis caused by volcanic dust veils. For the distinction whether $\delta^{13}C$ is predominantly determined by A_N or g_l the combined evaluation with $\delta^{18}O$ or TRW is needed. High $\delta^{18}O$ values indicate high VPD, which induces a reduction in stomatal conductance, reducing the back diffusion of depleted water molecules from the ambient air. This confirms a sunny CE 1993 at ALT with mild weather conditions according to observational data from the closest weather station (Table 2). Interestingly, we also find less negative values for $\delta^{13}C$ in the same period. This shows that the two isotopes correlate with each other and indicates the need for a combined evaluation of the C and O isotopes (Scheidegger et al., 2000) taking into account precautions as suggested by Roden and Siegwolf (2012).

4.2. Lag between volcanic events and response in tree rings

Most discussed events suggest a lag between the eruption and the tree-ring response for one year or more (Fig. 3). This lag is explained by the tree's use of stored carbohydrates, which are the substrate for needle and early wood production. These stored carbohydrates carry the isotopic signal of previous years and depend on their remobilization, as such the signals may be masked in freshly produced biomass. The delayed signal could also reflect the time needed for the dust veil to be transported to the study regions.

4.3. Temperature and sunshine duration changes after stratospheric volcanic eruptions

Correlation functions show that MXD and CWT (with the exception of TAY in the latter case), and to a lesser extent TRW chronologies, portray the strongest signals for summer (June-August) temperatures. In addition, significant information about sunshine duration can be derived from the YAK and ALT $\delta^{18}O$ series. Thus, we hypothesize that extremely narrow TRW and very negative anomalies observed in the MXD and CWT chronologies of YAK and to a lesser extent at ALT, along with low $\delta^{18}O$ values reflect cold and low sunshine duration conditions in summer. Presumably, the temperatures were below the threshold values for growth over much of the growing season (Körner, 2015). This hypothesis of a generalized regional cooling after both eruptions is further confirmed by the occurrence of frost rings at ALT site in CE 538, 1259 (Myglan et al., 2008; Guillet et al., 2017), as well as in neighboring Mongolia (D'Arrigo et al., 2001). The unusual cooling in CE 536-542 is also evidenced by a very small number of cells formed at YAK (Churakova (Sidorova) et al., 2014). Although $\delta^{18}O$ is an indirect proxy for needle temperature, low $\delta^{18}O$ values in CE 538, 542, 1258, and 1259 for YAK and in CE 536 for ALT are a result of low irradiation, leading to low temperature and low VPD (high stomatal conductance), both likely a result from volcanic dust veils. Similarly, in the aftermath of the Samalas eruption, the persistence of summer cooling is limited to CE 1258 and 1259 at the three studied sites, which is in line with findings of Guillet et al., (2017). Interestingly, a slight decrease in oxygen isotope chronologies, which can be related to low levels of summer sunshine duration (i.e. low leaf temperatures), allows for hypothesizing that cool conditions could have prevailed.

For all later high-magnitude CE eruptions, temperature-sensitive tree-ring proxies do not evidence a generalized decrease in summer temperatures. Paradoxically, the impacts of the Tambora eruption, known for its triggering of a widespread "year without summer" (Harrington, 1992), did only induce abnormal MXD at YAK in 1816, but no anomalies are observed at TAY and ALT, except for the positive deviation of $\delta^{13}C$ at TAY and the negative anomaly at ALT in CE 1817 (Fig. 2, Fig. 5, Fig. S1). While these findings may seem surprising, they are in line with the TRW and MXD reconstructions of Briffa et al. (1998) or Guillet et al. (2017), who found limited impacts of the CE 1815 Tambora eruption in Eastern Siberia and Alaska using TRW and MXD data only. The inclusion of CWT chronologies by Barinov et al. (2018) confirms the absence of a significant cooling signal after the second largest eruption of the last millennium (CE 1815) in larch trees of the Altai-Sayan mountain region.

Finally, in CE 1992, our results evidence cold conditions at YAK, which is consistent with weather observations showing that the below-average anomalies of summer temperatures (after Pinatubo eruption) were indeed limited to Northeastern Siberia (Robock, 2000). As both isotopes indicate a reduction in stomatal conductance, we found that warm (in agreement with MXD and CWT) and dry conditions were prevalent at ALT at this time. This isotopic constellation was confirmed by the positive relationships between VPD and $\delta^{18}O$ and $\delta^{13}C$ at ALT. However, temperature and sunshine duration are not always highly coherent over time due to the influence of other factors, like Arctic Oscillations as suggested for Fennoscandia regions by Loader et al. (2013).

4.4. Moisture changes

Water availability is a key parameter for Siberian trees as they are growing under extremely continental conditions with hot summers and cold winters, and even more so with very low annual precipitation (Table 2). Permafrost plays a crucial role and can be considered as a buffer for additional water sources during hot summers (Sugimoto et al., 2002; Boike et al., 2013; Saurer et al., 2016). Yet, thawed permafrost water is not always available to roots due to the surficial structure of the root plate or extremely cold water temperature (close to 0ºC), which can hardly be utilized by trees (Churakova (Sidorova) et al., 2016). Thus, Siberian trees are highly susceptible to drought, induced by dry and warm air during July and therefore the stable carbon isotopes can be sensitive indicators of such conditions. After volcanic eruptions, however, low light intensity due to dust veils induce low temperatures and reduced VPD, the driver for evapotranspiration. Under such conditions drought stress is unlikely to occur. However, the transition phases with changes from cool and moist to warm and dry conditions are more critical when drought is more likely to occur.

In our study, higher $\delta^{13}C$ values in tree-ring cellulose indicate increasing drought conditions as a consequence of reduced precipitation for two years after the CE 1815 volcanic eruption at TAY site. No further extreme hydro-climatic anomalies occurred at Siberian sites in the aftermath of the Pinatubo eruption.

4.5. Synthetized interpretation from the multi-parameter tree-ring proxies

Our analysis demonstrates the added value of a tree-ring derived multi-proxy approach to better capture the climatic variability after large volcanic eruptions. Besides the well-documented effects of temperature derived from TRW and MXD, CWT, stable carbon and oxygen isotopes in tree-ring cellulose provide important and complementary information about moisture and sunshine duration changes (an indirect proxy for leaf temperature effective for air-to-leaf VPD) after stratospheric volcanic eruptions.

Our results reveal the complex behavior of the Siberian climatic system to the stratospheric volcanic eruptions of the Common Era. The CE 535 and CE 1257 Samalas eruptions caused substantial cooling – very likely induced by dust veils (Churakova (Sidorova) et al., 2014; Guillet et al., 2017; Helama et al., 2018) – as well as humid conditions at both the high-latitude and high-altitude sites. Conversely, only local and limited climate responses were observed after the CE 1641 Parker, 1815 Tambora, and 1991 Pinatubo eruptions. Similar site-dependent impacts referred to the coldest summers of the last millennium in the Northern Hemisphere based on TRW and MXD reconstructions (Schneider et al., 2015; Stoffel et al., 2015; Wilson et al., 2016; Guillet et al., 2017). This absence of widespread and intense cooling or missing drastic changes in hydrological regime over vast regions of Siberia may result from the location and strength of the volcanic eruption, atmospheric transmissivity as well as from the modulation of radiative forcing effects by regional climate variability. These results are consistent with other regional studies, which interpreted the spatial-temporal heterogeneity of tree responses to past volcanic events (Wiles et al., 2014; Esper et al., 2017; Barinov et al., 2018) in terms of regional climates.

5. Conclusions

In this study, we demonstrate that the consequences of large volcanic eruptions on climate are rather complex between sites and among events. The different locations and magnitudes of eruptions, but also regional climate variability, may explain some of this heterogeneity. We show that each tree-ring and isotope proxy alone cannot provide the full information of the volcanic impact on climate, but that they, when combined, contribute to the formation of the full picture, which is critical for a comprehensive description of climate dynamics induced by volcanism and the inclusion of these phenomena in global climate models.

The analyses with a larger number of samples in the investigations of Siberian and other Northern Hemispheric sites will indeed to provide higher certainty in terms of data interpretation of climatic dynamics of these boreal regions. However, the multi-proxy approach as applied in our study also provides a strong set of complementary information to the research field, as it allows the refinement of the interpretations and thus improves our understanding of the heterogeneity of climatic signals after CE stratospheric volcanic eruptions, as recorded in multiple tree-ring and stable isotope parameters.

Author contribution: TRW analysis was performed at V.N. Sukachev Institute of Forest SB RAS by O.V. Churakova (Sidorova), D.V. Ovchinnikov, V.S. Myglan and O.V. Naumova. CWT analysis was carried out at the V. N. Sukachev Institute of Forest SB RAS, Krasnoyarsk, Russia by M.V. Fonti and at the University of Arizona by I.P. Panyushkina. Stable isotope analysis was conducted at the Paul Scherrer Institute (PSI), by O.V. Churakova (Sidorova), M. Saurer, and R. Siegwolf. MXD measurements were realized with a DENDRO Walesh 2003 densitometer at WSL and at the V.N. Sukachev Institute of Forest SB RAS, Krasnoyarsk, Russia by O.V. Churakova (Sidorova) and A.V. Kirdyanov. Samples from YAK and TAY were collected by M.M. Naurzbaev. All authors contributed significantly to the data analysis and paper writing.

Acknowledgements: This work was supported by Marie Curie International Incoming Fellowship [EU_ISOTREC 235122], Re-Integration Marie Curie Fellowship [909122] and UFZ scholarship [2006], RFBR [09-05-98015_r_sibir_a] granted to Olga V. Churakova (Sidorova); SNSF Matthias Saurer [200021_121838/1]; Era.Net RusPlus project granted to Markus Stoffel [SNF IZRPZ0_164735] and RFBR [№ 16-55-76012 Era_a] granted to Eugene A. Vaganov; project granted to Vladimir S. Myglan RNF, Russian Scientific Fond [№ 15-14-

30011]; Alexander V. Kirdyanov was supported by the Ministry of Education and Science of the Russian Federation [#5.3508.2017/4.6] and RSF [#14-14-00295]; Scientific School [3297.2014.4] granted to Eugene A. Vaganov; and US National Science Foundation (NSF) grants [#9413327, #970966, #0308525] to Malcolm K. Hughes and US CRDF grant # RC1-279, to Malcolm K. Hughes and Eugene A. Vaganov. We thank Tatjana Boettger for her support and access to the stable isotope facilities within UFZ Haale/Saale scholarship 2006; Anne Verstege, Daniel Nievergelt for their help with sample preparation for the MXD and Paolo Cherubini for providing lab access at the Swiss Federal Institute for Forest, Snow and Landscape Research (WSL).

We thank two anonymous reviewers and handling Editor Juerg Luterbacher for their constructive comments on this manuscript.

Figure legends

Fig. 1. Location of the study sites (stars) and known volcanos from the tropics (black dots) considered in this study (a). Annual tree-ring width index (light lines) and smoothed by 51-year Hamming window (bold lines) from the northeastern Yakutia (YAK - **blue**, b) (Hughes et al., 1999; Sidorova and Naurzbaev 2002; Sidorova 2003), eastern Taimyr (TAY - **green**, c) (Naurzbaev et al., 2002), and Russian Altai (ALT - **red**, d) (Myglan et al., 2009). Photos show the larch stnads at YAK, TAY (M.M. Naurzbaev) and ALT (V.S. Myglan) sites.

Fig. 2. Normalized (z-score) individual tree-ring index chronologies (TRW, **black**), maximum latewood density (MXD, **purple**), cell wall thickness (CWT, **green**), $\delta^{13}C$ (**red)** and $\delta^{18}O$ (**blue**) in tree-ring cellulose chronologies from northeastern Yakutia (YAK), eastern Taimyr (TAY) and Altai (ALT) for the specific periods 520-560, 1242-1286, 1625-1660, 1790-1835, 1950-2000 before and after the eruptions CE 535, 540, 1257, 1640, 1815 and 1991 are presented. Vertical lines show year of the eruptions.

Fig. 3. Superposed epoch analysis (SEA) of $\delta^{18}O$, $\delta^{13}C$, CWT, TRW, and MXD chronologies for the Yakutia (YAK), Taimyr (TAY), and Altai (ALT) sites, summarizing negative anomalies 15 years before and 20 years after the volcanic eruptions in CE 535, 540, 1257, 1640, 1815, and 1991. Statistically negative anomalies are marked with a red star (*$p<0.05$).

Fig. 4. Significant correlation coefficients between tree-ring parameters: TRW, MXD, CWT, $\delta^{13}C$ and $\delta^{18}O$ versus weather station data: temperature (T, red), precipitation (P, blue), vapor

pressure deficit (VPD, green), and sunshine duration (S, yellow) from September of the previous year to August of the current year for three study sites were calculated. Table 2 lists stations and periods used in the analysis.

Fig. 5. Responses of larch trees from Yakutia (YAK), Taimyr (TAY) and Altai (ALT) to volcanic eruptions (Table 1). Squares, rhombs, circles, and triangles indicate the years following each eruption that can be considered as very extreme (negative values < 5th percentile of the PDFs, intensive color), extreme (negative values >5th, <10th percentile of the PDFs, light color) and non-extreme (>10th percentile of the PDFs, white color). July temperature changes are presented with squares. Summer vapor pressure deficit (VPD) variability is shown with circles. July precipitations are presented with rhombs, and July sunshine duration is shown as triangles.

Table 1. List of stratospheric volcanic eruptions used in the study

Table 2. Tree-ring sites in northeastern Yakutia (YAK), eastern Taimyr (TAY), and Altai (ALT) and weather stations used in the study. Monthly air temperature (T, °C), precipitation (P, mm), sunshine duration (S, h/month) and vapor pressure deficit (VPD, kPa) data were downloaded from the meteorological database: http://aisori.meteo.ru/ClimateR.

Fig. S1. Probability density function (Pdf) computed for each of the tree-ring parameter for northeastern Yakutia (YAK), eastern Taimyr (TAY) and Russian Altai (ALT). Tree-ring parameters (TRWi - **black**, MXD – **purple**, CWT – **green**, $\delta^{18}O$ - **blue** and $\delta^{13}C$ - **red**) in bold lines represent the probability density function. Dotted lines represent the anomalies (z-score) observed for the first and second years following the CE 535, 540, 1257, 1640, 1815 and 1991 volcanic eruptions for each tree-ring parameter.

References

Abaimov, A.P., Bondarev, A.I., Yzrzanova, O.V., Shitova, S.A.: Polar forests of Krasnoyarsk region. Nauka Press, Novosibirsk. 208 p, 1997.

Battipaglia, G., Cherubini, P., Saurer, M., Siegwolf, R.T.W., Strumia, S., Cotrufo, M.F.: Volcanic explosive eruptions of the Vesuvio decrease tree-ring growth but not photosynthetic rates in the surrounding forests. Global Change Biology. 13, 1-16, 2007.

Barinov, V.V., Myglan, V.S., Taynik, A.V., Ojdupaa, O.Ch., Agatova, A.R., Churakova (Sidorova) O.V.: Extreme climatic events in Altai-Sayan region as indicator of major volcanic eruptions. Geophysical processes and biosphere. 17, 45-61, 2018. doi: 10.21455/GPB2018.3-3.

Boettger T., Haupt, M., Knöller, K., Weise, S., Waterhouse, G.S. … Schleser, G.H.: Wood cellulose preparation methods and mass spectrometric analyses of $\delta^{13}C$, $\delta^{18}O$, and non ex-changeable $\delta^{2}H$ values in cellulose, sugar, and starch: An inter-laboratory comparison. Anal. Chem. 79, 4603–4612, doi:10.1021/ac0700023, 2007.

Boike, J., Kattenstroth, B., Abramova, K., Bornemann, N., Cherverova, A., Fedorova, I., Fröb, K., Grigoriev, M., Grüber, M., Kutzbach, L., Langer, M., Minke, M., Muster, S., Piel, K., Pfeiffer, E.-M., Stoff, G., Westermann, S., Wischnewski, K., Wille, C., Hubberten, H.-W.: Baseline characteristics of climate, permafrost and land cover from a new permafrost observatory in the Lena Rive Delta, Siberia (1998-2011). Biogeosciences. 10, 2105-2128, 2013.

Briffa, K.R., Jones, P.D., Schweingruber, F.H., Osborn, T.J.: Influence of volcanic eruptions on Northern Hemisphere summer temperature over the past 600 years. Nature. 393, 450–455, 1998.

Bryukhanova, M.V., Fonti, P., Kirdyanov, A.V., Siegwolf, R., Saurer, M., Pochebyt, N.P., Churakova (Sidorova), O.V., Prokushkin, A.S.: The response of $\delta^{13}C$, $\delta^{18}O$ and cell anatomy of *Larix gmelinii* tree rings to differing soil active layer depths. Dendrochronologia. 34, 51-59, 2015.

Büntgen, U., Myglan, V.S., Ljungqvist, F.C., McCormick, M., Di Cosmo, N., Sigl M., ….Kirdyanov, A.V.: Cooling and societal change during the Late Antique Little Ice Age from 536 to around 660 AD. Nature Geoscience. 9, 231-236, 2016.

Castagneri, D., Fonti, P., von Arx, G., Carrer, M.: How does climate influence xylem morphogenesis over the growing season? Insights from long-term intra-ring anatomy in *Picea abies*. Annals of Botany. 19, 1011-1020, doi:10.1093/aob/mcw274, 2017.

Cernusak, L., Ubierna, N., Winter, K., Holtum, J.A.M., Marshall, J.D., Farquhar, G.D.: Environmental and physiological determinants of carbon isotope discrimination in terrestrial Plants. Transley Review New Phytologist. 200, 950-965, 2013.

Cernusak, L., Barbour, M., Arndt, S., Cheesman, A., English, N., Field, T., Helliker, B., Holloway-Phillips, M., Holtum, J., Kahmen, A., Mcnerney F, Munksgaard N, Simonin K, Song X, Stuart-Williams H, West J and Farquhar G.: Stable isotopes in leaf water of terrestrial plants. Plant, Cell & Environment. 39 (5), 1087-1102, 2016.

Churakova (Sidorova), O.V., Bryukhanova, M., Saurer, M., Boettger, T., Naurzbaev, M., Myglan, V.S., Vaganov, E.A., Hughes, M.K., Siegwolf, R.T.W.: A cluster of stratospheric volcanic eruptions in the AD 530s recorded in Siberian tree rings. Global and Planetary Change. 122, 140-150, 2014.

Churakova (Sidorova), O.V., Shashkin, A.V., Siegwolf, R., Spahni, R., Launois, T., Saurer M., Bryukhanova, M.V., Benkova, A.V., Kupzova, A.V., Vaganov, E.A., Peylin, P., Masson-Delmotte, V., Roden, J.: Application of eco-physiological models to the climatic interpretation of $\delta^{13}C$ and $\delta^{18}O$ measured in Siberian larch tree-rings. Dendrochronologa, doi:10.1016/j.dendro.2015.12.008, 2016.

Cook, E., Briffa, K., Shiyatov, S., Mazepa, V.: Tree-ring standardization and growth trend estimation. In: Methods of dendrochronology: applications in the environmental sciences, Eds: Cook, E.R., Kairiukstis, L.A. 104-123, 1990.

Cook, E.R., Krusic, P.J.: A Tree-Ring Standardization Program Based on De-trending and Autoregressive Time Series Modeling, with Interactive Graphics (ARSTAN). (Ed. by E.R., Cook and P.J., Krusic), 2008.

Craig, H.: Isotopic variations in meteoric waters. Science. 133, 1702– 1703, 1961.

Crowley, T.J., Unterman, M.B.: Technical details concerning development of a 1200 yr. proxy index for global volcanism. Earth Syst. Sci. Data. 5, 187-197, 2013.

Cuny, H.E., Rathgeber, C.B.K., Frank, D., Fonti, P., Fournier, M.: Kinetics of tracheid development explain conifer tree-ring structure. New Phytologist. 203, 1231–1241, 2014.

D'Arrigo, R.D., Jacoby, G.C., Frank, D., Pederson, N.D., Cook, E., Buckly, B.M., Nachin, B., Mijidorj, R., Dugarjav, C.: 1738-years of Mongolian temperature variability inferred from a tree-ring width chronology of Siberian pine. Geophisycal Research Letters. Vol. 28 (3), 543-546, 2001.

Dansgaard, W.: Stable isotopes in precipitation. Tellus. 16, 436–468, 1964.

Dawson, T.E., Mambelli, S., Plamboeck, A.H., Templer, P.H., Tu, K.P.: Stable isotopes in plant ecology Ann. Review of Ecology and Systematics. 33, 507-559, 2004.

Dongmann, G., Förstel, H., Wagener, K.: ^{18}O-rich oxygen from land photosynthesis. Nature New Biol. 240, 127–128, 1972.

Eschbach, W., Nogler, P., Schär, E., Schweingruber, F.H.: Technical advances in the radiodensitometrical determination of wood density. Dendrochronologia. 13, 155–168, 2015.

Esper, J., Büntgen, U., Hartl-Meier, C., Oppenheimer, C., Schneider, L.: Northern Hemisphere temperature anomalies during 1450s period of ambiguous volcanic forcing. Bull. Volcanology. 79, 41, 2017.

Esper, J., St. George, S., Anchukaitis, K., D'Arrigo, R., Ljungqvist, F., Luterbacher, J., Schneider, L., Stoffel, M., Wilson, R., Büntgen, U.: Large-scale, millennial-length temperature reconstructions from tree-rings. Dendrochronologia. 50, 81–90, 2018.

Farquhar, G. D.: Eds. Stable Isotopes and Plant Carbon-Water Relations. Academic Press, San Diego. 47–70, 1982.

Farquhar, G.D., Ehleringer, J.R., Hubick, K.T.: Annu. Rev. Plant Physiol. Plant Mol. Biol. 40, 503 p, 1989.

Farquhar, G.D., Lloyd, J.: Carbon and oxygen isotope effects in the exchange of carbon dioxide between terrestrial plants and the atmosphere. In: Ehleringer, J.R., Hall, A.E., Farquhar, G.D. (Eds) Stable Isotopes and Plant Carbon-Water Relations. Academic Press, San Diego, 47–70, 1993.

Fonti, P., Bryukhanova, M.V., Myglan, V.S., Kirdyanov, A.V., Naumova, O.V., Vaganov, E.A.: Temperature-induced responses of xylem structure of *Larix sibirica* (Pinaceae) from Russian Altay. American Journal of Botany. 100 (7), 1-12, 2013.

Francey, R.J., Allison, C.E., Etheridge D.M., Trudinger, C.M., Langenfelds, R.L., Michel, E., Steele, L.P.: A 1000-year high precision record of $\delta^{13}C$ in atmospheric CO_2. Tellus. Ser. B (51), 170-193, 1999.

Fritts, H.C.: Tree-rings and climate. London. New York; San Francisco: Acad. Press. 567 p, 1976.

Furst, G.G.: Methods of Anatomical and Histochemical Research of Plant Tissue. Nauka, Moscow. 156 p, 1979.

Gao, C., Robock, A., Ammann, C.: Volcanic forcing of climate over the past 1500 years: An improved ice core-based index for climate models. J. Geophys. Res. Atmos. 113:D23111. doi:10.1029/2008jd010239, 2008.

Gennaretti, F., Huard, D., Naulier, M., Savard, M., Bégin, C., Arseneault, D., Guiot, J.: Bayesian multiproxy temperature reconstruction with black spruce ring widths and stable isotopes from the northern Quebec taiga. Clym. Dyn. doi: 10.1007/s00382-017-3565-5, 2017.

Gillett, N.P., Weaver, A.J., Zwiers, F.W. Wehner, M.F.: Detection of volcanic influence on global precipitation. Geophysical Research Letters. 31 (12), doi:10.1029/2004GL020044 R, 2004.

Groisman, P.Ya.: Possible regional climate consequences of the Pinatubo eruption. Geophys. Res. Lett., 19, 1603–1606, 1992.

Gu, L., Baldocchi, D.D., Wofsy, S.C., Munger, J.W., Michalsky, J.J., Urbanski, S.P., Boden, T.A.: Response of a deciduous forest to the Mount Pinatubo eruption: Enhanced photosynthesis, Science. 299 (5615), 2035–2038, 2003.

Guillet, S., Corona, C., Stoffel, M., Khodri M., Lavigne F., Ortega, P.,….Oppenheimer, C.: Climate response to the 1257 Samalas eruption revealed by proxy records. Nature geoscience, doi:10.1038/ngeo2875, 2017.

Hansen, J., Sato, M., Ruedy, R., Lacis, A., Asamoah, K., Borenstein S,, ….Wilson, H.: A Pinatubo climate modeling investigation. In The Mount Pinatubo Eruption: Effects on the Atmosphere and Climate, NATO ASI Series Vol. I 42. G. Fiocco, D. Fua, and G. Visconti, Eds. Springer-Verlag, 233-272, 1996.

Harrington, C.R.: The Year without a summer? World climate in 1816. Ottawa: Canadian Museum of Nature, ISBN 0660130637, 1992.

Helama, S., Arppe, L., Uusitalo, J., Holopainen, J., Mäkelä, H.M., Mäkinen, H., Mielikäinen, K., Nöjd, P., Sutinen, R., Taavitsainen, J.-P., Timonen, M., Oinonen, M.: Volcanic dust veils from sixth century tree-ring isotopes linked to reduced irradiance, primary production and human health. Scientific reports 8, 1339, doi:10.1038/s41598-018-19760-w, 2018.

Hughes, M.K., Vaganov, E.A., Shiyatov, S.G., Touchan, R. & Funkhouser, G.: Twentieth-century summer warmth in northern Yakutia in a 600-year context. The Holocene. 9(5), 603-608, 1999.

Iles, C.E., Hegerl, G.C.: The global precipitation response to volcanic eruptions in the CMIP5 models. Environ. Res. Lett. 9, doi:10.1088/1748-9326/9/10/104012, 2014.

Joseph, R., Zeng, N.: Seasonally modulated tropical drought induced by volcanic aerosol. J. Climate, 24, 2045–2060, 2011.

Kirdyanov, A.V., Treydte, K.S., Nikolaev, A., Helle, G., Schleser, G.H.: Climate signals in tree-ring width, wood density and $\delta^{13}C$ from larches in Eastern Siberia (Russia) Chemical Geology, 252, 31-41, 2008. doi:10.1016/j.chemgeo.2008.01.023

Körner, Ch.: Paradigm shift in plant growth control. Curr. Opinion Plant Biol. 25, 107-114, 2015.

Lavigne, F., Degeai, J.-P., Komorowski, J.-C., Guillet, S., Robert, V., Lahitte, P., Oppenheimer, C., Stoffel, M., Vidal, C.M., Suro, I.P., Wassmer, P., Hajdas, I., Hadmoko, D.S., Belizal, E.: Source of the great A.D. 1257 mystery eruption unveiled, Samalas volcano, Rinjani Volcanic Complex, Indonesia. Proc Natl Acad Sci 110, 16742–16747, doi:10.1073/pnas.1307520110, 2013.

Lenz, O., Schär, E., Schweingruber F.H.: Methodische Probleme bei der radiographisch-densitometrischen Bestimmung der Dichte und der Jahrrinbreiten von Holz. Holzforschung, 30, 114-123, 1976.

Loader, N.J., Robertson, I., Barker, A.C., Switsur, V.R., Waterhouse, J.S.: Improved technique for the batch processing of small whole wood samples to alpha-cellulose. Chemical Geology. 136, 313-317, 1997.

Loader, N.J., Young, G.H.F., Grudd, H., McCarroll.: Stable carbon isotopes from Torneträsk, norther Sweden provide a millennial length reconstruction of summer sunshine and its relationship to Arctic circulation. Quaternary Science Reviews. 62, 97-113, 2013.

McCarroll, D., Loader, N.J.: Stable isotopes in tree rings. Quaternary Science Review. 23, 771-801, 2004.

Meronen, H., Henriksson, S.V., Räisänen, P., Laaksonen, A.: Climate effects of northern hemisphere volcanic eruptions in an Earth System Model. Atmospheric Research, 114-115: 107-118, 2012.

Munro, M.A.R., Brown, P.M., Hughes, M.K., Garcia, E.M.R.: Image analysis of tracheid dimensions for dendrochronological use. Radiocarbon, Eds. by M.D. Dean, J. Swetnam T), pp. 843-851. Tucson, Arizona, 1996.

Myglan, V.S., Oidupaa, O. Ch., Kirdyanov, A.V., Vaganov, E.A.: 1929-year tree-ring chronology for Altai-Sayan region (Western Tuva). Journal of archeology, ethnography and anthropology of Eurasia. 4 (36), 25-31, 2008.

Naurzbaev, M.M., Vaganov, E.A., Sidorova, O.V., Schweingruber, F.H.: Summer temperatures in eastern Taimyr inferred from a 2427-year late-Holocene tree-ring chronology and earlier floating series. The Holocene. 12(6), 727-736, 2002.

Panofsky, H.A., Brier, G.W.: Some applications of statistics to meteorology. University Park, PA. Mineral industries extension services, college of mineral industries, Pennsylvania State University, 224 p, 1958.

Panyushkina, I.P., Hughes, M.K., Vaganov, E.A., Munro, M.A.R.: Summer temperature in northern Yakutia since AD 1642 reconstructed from radial dimensions of larch tracheids. Canadian Journal of Forest Research. 33, 1-10, 2003.

Peng, Y., Shen, C., Wang, W.-C., Xu, Y.: Response of summer precipitation over Eastern China to large volcanic eruptions. Journal of Climate. 23, 818-824, 2009.

R Core Team.: R: A Language and Environment for Statistical Computing. Vienna, Austria, 2016.

Robock, A.: Volcanic eruptions and climate. Reviews of Geophysics. 38(2), 191-219, 2000.

Robock, A., Liu, Y.: The volcanic signal in Goddard Institute for Space Studies three-imensional model simulations. J. Climate. 7, 44-55, 1994.

Roden, J.S., Siegwolf, R: Is the dual isotope conceptual model fully operational? Tree Physiology. 32, 1179-1182, 2012.

Saurer, M., Robertson, I., Siegwolf, R., Leuenberger, M.: Oxygen isotope analysis of cellulose: an interlaboratory comparison. Analytical cemistry, 70, 2074-2080, 1998.

Saurer, M., Kirdyanov, A. V., Prokushkin, A. S., Rinne, K. T., Siegwolf, R.T.W.: The impact of an inverse climate-isotope relationship in soil water on the oxygen-isotope composition of *Larix gmelinii* in Siberia. New Phytologist. 209(3), 955-964, 2016.

Scheidegger, Y., Saurer, M., Bahn, M., Siegwolf, R.: Linking stable oxygen and carbon isotopes with stomatal conductance and photosynthetic capacity: a conceptual model. Oecologia. 125, 350–357. doi: 10.1007/s004420000466, 2000.

Schneider, L., Smerdon, J.E., Büntgen, U., Wilson, R.J.S., Myglan, V.S., Kirdyanov, A.V., Esper, J.: Revising mid-latitude summer temperatures back to A.D. 600 based on a wood density network. Geophys. Res. Lett. 42, GL063956, doi:10.1002/2015gl063956, 2015.

Schweingruber, F.H.: Tree rings and environment dendroecology. Paul Haupt Publ Bern, Stuttgart, Vienna 1996. pp. 609, 1996.

Sidorova, O.V., Naurzbaev, M.M.: Response of *Larix cajanderi* to climatic changes at the upper timberline and in the Indigirka River valley. Lesovedenie (in Russian). 2, 73-75, 2002.

Sidorova, O.V.: Long-term climatic changes and the larch radial growth on the northern Middle Siberia and the Northeastern Yakutia in the Late Holocene. Abs. PHD Diss, V.N. Sukachev Institute of Forest, Krasnoyarsk, 2003.

Sidorova, O.V., Naurzbaev, M.M., Vaganov, E.A.: Response of tree-ring chronologies growing on the Northern Eurasia to powerful volcanic eruptions. Problems of ecological monitoring and ecosystem modeling, XX, 60-72, 2005.

Sidorova, O.V., Saurer, M., Myglan, V.S., Eichler, A., Schwikowski, M., Kirdyanov, A.V., Bryukhanova, M.V., Gerasimova, O.V., Kalugin, I., Daryin, A., Siegwolf, R.: A multi-proxy approach for revealing recent climatic changes in the Russian Altai. Climate Dynamics, 38 (1-2), 175–188, 2011.

Sidorova, O.V., Siegwolf, R., Myglan, V.S., Loader, N.J., Helle, G., Saurer, M.: The application of tree-rings and stable isotopes for reconstructions of climate conditions in the Altai-Sayan Mountain region. Climatic Changes, doi: 10.1007/s10584-013-0805-5, 2012.

Sidorova, O.V., Siegwolf, R., Saurer, M., Naurzbaev, M., Shashkin, A.V., Vaganov, E.A.: Spatial patterns of climatic changes in the Eurasian north reflected in Siberian larch tree-ring parameters and stable isotopes. Global Change Biology, doi: 10.1111/j.1365-2486.2009.02008.x, 16, 1003-1018, 2010.

Sidorova, O.V., Siegwolf, R.T.W., Saurer, M., Naurzbaev, M.M., Vaganov, E.A.: Isotopic composition ($\delta^{13}C$, $\delta^{18}O$) in Siberian tree-ring chronology. Geophysical research Biogeosciences. 113, 1-13, 2008.

Sigl, M., Winstrup, M., McConnell, J.R.: Timing and climate forcing of volcanic eruptions for the past 2500 years. Nature. 523, 543-549. doi:10.1038/nature14565, 2015.

Sprenger, M., Tetzlaff, D., Buttle, J. M., Laudon, H., Leistert, H., Mitchell, C., Snelgrove, J., Weiler, M., Soulsby, C.: Measuring and modelling stable isotopes of mobile and bulk soil water, Vadose Zone Journal, https://doi.org/10.2136/vzj2017.08.0149, 20, 2017.

Sternberg, L.S.O.: Oxygen stable isotope ratios of tree-ring cellulose: The next phase of understanding. New Phytologist. 181 (3), 553-562, 2009.

Stirzaker, D.: Elementary Probability density functions. Cambridge. Sec. Ed. 538 p, 2003.

Stoffel, M., Khodri, M., Corona, C., Guillet, S., Poulain, V., Bekki, S., Guiot, J., Luckman, B.H., Oppenheimer, C., Lebas, N., Beniston, M., Masson-Delmotte, V.: Estimates of volcanic-induced cooling in the Northern Hemisphere over the past 1500 years. Nature Geoscience. 8, 784–788, 2015.

Stothers, R.B.: Climatic and Demographic Consequences of the Massive Volcanic Eruption of 1258. Climatic Change. 45, 361-374, 2000.

Stothers, R.B.: Mystery cloud of AD 536. Nature. 307, 344-345, doi:10.1038/307344a0, 1984.

Sugimoto, A., Yanagisawa, N., Fujita, N., Maximov, T.C.: Importance of permafrost as a source of water for plants in east Siberian taiga. Ecological Research. 17 (4), 493-503, 2002.

Toohey, M., Sigl, M.: Volcanic stratospheric sulphur injections and aerosol optical depth from 500 BCE to 1900 CE. Earth System Science Data. doi:10.5194/essd-9-809-2017, 2017.

Vaganov, E.A., Hughes, M.K., Kirdyanov, A.K., Schweingruber, F.H., Silkin, P.P.: Influence of snowfall and melt timing on tree growth in subarctic Eurasia. Nature. 400, 149-151, 1999.

Vaganov, E.A., Hughes, M.K., Shashkin, A.V.: Growth dynamics of conifer tree rings. Springer Verlag, Berlin., pp. 353, 2006.

Wegmann, M., Brönnimann, S., Bhend, J., Franke, J., Folini, D., Wild, M., Luterbacher, J.: Volcanic influence on European summer precipitation through monsoons: Possible cause for “years without summer”. AMS, doi.org/10.1175/JCLI-D-13-00524.1, 2014.

Wigley, T.M.L., Briffa, K.R., Jones, P.D.: On the Average Value of Correlated Time Series, with Applications in Dendroclimatology and Hydrometeorology. Journal of Climate and Applied Meteorology. 23 (2), 201-213, doi:10.1175/15200450(1984)023.0201, 1984.

Wiles, G.C., D’Arrigo, R.D., Barclay, D., Wilson, R.S., Jarvis, S.K., Vargo, L., Frank, D.: Surface air temperature variability reconstructed with tree rings for the Gulf of Alaska over the past 1200 years. The Holocene. 6, 10.1177/0959683613516815, 2014.

Wilson, R.J.S., Anchukaitis, K., Briffa, K. et al.: Last millennium Northern Hemisphere summer temperatures from tree rings. Part I: the long-term context. Quaternary Science Review. 134, 1–18, 2016.

Zielinski, G.A., Mayewski, P.A., Meeker, L.D., Whitlow, S., Twickler, M.S., Morrison, M., Meese, D.A., Gow A.J., Alley, R.B.: Record of volcanism since 7000 BC from the

GISP2 Greenland ice core implications for the volcano-climate system. Science. 264 (5161), 948-952, 1994.

Zielinski, G.A.: Use of paleo-records in determining variability within the volcanism-climate system. Quaternary Science Reviews. 19, 417-438, 2000.

Siberian tree-ring and stable isotope proxies as indicators of temperature and moisture changes after major stratospheric volcanic eruptions

Olga V. Churakova (Sidorova)[1,2*], Marina V. Fonti[2], Matthias Saurer[3,4], Sébastien Guillet[1], Christophe Corona[5], Patrick Fonti[3], Vladimir S. Myglan[6], Alexander V. Kirdyanov[2,7,8], Oksana V. Naumova[6], Dmitriy V. Ovchinnikov[7], Alexander V. Shashkin[2,7], Irina P. Panyushkina[9], Ulf Büntgen[3,8], Malcolm K. Hughes[9], Eugene A. Vaganov[2,7,10], Rolf T.W. Siegwolf[3,4], Markus Stoffel[1,11,12]

[1]*Institute for Environmental Sciences, University of Geneva, CH-1205 Geneva, 66 Bvd Carl Vogt, Switzerland*

[2]*Institute of Ecology and Geography, Siberian Federal University RU-660049 Krasnoyarsk, Svobodniy pr 79/10, Russia*

[3]*Swiss Federal Institute for Forest, Snow and Landscape Research WSL, Zürcherstrasse 111, CH-8903 Birmensdorf, Switzerland*

[4]*Paul Scherrer Institute, CH- 5232 Villigen - PSI, Switzerland*

[5]*Université Blaise Pascal, Geolab, UMR 6042 CNRS, 4 rue Ledru, F-63057 Clermont-Ferrand, France*

[6]*Institute of Humanities, Siberian Federal University RU-660049 Krasnoyarsk, Svobodniy pr 82, Russia*

[7]*V.N. Sukachev Institute of Forest SB RAS, Federal Research Center "Krasnoyarsk Science Center SB RAS" RU-660036 Krasnoyarsk, Akademgorodok 50, bld. 28, Russia*

[8]*Department of Geography, University of Cambridge, Downing Place, Cambridge CB2 3EN*

[9]*Laboratory of Tree-Ring Research, University of Arizona, 1215 E. Lowell St., Tucson, 85721, USA*

[10]*Siberian Federal University, Rectorate, RU-660049 Krasnoyarsk, Svobodniy pr 79/10, Russia*

[11]*dendrolab.ch, Department of Earth Sciences, University of Geneva, 13 rue des Maraîchers, CH-1205 Geneva, Switzerland*

[12]*Department F.A. Forel for Environmental and Aquatic Sciences, University of Geneva, 66 Boulevard Carl-Vogt, CH-1205 Geneva, Switzerland*

Corresponding author: Olga V. Churakova (Sidorova)*

E-Mail: olga.churakova@hotmail.com

Deleted: *and*

Deleted: *Environmental*

Abstract

Stratospheric volcanic eruptions have far-reaching impacts on global climate and society. Tree rings can provide valuable climatic information on these impacts across different spatial and temporal scales. To detect temperature and hydro-climatic changes after strong stratospheric volcanic eruptions for the last 1500 years (CE 535 Unknown, CE 540 Unknown, CE 1257 Samalas, CE 1640 Parker, CE 1815 Tambora, and CE 1991 Pinatubo), we measured and analyzed tree-ring width (TRW), maximum latewood density (MXD), cell wall thickness (CWT), and $\delta^{13}C$ and $\delta^{18}O$ in tree-ring cellulose chronologies of climate-sensitive larch trees from three different Siberian regions (Northeastern Yakutia - YAK, Eastern Taimyr – TAY, and Russian Altai – ALT).

All tree-ring proxies proved to encode a significant and specific climatic signal of the growing season. Our findings suggest that TRW, MXD, and CWT show strong negative summer air temperature anomalies in 536, 541-542, and 1258-1259 at all study regions. Based on $\delta^{13}C$, 536 was extremely humid in YAK, 537-538 in TAY. No extreme hydro-climatic anomalies occurred at Siberian sites after the volcanic eruptions in 1640, 1815 and 1991, except for 1817 in ALT. The signal stored in $\delta^{18}O$ indicated significantly lower summer sunshine duration in 536, 541-542, 1258-1259 in YAK, and 536 in ALT. Our results show that trees growing at YAK and ALT mainly responded the first year after the eruptions, whereas at TAY, the growth response occurred after two years.

The fact that differences exist in climate responses to volcanic eruptions – both in space and time – underlines the added value of a multiple tree-ring proxy assessment. As such, the various indicators used clearly help to provide a more realistic picture of the impact of volcanic eruption to past climate dynamics, which is fundamental for an improved understanding of climate dynamics, but also for the validation of global climate models.

Deleted: (535, 540, 1257, 1640, 1815, and 1991)

Deleted: sites

Deleted: and

Deleted: , whereas 541 was humid in ALT, but led to at least two dry summers across two Siberian sites following the 1257 eruption.

Deleted: These

Key words: Dendrochronology, δ^{13}C and δ^{18}O in tree-ring cellulose, tree-ring width, maximum latewood density, cell wall thickness, temperature, precipitation, sunshine duration, vapor pressure deficit

1. Introduction

Major stratospheric volcanic eruptions can modify the Earth's radiative balance and substantially cool the troposphere. This is due to the massive injection of sulphate aerosols, which reduce the surface temperatures on timescales ranging from months to years (Robock, 2000). Volcanic aerosols significantly absorb terrestrial radiation and scatter incoming solar radiation, resulting in a cooling that has been estimated to about 0.5°C during the two years following the Mount Pinatubo eruption in June 1991 (Hansen et al., 1996).

Since trees – as living organisms – are impacted in their metabolism by environmental changes, their responses to these changes are recorded in the biomass, as it is found in tree-ring parameters (Schweingruber, 1996). The decoding of tree-ring archives is used to reconstruct past climates. A summer cooling of the Northern Hemisphere ranging from 0.6°C to 1.3°C has been reported after the strongest known volcanic eruptions of the past 1500 years: CE 1257 Samalas, 1815 Tambora and 1991 Pinatubo based on temperature reconstructions using tree-ring width (TRW) and maximum latewood density (MXD) records (Briffa et al., 1998; Schneider et al., 2015; Stoffel et al., 2015; Wilson et al., 2016; Esper et al., 2017, 2018; Guillet et al., 2017; Barinov et al., 2018).

Climate simulation show, significant changes in the precipitation regime after large volcanic eruptions. These include, among others, rainfall deficit in monsoon prone regions and in Southern Europe (Joseph and Zeng, 2011) and wetter than normal conditions in Northern Europe (Robock and Liu 1994; Gillet et al., 2004; Peng et al., 2009; Meronen et al., 2012; Iles et al., 2013; Wegmann et al., 2014). However, despite recent advances in the field, the impacts of

Deleted: These different climatic responses in space and time evidence the added value of a multiple tree-ring proxies assessment to provide a more realistic picture of the impact of volcanic eruption to past climate dynamics, which is fundamental to validate global climate models. ¶

Deleted: drought,

Deleted: substantially

Deleted: are able to

Deleted: The cooling associated with the radiative effects of v

Deleted: , which

Deleted: (NH)

Deleted: ,

Deleted: 1452/3 Unknown, 1600 Huaynaputina, and

Deleted: eruptions

Deleted: econstructions

Deleted: According to c

Deleted: s

Deleted: can also be expected

Deleted: ; t

Deleted: as well as

stratospheric volcanic eruptions on hydro-climatic variability at regional scales remain largely unknown. Therefore, further knowledge about moisture anomalies is critically needed, especially at high-latitude sites where tree growth is mainly limited by summer temperatures.

As dust and aerosol particles of large volcanic eruptions affect primarily the radiation regime, three major drivers of plant growth (i.e. photosynthetic active radiation (PaR), temperature and vapor pressure deficit (VPD)) will be affected by volcanic activity. This is reflected in reduced TRW as a result of reduced photosynthesis but even more so due to low temperature. As cell division is temperature dependent, its rate (tree-ring growth) will exponentially decrease with decreasing temperature below +3°C (Körner, 2015), outweighing the "low light / low-photosynthesis" effect by far.

Furthermore, over the last years, some studies using mainly carbon isotopic signals ($\delta^{13}C$) in tree rings showed eco-physiological responses of trees to volcanic eruptions at mid- (Battipaglia et al., 2007) or high- (Gennaretti et al., 2017) latitudes. By contrast, a combination of both carbon ($\delta^{13}C$) and oxygen ($\delta^{18}O$) isotopes in tree rings has been employed only rarely to trace volcanic eruptions in high-latitude or high-altitude proxy records (Churakova (Sidorova) et al., 2014).

Application of TRW, MXD and cell wall thickness (CWT) as well as $\delta^{13}C$ and $\delta^{18}O$ in tree cellulose chronologies is a promising way to disentangle hydro-climatic variability as well as winter and early spring temperatures at high-latitude and high-altitude sites (Kirdyanov et al., 2008; Sidorova et al., 2008, 2010, 2011; Churakova (Sidorova) et al., 2014; Castagneri et al., 2017). In that sense, recent CWT measurements allowed generating high-resolution, seasonal information of water and carbon limitations on growth during springs and summers (Panyushkina et al., 2003; Sidorova et al., 2011; Fonti et al., 2013; Bryukhanova et al., 2015). Depending on site conditions, $\delta^{13}C$ variations reflect light (stand density) (Loader et al., 2013), water availability (soil properties) and air humidity (proximity to open waters, i.e. rivers, lakes, swamps

Deleted: the

Deleted: by

Deleted: CE

Deleted: Approaches including

Deleted: are

Deleted: s

Deleted: ,

Deleted: work has

Deleted: the retrieval of

Deleted: on

Deleted: from

Deleted: CWT measurements

and orography) as these parameters have been recognized to modulate stomatal conductance (g_l) controlling carbon isotopic discrimination.

Depending on the study site, a decrease in the carbon isotope ratio can be expected after stratospheric volcanic eruptions due to limited photosynthetic activity and higher stomatal conductance, which in turn would be the result of decreased temperatures, VPD, and a reduction in light intensity. By contrast, volcanic eruptions have also been credited for an increase in photosynthesis as dust and aerosol particles cause an increased light scattering, compensating for the light reduction (Gu et al., 2003). A significant increase in $\delta^{13}C$ values in tree-ring cellulose should be interpreted as an indicator of drought (stomatal closure) or high photosynthesis (Farquhar et al., 1982). In the past, very little attention has been paid to the elemental and isotopic composition of tree rings for years during which they may have been subjected to the climatic influence of powerful, but remote, and often tropical, volcanic eruptions.

In this study, we aim to fill this gap by investigating the response of different components of the Siberian climate system (i.e. temperature, precipitations, VPD, and sunshine duration) to stratospheric volcanic events of the last 1500 years. By doing so, we seek to extend our understanding of the effects of volcanic eruptions on climate by combining multiple climate sensitive variables measured in tree rings that were formed around the time of the major volcanic eruptions (Table 1). We focus our investigation on remote tree-ring sites in Siberia, two at high latitudes (northeastern Yakutia - YAK and eastern Taimyr - TAY), and one at high altitude (Russian Altai - ALT), for which long tree-ring chronologies were developed previously with highly climate sensitive trees. We assemble a dataset from five tree-ring proxies: TRW, MXD, CWT, $\delta^{13}C$ and $\delta^{18}O$ in larch tree-ring cellulose chronologies in order to: (1) determine the major climatic drivers of the tree-ring proxies and to evaluate their individual and integrative response to climate change, and to (2) reconstruct the climatic impacts of volcanic eruptions over specific periods of the past (Table 1).

Deleted: ¶
Deleted: limited
Deleted: given
Deleted: in
Deleted: ,
Deleted: see
Deleted: ,
Deleted: where
Deleted: with high climate sensitivity exist
Deleted: developed
Deleted: including
Deleted: stable isotope
Deleted: derived from larch trees with the goal
Deleted: to
Deleted: above mentioned
Deleted: suitability
Deleted:
Deleted: in terms of climate responsiveness, for each proxy separately and in combination; and based on these analyses
Deleted: to
Deleted: effect
Deleted: the strong
Deleted: of

2. Material and methods

2.1. Study sites

The study sites are situated in Siberia (Russian Federation), far away from industrial centers (and 1500–3400 km apart from each other), in the zone of continuous permafrost in northeastern Yakutia (YAK, 69°N, 148°E), eastern Taimyr (TAY, 70°N, 103°E), and mountain permafrost in Altai (ALT, 50°N, 89°E) (Fig. 1a, Table 2). Tree-ring samples were collected during several field trips and included old relict wood and living larch trees: *Larix cajanderi* Mayr (up to 1216 years) in YAK, *Larix gmelinii* Rupr. (max. 640 years) in TAY and *Larix sibirica* Ldb. (max. 950 years) in ALT. TRW chronologies have been developed and published in the past (Fig. 1, Hughes et al., 1999; Sidorova and Naurzbaev, 2002; Sidorova, 2003 for YAK; Naurzbaev et al., 2002; Panyushkina et al., 2003 for TAY; Myglan et al., 2008 for ALT).

Due to the remote location of our study sites, we used meteorological data from monitored weather stations located at distances ranging from 50-200 km from the sampled sites. Temperature data from these weather stations are significantly correlated (r>0.91; $p<0.05$) with gridded data (http://climexp.knmi.nl). However, poor correlation is found with precipitation data (r<0.45; $p<0.05$), most likely is the result of the local topography (Churakova (Sidorova) et al., 2016).

Mean annual air temperature is lower at the high-latitude YAK and TAY sites than at the high-altitude ALT site (Table 2). Annual precipitation is low (153-269 mm year^{-1}) for all study sites. The growing season calculated with a growth threshold of +5ºC (Fritts 1976; Schweingruber 1996) is very short (50-120 days) at all locations (Table 2). Sunshine duration is higher at YAK and TAY (ca. 18-20 h/day in summer) compared to ALT (ca. 18 h/day in summer) (Sidorova et al., 2005; Myglan et al., 2008; Sidorova et al., 2011; Churakova (Sidorova) et al., 2014).

Deleted:
Deleted:
Deleted: s characterized by
Deleted:
Deleted: the
Deleted: mountains
Deleted: expeditions
Deleted: d
Deleted: ,
Deleted: max.
Deleted: localization
Deleted: sampling
Field Code Changed
Formatted: Font: Italic, Not Highlight
Deleted: as a
Deleted: representing local effects
Deleted: totals are very
Deleted: vegetation period
Deleted: for tree growth

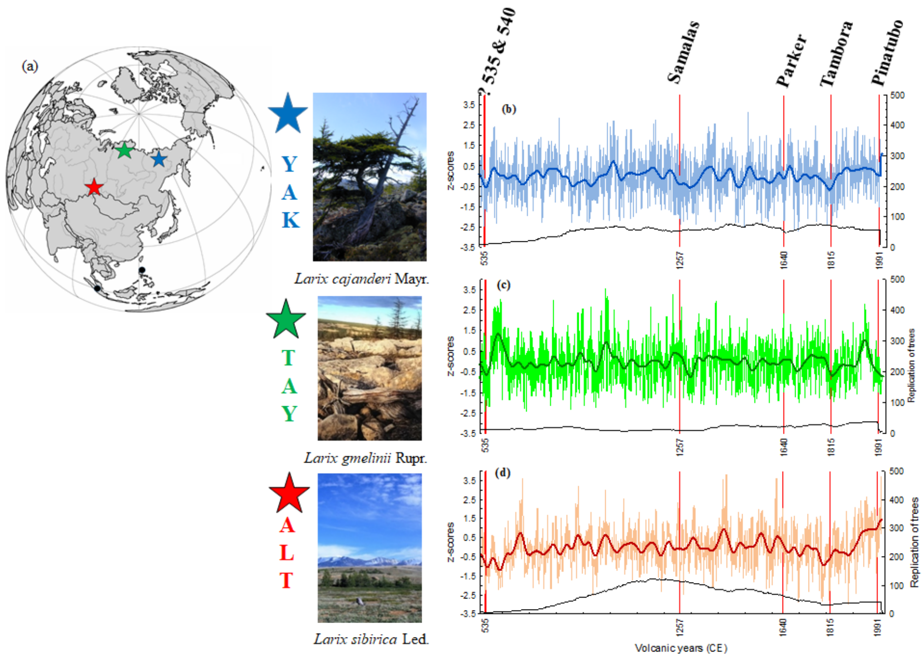

Fig. 1. Location of the study sites (stars) and known volcanous from the tropics (black dots) considered in this study (a). Annual tree-ring width index (light lines) and smoothed by 51-year Hamming window (bold lines) chronologies from northeastern Yakutia (YAK - **blue**, b) (Hughes et al., 1999; Sidorova and Naurzbaev, 2002; Sidorova, 2003), eastern Taimyr (TAY - **green**, c) (Naurzbaev et al., 2002), and Russian Altai (ALT - **red**, d) (Myglan et al., 2009). Photos show the the larchstands at YAK, TAY (M.M. Naurzbaev) and ALT (V.S. Myglan) sites.

2.2. Selection of volcanic events and larch subsamples

Identification of the events used in this study was based on volcanic aerosols deposited in ice core records (Zielinski 1994; Robock 2000), and more precisely on Toohey and Sigl (2017), where the authors listed the top 20 eruptions over the past 2,000 years, based on volcanic stratospheric sulfur injection (VSSI). From that list, we selected those reconstructed VSSI

Deleted: Map with the l
Deleted: s
Deleted: volcanic
Deleted: eruptions
Deleted: were constructed based on
Deleted: trees
Deleted: (Photos: V. Myglan – ALT,
Deleted:
Deleted: – YAK, TAY
Deleted: .
Formatted: Pattern: Clear
Deleted: analyzed
Formatted: Pattern: Clear
Deleted: from
Deleted: in terms of
Formatted: Pattern: Clear
Deleted: in a new ice core-based volcanic forcing reconstruction
Deleted: Our sub-criteria is based on literature review of

and events that are well reported in tree-ring proxies that may thus have had a noticeable impact on the forest ecosystems in high-latitude and high-altitude regions (Briffa et al., 1998; D'Arrigo et al., 2001; Churakova (Sidorova) et al., 2014; Büntgen et al., 2016; Gennaretti et al., 2017; Helama et al., 2018). Therefore, based on our previously published TRW and newly developed MXD, CWT, $\delta^{13}C$ and $\delta^{18}O$ in tree-ring cellulose chronologies, we selected periods CE 520-560, 1242-1286, 1625-1660, 1790-1835, and 1950-2000 with strong volcanic eruptions in CE 535, 540, 1257, 1640, 1815, and 1991, as they have had far-reaching climatic effects (Table 1). The recent period 1950-2000 is used to calibrate the tree-ring proxy against available climate data.

Tree-ring material was prepared from the 2000-yr long TRW chronologies available at each of the sites from the previous studies (Fig. 1 b-d). According to the level of conservation of the material, the largest possible number of samples was prepared for each of the proxies. Unlike TRW, which could be measured on virtually all samples, some of the material was not available with sufficient quality to allow for tree-ring anatomy and stable isotope analysis. We therefore use a smaller sample size for CWT (n=4) and stable isotopes (n=4) than for TRW (n=12) or MXD (n=12). Nonetheless, replications are still comparable with those used in reference papers on stable isotopes and CWT (Loader et al., 1997; Panyushkina et al., 2003).

Deleted: from

Deleted: 2016

Deleted: the years, characterized by strong volcanic eruptions with far-reaching climatic effect, namely the years

Deleted: CE 535, 540, 1257, 1640, 1815, and 1991. Therefore, to investigate climatic impacts of these eruptions in Siberian regions, we selected periods around (± 10 years): CE 525-545, 1247-1267, 1630-1650, 1805-1825, and 1950-2000, with the latter being used to calibrate tree-ring proxy versus available climate data (Table 2).

Deleted: M

Deleted: in the fields of

Deleted:

Deleted: and isotope analyses

Table 1. List of stratospheric volcanic eruptions used in the study.

Study period (CE)	Date of eruption Month/Day/Year	Volcano name	Volcanic Explosivity Index (VEI)	Location, coordinates	References
520-560	NA/NA/535	Unknown	?	Unknown	Stothers, 1984
	NA/NA/540	Unknown	?	Unknown	Sigl et al., 2015; Toohey, Sigl 2017
1242-1286	May-October/NA/ 1257	Samalas	7	Indonesia, 8.42°N, 116.47°E	Lavigne et al., 2013; Stothers, 2000; Sigl et al., 2015
1625-1660	December/26/1640	Parker	5	Philippines, 6°N, 124°E	Zielinski et al., 1994; 2000
1790-1835	April/10/1815	Tambora	7	Indonesia, 8°S, 118°E	Zielinski et al., 1994; 2000
1950 - 2000	June/15/1991	Pinatubo	6	Philippines, 15°N, 120°E	Zielinski et al., 1994; Sigl et al., 2015

NA – not available.

Deleted: 525-545

Formatted Table

Deleted: 1247-1267

Deleted: 1630-1650

Deleted: 1805-1825

Table 2. Tree-ring sites in northeastern Yakutia (YAK), eastern Taimyr (TAY), and Altai (ALT) and weather stations used in the study. Monthly air temperature (T, °C), precipitation (P, mm), sunshine duration (S, h/month) and vapor pressure deficit (VPD, kPa) data were downloaded from the meteorological database: http://aisori.meteo.ru/ClimateR.

Site	Tree species	Location	Weather station	Meteorological parameters				Length of growing season (day)	Thawing permafrost depth (max, cm)	Annual air temperature (°C)	Annual precipitation (mm)
				T (°C)	P (mm)	S (h/month)	VPD (kPa)				
				Periods							
YAK	*Larix cajanderi* Mayr.	69°N, 148°E	Chokurdach 62°N, 147°E, 61 m. a.s.l.	1950-2000	1966-2000	1961-2000	1950-2000	50-70*	20-50*	-14.7	205
TAY	*Larix gmelinii* Rupr.	70°N, 103°E	Khatanga 71°N, 102°E, 33m. a.s.l.	1950-2000	1966-2000	1961-2000	1950-2000	90**	40-60**	-13.2	269
ALT	*Larix sibirica* Ledeb.	50°N, 89°E	Mugur Aksy 50°N, 90°E 1850 m. a.s.l.	1963-2000	1966-2000			90-120***	80-100***	-2.7	153
			Kosh-Agach 50°N, 88°E 1758 m.a.s.l.			1961-2000	1950-2000				

*Abaimov, 1996; Hughes et al., 1999; Churakova (Sidorova) et al., 2016

**Naurzbaev et al., 2002

***Sidorova et al., 2011

Deleted: Summary of t

Deleted: used

Deleted: available

Deleted: S

Deleted: vegetation

Deleted: period

2.3. Tree-ring width analysis

Ring width of 12 trees was re-measured for each selected period. Cross-dating was checked by comparison with the existing complete 2000-yr TRW chronologies (Fig. 1). The TRW series were standardized using the ARSTAN program (Cook and Krusic, 2008) based on the negative exponential curve (k>0) or a linear regression (any slope) prior to bi-weight robust averaging (Cook and Kairiukstis 1990). Signal strength in regional TRW chronologies was assessed with the Expressed Population Signal (EPS) statistics as it measures how well the finite sample chronology compares with a theoretical population chronology based on an infinite number of trees (Wigley et al., 1984). Mean inter-series correlation (RBAR) and EPS values of stable isotope chronologies were calculated for the period 1950-2000, for which individual trees were analyzed separately. All series have RBAR ranges between 0.59 and 0.87, the common signal exceeds the EPS > 0.85 threshold of 0.85. Before 1950, we used pooled cellulose only. For all other tree-ring parameters and studied periods, the EPS exceeds the threshold of 0.85, and RBAR values range from 0.63 to 0.94.

Deleted: We show the common signal with an EPS > 0.85 and

2.4. Image analysis of cell wall thickness (CWT)

Analysis of wood anatomy was performed for all studied periods with an AxioVision scanner (Carl Zeiss, Germany). Micro-sections were prepared using a sliding microtome and stained with methyl blue (Furst, 1979). Tracheids in each tree ring were measured along five radial files of cells (Munro et al., 1996; Vaganov et al., 2006) selected for their larger tangential cell diameter (T). For each tracheid, CWT was computed separately. In a second step, tracheid anatomical parameters were averaged for each tree ring. Site chronologies are presented for the complete annual ring chronology without standardization due to the absence of low-frequency trend. CWT data from ALT for the periods 1790-1835 and 1950-2000 were used from the past studies (Sidorova et al., 2011; Fonti

Deleted: ical features

Deleted: every

et al., 2013) and for YAK for the period from 1600-1980 from Panyushkina et al. (2003). Unfortunately, the remaining sample material for the CE 536 ring at TAY was insufficient to produce a clear signal. As a result, CWT is missing for CE 536 at TAY (Fig. 2).

Deleted: anatomical

2.5. Maximum latewood density (MXD)

Maximum latewood density chronologies from ALT were available for the period CE 600-2007 from Schneider et al. (2015) and Kirdyanov A.V. (personal communication), and for YAK and TAY the period CE 1790-2004 from Sidorova et al. (2010). For any of the other periods, at least six cross-sections (for CE 520-560, only four sections could be used, as this period is not as well replicated) were sawn with a double-bladed saw, to a thickness of 1.2 mm, at right angles to the fiber direction. Samples were exposed to X-rays for 35-60 min (Schweingruber, 1996). MXD measurements were obtained with a resolution of 0.01 mm, and brightness variations transferred into (g/cm^3) using a calibration wedge (Lenz et al., 1976; Eschbach et al., 1995) from a Walesch X-ray densitometer 2003. All MXD series were detrended in ARSTAN by calculating subtractions from straight-line functions (Fritts, 1976). Site chronologies were developed for each volcanic period using the bi-weight robust averaging.

Deleted: Schneider et al. (2015)

Deleted: 516

2.6. Stable carbon ($\delta^{13}C$) and oxygen ($\delta^{18}O$) isotopes in tree-ring cellulose

During photosynthetic CO_2 assimilation $^{13}CO_2$ is discriminated against $^{12}CO_2$, leaving the newly produced assimilates depleted in ^{13}C. The carbon isotope discrimination ($^{13}\Delta$) is partitioned in the diffusional component with a = 4.4‰ and the biochemical fractionation with b = 27‰, for C3 plants, during carboxylation via Rubisco. The $^{13}\Delta$ is directly proportional to the c_i/c_a ratio, where c_i is the leaf intercellular, and c_a the ambient CO_2 concentration. This ratio reflects the balance between stomatal conductance (g_l) and photosynthetic rate (A_N). A decrease in g_l at a given A_N results in a decrease of $^{13}\Delta$, as c_i/c_a decreases and vice versa. The same is true when A_N increases or decreases at a given g_l. Since CO_2 and H_2O gas exchange are strongly interlinked with the C-isotope fractionation $^{13}\Delta$ is controlled by the same environmental variables i.e. PaR, CO_2, VPD and temperature (Farquhar et al., 1982, 1989; Cernusak et al., 2013).

The oxygen isotopic compositions of tree-ring cellulose record the $\delta^{18}O$ of the source water derived from precipitation, which itself is related to temperature variations at middle and high latitudes (Craig, 1961; Dansgaard, 1964). It is modulated by evaporation at the soil surface and to a larger degree by evaporative and diffusion processes in leaves; the process is largely controlled by the vapor pressure deficit (Dongmann et al., 1972, Farquhar and Loyd, 1993, Cernusak et al., 2016). A further step of fractionation occurs as sugar molecules are transferred to the locations of growth (Roden et al., 2000). During the formation of organic compounds the biosynthetic fractionation leads to a positive shift of the $\delta^{18}O$ values by 27‰ relative to the leaf water (Sternberg, 2009). The oxygen isotope variation in tree-ring cellulose therefore reflects a mixed climate information, often dominated by a temperature, source water or sunshine duration modulated by the VPD influence.

Deleted: a

The cross-sections of relict wood and cores from living trees used for the TRW, MXD and CWT measurements were then selected for the isotope analyses. We analyzed four subsamples for each studied period according to the standards and criteria described in Loader et al. (2013). The first 50 yrs. of each sample were excluded to limit juvenile effects (McCarroll and Loader, 2004). After splitting annual rings with a scalpel, the whole wood samples were enclosed in filter bags. α-cellulose extraction was performed according to the method described by Boettger et al. (2007). For the analyses of $^{13}C/^{12}C$ and $^{18}O/^{16}O$ isotope ratios, 0.2-0.3 mg and 0.5-0.6 mg of cellulose were weighed for each annual ring, into tin and silver capsules, respectively. Carbon and oxygen isotopic ratios in cellulose were determined with an isotope ratio mass spectrometer (Delta-S, Finnigan MAT, Bremen, Germany) linked to two elemental analyzers (EA-1108, and EA-1110 Carlo Erba, Italy) via a variable open split interface (CONFLO-II, Finnigan MAT, Bremen, Germany). The $^{13}C/^{12}C$ ratio was determined separately by combustion under oxygen excess at a reactor temperature of 1020°C. Samples for $^{18}O/^{16}O$ ratio measurements were pyrolyzed to CO at 1080°C

(Saurer et al., 1998). The instrument was operated in the continuous flow mode for both, the C and O isotopes. The isotopic values were expressed in the delta notation multiplied by 1000 relative to the international standards (Eq. 1):

$$\delta \text{ sample} = R_{sample}/R_{standard}-1 \qquad \text{(Eq. 1)}$$

where R_{sample} is the molar fraction of $^{13}C/^{12}C$ or $^{18}O/^{16}O$ ratio of the sample and $R_{standard}$ the molar fraction of the standards, Vienna Pee Dee Belemnite (VPDB) for carbon and Vienna Standard Mean Ocean Water (VSMOW) for oxygen. The precision is $\sigma \pm 0.1$‰ for carbon and $\sigma \pm 0.2$‰ for oxygen. To remove the atmospheric $\delta^{13}C$ trend after CE 1800 from the carbon isotope values in tree rings (i.e. Suess effect, due to fossil fuel combustion) we used atmospheric $\delta^{13}C$ data from Francey et al. (1999), http://www.cmdl.noaa.gov./info/ftpdata.html). These corrected series were used for all statistical analyses. The $\delta^{18}O$ cellulose series were not detrended.

2.7. Climatic data

Meteorological series were obtained from local weather stations close to the study sites and used for the computation of correlation functions between tree-ring proxies and monthly climatic parameters (Table 2).

Deleted: Sunshine duration data were obtained from available Kosh-Agach meteorological station (http://aisori.meteo.ru/ClimateR).

2.8. Statistical analysis

All chronologies for each period were normalized to z-scores (Fig. 2). To assess post-volcanic climate variability, we used Superposed Epoch Analysis (SEA, Panofsky and Brier, 1958) with the five proxy chronologies available at each of the three study sites. In this study, intervals of 15 years before and 20 years after a volcanic eruption were analyzed. SEA is applied to the six annually dated volcanic eruptions (Table 1).

Deleted: experiment

Deleted: the

Deleted: 10

To test the sensitivity of the studied tree-ring parameters to climate, bootstrap correlation functions have been computed between proxy chronologies and monthly climate predictors using the 'bootRes' package of R software (R Core Team 2016) for the period 1950 (1966)-2000.

To estimate whether volcanic years can be considered as extreme, we computed Probability Density Functions (PDFs, Stirzaker, 2003) for each study site and for each tree-ring parameter over a period of 219 years for which measurements are available (Fig. S1). A year is considered (very) extreme, if the value of a given parameter is below the (5th) 10th percentile of the PDF.

3. Results

3.1. Anomalies in tree-ring proxy chronologies after stratospheric volcanic eruptions

Normalized TRW chronologies show negative deviations the year following the eruptions at all studied sites (Fig. 2). Regarding CWT, a strong decrease is observed in CE 537 at all study sites. Only two layers of cells were formed in CE 537 (-1.8σ) and 541 (-2.4σ) for YAK as compared to the 11-20 layers of cells formed on average during "normal" years. In addition, we also observe the formation of frost rings in ALT between CE 536 and 538, as well as in 1259. An abrupt CWT decrease is recorded in TAY in 537 (-3.1σ).

Furthermore, we revealed decreasing MXD values at ALT (-4.4 σ) in CE 537 and YAK (-2.8 σ) in CE 536. However, for TAY, data show a less pronounced pattern of MXD variation (Fig. 2). In this regard, the sharpest decrease was observed in the CWT chronologies from YAK in CE 540 (-1.9σ) and 541 (-2.4σ), whereas the response was smaller in TAY and ALT for the same years (Fig. 2). The ALT $\delta^{18}O$ chronology recorded a drastic decrease in 536 CE with (- 4.8 σ) (Fig. 2, Fig. S1). A $\delta^{18}O$ decrease for YAK was found after the CE 1257 Samalas in CE 1258 (-1.5 σ) and in 1259 (-2.9σ), which is opposite to the increased $\delta^{18}O$ value found in CE 1259 at ALT (Fig. 2; Fig. S1).

Regarding the carbon isotope ratio, negative anomalies are observed in ALT already in 1258 (-2.3σ). The CE 540 eruption was less clearly recorded in tree-ring proxies from TAY, compared to YAK and ALT (Fig. 2). With respect to the CE 1257 Samalas eruption (Fig. 2), the year following the eruption was recorded as very extreme in the TRW, MXD, $\delta^{18}O$, while less extreme in CWT

Deleted: 221

Deleted: We applied unpaired t-test statistics to check significance between each proxy and each site.

Deleted: 536

Deleted: at YAK and ALT

Deleted: 536

Deleted: for

Deleted: , we found less pronounced patterns of the MXD variation (Fig. 2).

Deleted: (-2.4σ) in CE 540

Deleted: compared to a smaller response in TAY and ALT

Deleted: YAK and TAY, and – to a lesser extent – in ALT. The CE 540 eruption was less clearly recorded in tree-ring proxies from TAY, compared to YAK and ALT (Fig. 2).

and $\delta^{13}C$ from YAK. ALT chronologies show a synchronous decrease for all proxies following two years after the eruption (Fig. 2, Fig. S1).

Deleted: see

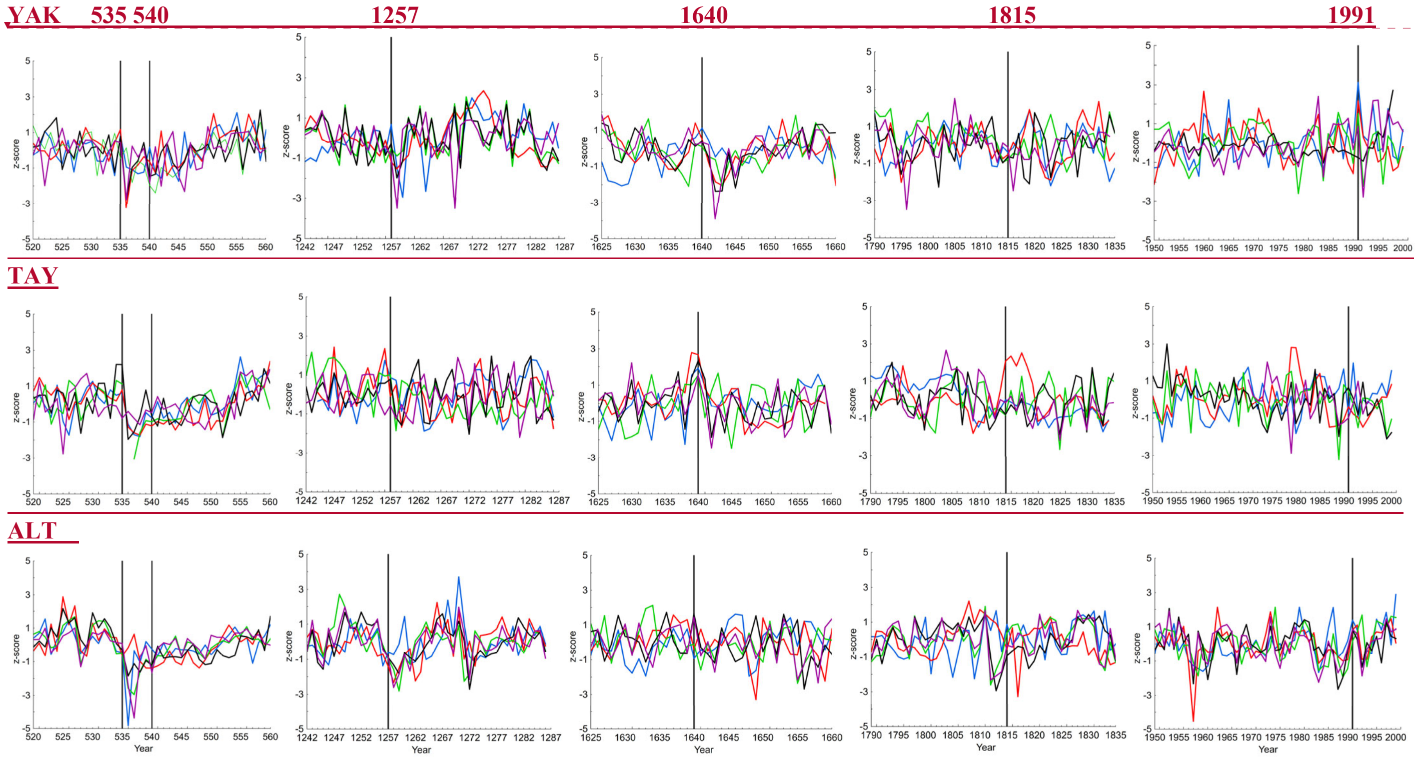

Fig. 2. Normalized (z-score) individual tree-ring index chronologies (TRW, **black**), maximum latewood density (MXD, **purple**), cell wall thickness (CWT, **green**), $\delta^{13}C$ (**red**) and $\delta^{18}O$ (**blue**) in tree-ring cellulose chronologies from northeastern Yakutia (YAK), eastern Taimyr (TAY) and

Deleted: YAK 535 540 1257 1640 1815 1991¶

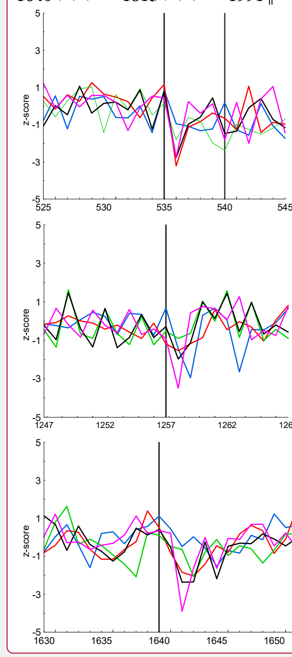

... [1]

Altai (ALT) for the specific periods CE 520-560, 1242-1286, 1625-1660, 1790-1835, 1950-2000 before and after the eruptions CE 535, 540, 1257, 1640, 1815 and 1991 are presented. Vertical lines show year of the eruptions.

The impacts of the more recent CE 1640 Parker, 1815 Tambora, and 1991 Pinatubo eruptions are, by contrast, far less obvious. In CE 1642, decreasing values are observed in all tree-ring proxies from the high-latitude sites YAK and TAY, whereas tree-ring proxies are not clearly affected at ALT (Fig. 2; Fig. S1).

Deleted: mainly for the TRW and MXD, less for $\delta^{13}C$ and $\delta^{18}O$)

Hardly any strong anomalies are observed in CE 1816 in Siberia regardless of the site and the tree-ring parameter analyzed. The ALT $\delta^{13}C$ value (-3.3σ) in CE 1817 and YAK MXD (-2.4σ) in 1816 can be seen as an exception to the rule here as they evidenced extreme values, respectively (Fig. S1).

Finally, the Pinatubo eruption is mainly captured by the MXD (-2.8σ) in CE 1992 and CWT (-2.2σ) chronologies from YAK. Simultaneous decreases of all tree-ring proxies from ALT are observed in 1993 (Fig. 2), which, however, cannot be classified as extreme (Fig. S1).

Deleted: mainly by MXD

Deleted: , S1

Overall, the SEA (Fig. 3) shows that volcanic eruptions centered around CE 535, 540, 1257, 1640, 1815, and 1991 have lead to decreasing values for all tree-ring proxies following next two years afterwards. A short-term response by two years after the eruptions is observed in the TRW and CWT proxies for TAY, while for YAK and ALT, the CWT decrease lasts longer (up to 5-6 years in ALT and YAK, respectively) (Fig. 3). The $\delta^{18}O$ isotope chronologies (z-score) show a distinct decrease the year after the eruptions. At ALT, however, the duration of negative anomalies were shorter (5 years) than at the high-latitude TAY (12 years) and YAK (9 years) sites. At the YAK site, two negative years followed the events, intermitted with one positive value, to remain negative again during the following 7 years. The duration of negative anomalies recorded in $\delta^{13}C$ values (z-score) lasts also longer at the high-latitude YAK site – (10 years) after the eruptions and 13 years at TAY compared to 7 years at ALT (Fig. 3).

Deleted: the high spatiotemporal variability and complexity of the response of the Siberian climate system to the largest volcanic events over past millennium (CE 535, 540, 1257, 1640, 1815 and 1991).

Deleted: A short-term response by two years after the eruptions is observed in the CWT proxies for TAY, while for YAK and ALT, the CWT decrease lasts longer (up to 5-6 years in ALT and YAK, respectively) (Fig. 3). The behavior of isotope chronologies is rather more complex, with a distinct decrease in $\delta^{13}C$ at the high-latitude sites (YAK, TAY), whereas $\delta^{18}O$ series are impacted mainly at the high-latitude YAK and high-altitude ALT sites. We find significant differences ($p=0.014$, $df=40$, $n=21$) between averaged $\delta^{13}C$ chronologies of the YAK and ALT sites. SEA for TRW and MXD show a more drastic decrease of values during the first year, mainly for TRW from YAK, and MXD from ALT when compared to other proxies and study sites (Fig. 3).¶

The largest decrease in the MXD values (in terms of z-score) is found at the high-latitude YAK site. The SEA for TRW, MXD, $\delta^{13}C$ and CWT from YAK as well as TRW and MXD from

ALT show a more drastic decrease of values during the first year when compared to other proxies and study sites (Fig. 3).

$\delta^{18}O$ YAK TAY ALT

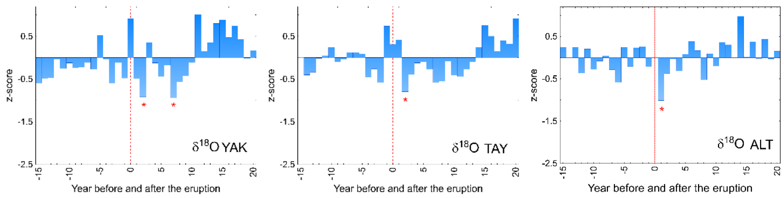

$\delta^{13}C$

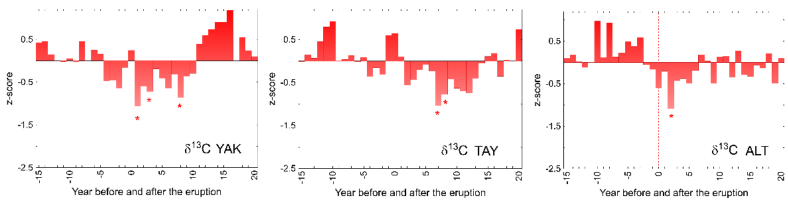

CWT

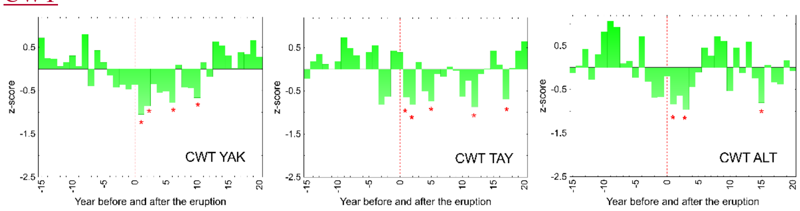

TRW

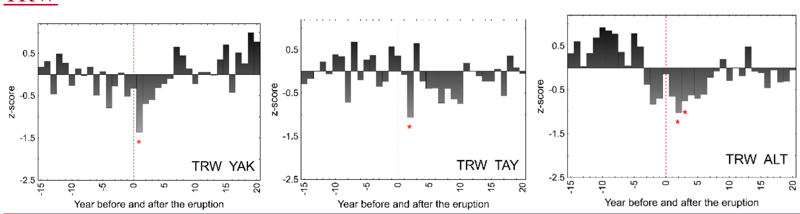

MXD

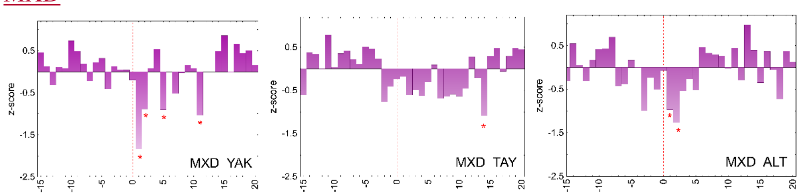

Fig. 3. Superposed epoch analysis (SEA) of $\delta^{18}O$, $\delta^{13}C$, CWT, TRW, and MXD chronologies for the Yakutia (YAK), Taimyr (TAY), and Altai (ALT) sites, summarizing negative anomalies 15 years before and 20 years after the volcanic eruptions in CE 535, 540, 1257, 1640, 1815, and 1991. Statistically negative anomalies are marked with a red star (*$p<0.05$).

3.2. Tree-ring proxies versus meteorological series

3.2.1. Monthly air temperatures and sunshine duration

Bootstrapped functions calculated for the instrumental period (1950-2000) show significant positive correlations ($p<0.05$) between TRW and MXD chronologies and mean summer (June-July) temperatures at all sites. Temperatures at the beginning (June) and the end of the growing season (mid-August) influenced the MXD chronology in ALT (r = 0.57) and YAK (r = 0.55), respectively (Fig. 4). July temperatures appear as a key factor for determining tree growth as they significantly impact CWT, $\delta^{13}C$, and $\delta^{18}O$ (with the exception of TAY for the latter) chronologies (r=0.28-0.60) at YAK and ALT.

Correlation analysis between July temperature and July sunshine duration showed significant correlation for YAK (r=0.56) and ALT (r=0.34). July sunshine duration are strongly and positively correlated with $\delta^{18}O$ in larch tree-ring cellulose chronologies from YAK (r=0.73) and ALT (r=0.51) for the period 1961-2000 (available sunshine duration data set).

Deleted: ¶
¶
¶
YAK TAY ALT ¶
$\delta^{18}O$ ¶

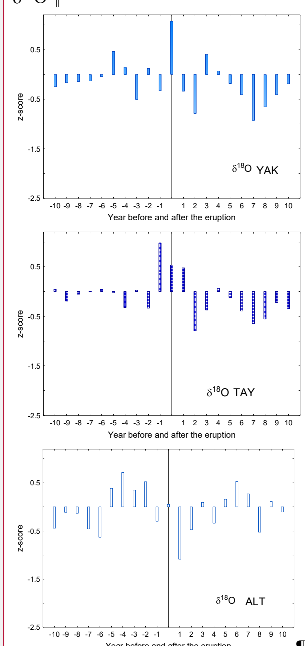

$\delta^{13}C$¶ ... [2]

Deleted: established

Deleted: evidence

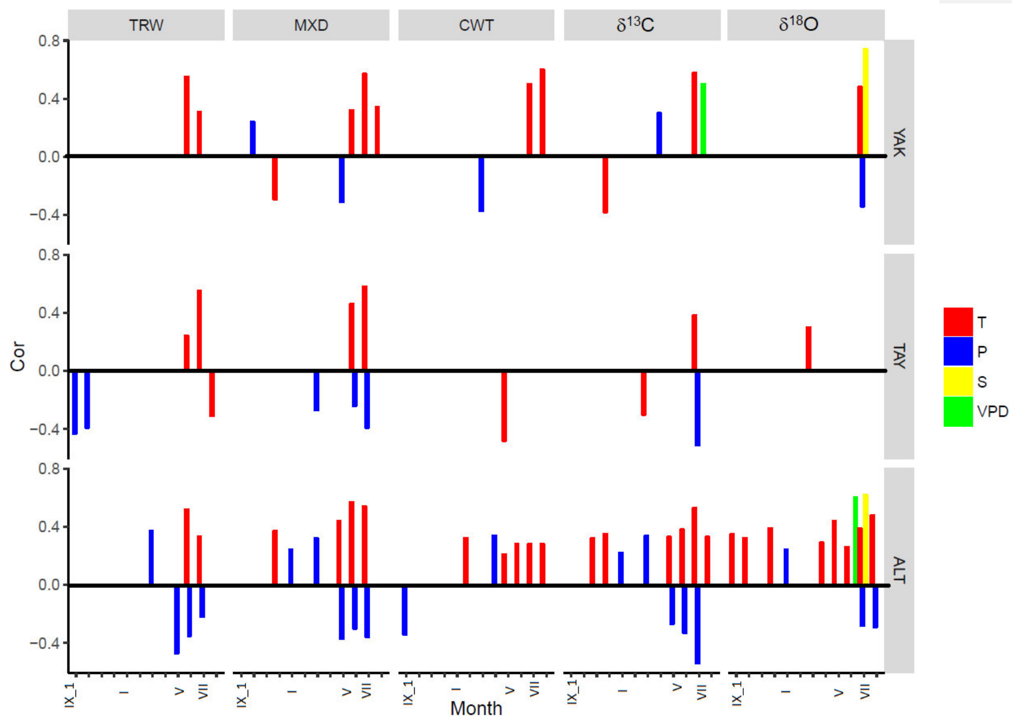

Fig. 4. Significant correlation coefficients between tree-ring parameters: TRW, MXD, CWT, $\delta^{13}C$ and $\delta^{18}O$ versus weather station data: temperature (T, red), precipitation (P, blue), vapor pressure deficit (VPD, green), and sunshine duration (S, yellow) from September of the previous year to August of the current year for three study sites were calculated. Table 2 lists stations and periods used in the analysis.

3.2.2. Monthly precipitation

The strongest July precipitation signal is observed at ALT (r=-0.54) and TAY (r=-0.51) with $\delta^{13}C$ chronologies ($p<0.05$). In addition, the ALT data shows a significant relationship ($p<0.05$) between March precipitation and TRW (r=0.37) and MXD (r=0.32), whereas April precipitation correlates positively with CWT (r=0.34), respectively. At YAK, July precipitation showed negative relationship with $\delta^{18}O$ in tree-ring cellulose (r=-0.34; $p<0.05$) only.

Deleted: Fig. 4. Significant correlation coefficients between tree-ring parameters: TRW, MXD, CWT, $\delta^{13}C$ and $\delta^{18}O$ versus weather station data: temperature (T, red), precipitation (P, blue), vapor pressure deficit (VPD, green), and sunshine duration (S, yellow) from September of the previous year to August of the current year for three study sites were calculated. Table 2 lists stations used in the analysis.¶

Deleted: at

Deleted: positive

Deleted: is observed

Deleted: ($p<0.05$)

Deleted: ,

Deleted: while

Deleted: is related

3.2.3. Vapor pressure deficit (VPD)

June VPD is significantly and positively correlated with the $\delta^{18}O$ chronology from ALT (r=0.67 $p<0.05$, respectively) for the period 1950-2000. The $\delta^{13}C$ in tree-ring cellulose from YAK correlate with July VPD only (r=0.69 $p<0.05$). We did not find a significant influence of VPD in TAY tree-ring and stable isotope parameters.

3.2.4. Synthesis of the climate data analysis

In summary, during the instrumental period of weather station observations (Table 2) summer temperature impacts TRW, MXD and CWT for the high-latitude sites (YAK, TAY), while summer precipitation affects stable carbon and oxygen isotopes (YAK, TAY, ALT), sunshine duration (YAK, ALT), and vapor pressure deficit (YAK, ALT).

Deleted: we found that

Deleted: mainly

Deleted: influenced

Deleted: were affected by summer precipitation

Deleted: signals

3.3. Response of Siberian larch trees to climatic changes after the major volcanic eruptions

Based on the statistical analysis above for the calibration period, we assumed that these relationships would not change over time and will provide information about climatic changes during the past volcanic periods (Fig. 5).

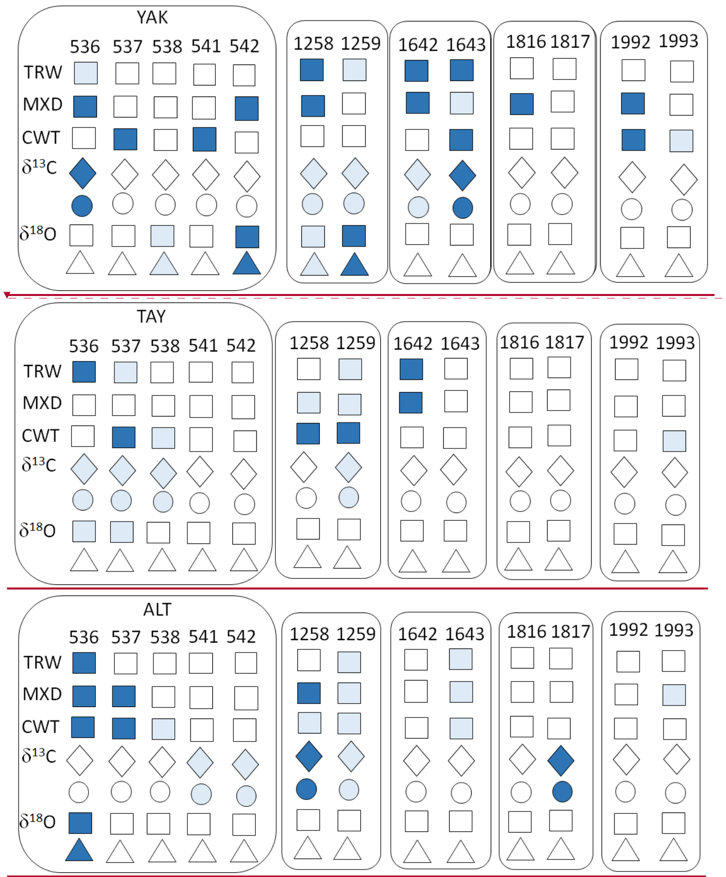

Fig. 5. Responses of larch trees from Yakutia (YAK), Taimyr (TAY) and Altai (ALT) to volcanic eruptions (Table 1). Squares, rhombs, circles, and triangles indicate the years following each eruption that can be considered as very extreme (negative values < 5th percentile of the PDFs, intensive color), extreme (negative values >5th, <10th percentile of the PDFs, light color) and non-extreme (>10th percentile of the PDFs, white color). July temperature changes are presented with squares. Summer vapor pressure deficit (VPD) variability is shown with circles. July precipitations are presented with rhombs, and July sunshine duration is shown as triangles.

Deleted:

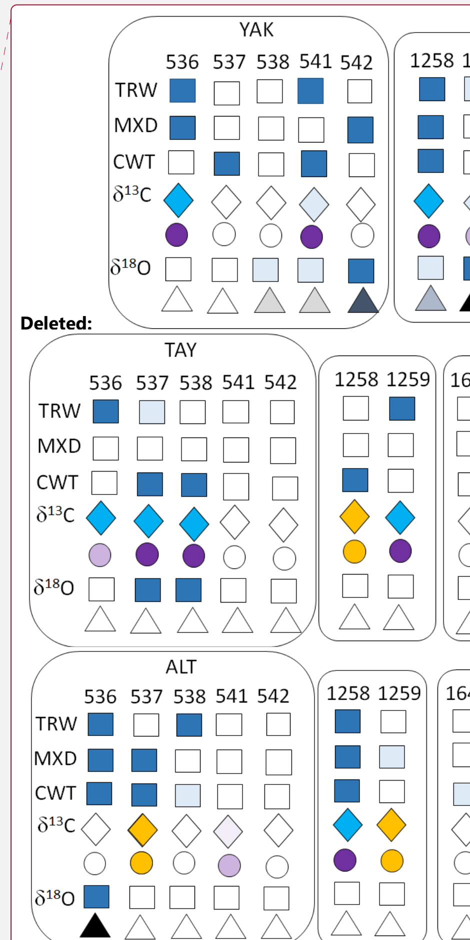

Fig. 5. Response of larch trees from Siberia to the CE volcanic eruptions (Table 1) with percentile of distribution considered as very extreme (< 5th, intensive color), extreme (>5th, <10th, light color) and non-extreme (>10th, white color). July temperature changes presented as a square from **heavy blue** (cold) to **light blue** (moderate). Summer vapor pressure deficit (VPD) variabilities are shown as a circle from **purple** (low), light purple (moderate decrease) to **orange** (increase, developing to dry air). July precipitation presented as a rhomb from **heavy turquoise** (wet), **light blue** (moderate) to **orange** (dry). Low July sunshine duration shown as black triangle, while high – as yellow.¶

3.3.1. Temperature proxies

We found strong negative summer air temperature anomalies at all sites after the CE 535 and 1257 volcanic eruptions. The temperature decrease was found in the TRW and CWT datasets at all sites, and also in the MXD datasets at YAK and ALT (Fig. 5). For the volcanic eruptions in later centuries, the evidence for a decrease in temperature was not as pronounced. Whereas no strong decline of summer temperature was found at ALT in CE 1642, we observe a slight decrease in TRW, MXD and CWT values in 1643. By contrast, a cold summer was recorded by most tree-ring parameters at YAK, except for $\delta^{18}O$. The absence of strong cooling is even more so striking during the years that followed the CE 1815 Tambora eruption: In CE 1816, only the MXD from YAK shows colder than normal conditions (Fig. 5). CE 1992 was recorded as a cold year in MXD and CWT from YAK, but again not at the other regions and by other proxies.

3.3.2. Moisture proxies: precipitation and VPD

Based on the climatological analysis with the local weather stations data (Table 2, Fig. 4) for all studied sites we considered $\delta^{13}C$ in tree-ring cellulose as a proxy for precipitation and vapor pressure deficit changes. Yet, CWT from ALT could be considered as a proxy with mixed temperature and precipitation signal (Fig. 4). Accordingly, the $\delta^{13}C$ values point to humid summers at YAK in 536, 1258, 1259, 1642 and 1643, at TAY in 536-538, and 1259, and at ALT the years of 541, 542, 1258, 1259 and 1817. Compared to other proxies and sites, the years of CE 536-538 were neither extremely humid nor dry at ALT (Fig. 5). No negative hydrological anomalies were recorded after the Tambora and Pinatubo eruptions at the high-latitude sites (YAK, TAY). However, positive anomalies were recorded in $\delta^{13}C$ values, pointing to dry conditions at TAY in CE 1817 (Fig. 2). A rather wet summer was reconstructed for the

Deleted: Namely

Deleted: ,

Deleted: drop

Deleted: in

Deleted: for

Deleted: nor 1643,

Deleted: an extreme cold in TAY for 1643 only, while still a cold summer in YAK for these two years based on the TRW chronology; 1816 was cold only in YAK (based on the CWT chronology), but not at the other sites. CE 1992 was recorded as a cold year in MXD and CWT from YAK, but again not for the other sites; CE 1993 was an extremely cold year for ALT based on CWT and $\delta^{18}O$, while also sunny, which is confirmed by local weather station data.

Deleted: chronologies

Deleted: proxies

Deleted: (VPD) changes

Deleted: , Fig. 5

Deleted: showed

Deleted: climate conditions

Deleted: for

Deleted: 541; for

Deleted: , 537,

Deleted: and in the year of

Deleted: for ALT.

Deleted: Opposite to other proxies and sites, the year of CE 537 in ALT was rather dry (Fig. 5). Dry conditions prevailed in CE 1258 in TAY, in CE 1259 in ALT, whereas wet anomalies were recorded in 1258 and 1259 in YAK. No anomalies were recorded for the CE 1642 event, irrespective of the sites. A rather wet summer was reconstructed for ALT in CE 1817 compared to 1816. CE 1992 in ALT was dry, which is consistent with weather station data (Fig. 5). Overall, there were mostly wet or humid anomalies at the high-latitude sites after the eruptions, but the response greatly varied between the different events.

high-altitude ALT site in CE 1817 compared to 1816 (Fig. 5). Overall, there were mostly humid anomalies after the eruptions at YAK site.

3.3.3. Sunshine duration proxies

Instrumental measurements of sunshine duration (Table 2) at YAK and ALT during the recent period showed a significant link with $\delta^{18}O$ cellulose. Based on this we conclude that sunshine duration decreased significantly after various eruptions at YAK (538, 542, 1258 and 1259) and in 536 at ALT site (Fig. 5).

Deleted: in

Deleted: in

Deleted: 541,

Deleted: in

Deleted: Conversely, summer 1993 in ALT was very sunny (Fig. 5).

4. Discussion

In this paper, we analyze climatic anomalies in years following selected large volcanic eruptions using long-term tree-ring multi-proxy chronologies for $\delta^{13}C$ and $\delta^{18}O$, TRW, MXD, CWT for the high-latitude (YAK, TAY) and high-altitude (ALT) sites. Since trees as living organisms respond to various climatic impacts, the carbon assimilation and growth patterns accordingly leave unique "finger prints" in the photosynthates, which is recorded in the wood of the tree rings specifically and individually for each proxy.

Deleted: ,

Deleted: of the CE

Deleted: ,

4.1. Evaluation of the applied proxies in Siberian tree-ring data

This study clearly shows that each proxy has to be analyzed and interpreted specifically for its validity on each studied site and evaluated for its suitability for the reconstruction of abrupt climatic changes.

The TRW in temperature-limited environments is an indirect proxy for summer temperature reconstructions, as growth is a temperature-controlled process. Temperature clearly determines the duration of the growing season and the rate of cell division (Cuny et al., 2014). Accordingly, low temperatures of growing season is recorded by narrow tree rings. The upper limit of temperature is species to tree species and biome. In most cases, tree growth is limited by drought rather than by high temperatures, since water shortage and VPD increase with increasing temperature. Still this does not make TRW a suitable proxy to determine the influence of water availability and air humidity, especially at the temperature-limited sites.

MXD chronologies obtained for the Eurasian subarctic record mainly a July-August temperature signal (Vaganov et al., 1999; Sidorova et al., 2010; Büntgen et al., 2016) and add valuable information about climate conditions toward the end of the growth season. Similarly, CWT is an anatomical parameter, which contains information on carbon sink limitation of the cambium due to extreme cold conditions (Panyushkina et al., 2003; Fonti et al., 2013; Bryukhanova et al., 2015). There is a strong signal of low cell number within a growing season, for example, strong decreasing CWT in CE 537 at YAK or the formation of frost rings at ALT in (CE 536-538, and 1259) has been shown in our study.

Low $\delta^{13}C$ values can be explained by a reduction in photosynthesis caused by volcanic dust veils. For the distinction whether $\delta^{13}C$ is predominantly determined by A_N or g_l the combined evaluation with $\delta^{18}O$ or TRW is needed. High $\delta^{18}O$ values indicate high VPD, which induces a reduction in stomatal conductance, reducing the back diffusion of depleted water molecules from the ambient air. This confirms a sunny year CE 1993 at ALT with mild weather conditions according to the observational data from the closest weather station (Table 2). Interestingly, we also find less negative values for $\delta^{13}C$ in the same period. This shows that the two isotopes correlate with each other and indicates the need for a combined evaluation of the C and O isotopes (Scheidegger et al., 2000) taking into account precautions as suggested by Roden and Siegwolf (2012).

4.2. Lag between volcanic events and response in tree rings

Deleted: temperatures are

Deleted: reflected

Deleted: in

Deleted: limit

Deleted: specific

Deleted: The clear signal about reduced number of cells within a season, for example, strong decreasing CWT in CE 536 at YAK or formation of frost rings in ALT (CE 536-538, 1259) has been shown in our study.¶

Deleted: in

Deleted: warm and dry

Most discussed events suggest a lag between the eruption and the tree ring response for one year or more (Fig. 3). This lag is explained by the tree's use of stored carbohydrates, which are the substrate for needle and early wood production. These stored carbohydrates carry the isotopic signal of previous years and depending on their remobilization, as such the signal may be masked in freshly produced biomass. The delayed signal could also reflect the time needed for the dust veil to be transported to the study regions.

Deleted: In m

Deleted: of the

Deleted: , we observe a certain delay – or

Deleted: –

Deleted: in tree rings

Deleted: of

Deleted: and use

Deleted: the signals

Deleted: sites

4.3. Temperature and sunshine duration changes after stratospheric volcanic eruptions

Correlation functions show that MXD and CWT (with the exception of TAY in the latter case), and to a lesser extent TRW chronologies, portray the strongest signals for summer (June-August) temperatures. In addition, significant information about sunshine duration can be derived from the YAK and ALT $\delta^{18}O$ series. Thus, we hypothesize that extremely narrow TRW and very negative anomalies observed in the MXD and CWT chronologies of YAK and to a lesser extent at ALT along with low $\delta^{18}O$ values reflect cold and low sunshine duration conditions in summer. Presumably, the temperatures were below the threshold values for growth over much of the growing season (Körner, 2015). This hypothesis of a generalized regional cooling after both eruptions is further confirmed by the occurrence of frost rings at ALT site in CE 538, 1259 (Myglan et al., 2008; Guillet et al., 2017), as well as in neighboring Mongolia (D'Arrigo et al., 2001). The unusual cooling in CE 536-542 is also evidenced by a very small number of cells formed at YAK (Churakova (Sidorova) et al., 2014). Although $\delta^{18}O$ is an indirect proxy for needle temperature, low $\delta^{18}O$ values in CE 538, 542 1258, and 1259 for YAK and in CE 536 at ALT are a result of low irradiation, leading to low temperature and low VPD (high stomatal conductance), both likely a result from volcanic dust veils.

Deleted: also

Deleted: ,

Deleted: in CE 536 and 1258

Deleted: (except for ALT in CE 1257)

Deleted: 536

Deleted: and

Similarly, in the aftermath of the Samalas eruption, the persistence of summer cooling is limited to CE 1259 only at the three study sites, which is in line with findings of Guillet et al., (2017).

Interestingly, a slight decrease in oxygen isotope chronologies, which can be related to low levels of summer sunshine duration (i.e. low leaf temperatures), allows for hypothesizing that cool conditions could have prevailed.

Deleted: –

Deleted: –

For all later high-magnitude CE eruptions, temperature-sensitive tree-ring proxies do not evidence a generalized drop in summer temperatures. Paradoxically, the impacts of the Tambora eruption, known for its triggering of a widespread "year without summer" (Harrington, 1992), did only induce abnormal MXD at YAK in 1816, but no anomalies are observed at sites TAY and ALT, except for the positive deviation of $\delta^{13}C$ in TAY and the negative anomaly at ALT in CE 1817 (Fig. 2; Fig. 5; Fig. S1). While these findings may seem surprising, they are in line with the TRW and MXD reconstructions of Briffa et al., (1998) or Guillet et al., (2017), who found limited impacts of the CE 1815 Tambora event in Eastern Siberia and Alaska using TRW and MXD data only. The inclusion of CWT chronologies by Barinov et al., (2018) confirms the absence of a significant cooling signal after the second largest eruption of the last millennium (CE 1815) in larch trees of the Altai-Sayan mountain region.

Deleted: for

Deleted: ALT

Deleted: The inclusion of CWT chronologies, not used in their reconstructions, further confirm the absence of a significant cooling in this region following the second largest eruption of the last millennium.

Finally, in CE 1992, our results evidence cold conditions in YAK, which is consistent with weather observations showing that the below-average anomalies in summer temperatures (after Pinatubo eruption) were indeed limited to Northeastern Siberia (Robock, 2000). As both isotopes indicate a reduction in stomatal conductance, we found that warm (in agreement with MXD and CWT) and dry conditions were prevalent for ALT at this time. This isotopic constellation was confirmed by the positive relationships between VPD and $\delta^{18}O$ and $\delta^{13}C$ for ALT.

However, temperature and sunshine duration are not always highly coherent over time due to the influence of other factors, like Arctic Oscillations as suggested for Fennoscandia regions by Loader et al. (2013).

Deleted: it was

4.4. Moisture changes

Water availability is a key parameter for Siberian trees as they are growing under extremely continental conditions with hot summers and cold winters, and even more so with very low annual precipitation (Table 2). Permafrost plays a crucial role and can be considered as a buffer for additional water sources during hot summers (Sugimoto et al., 2002; Boike et al., 2013; Saurer et al., 2016). Yet, thawed permafrost water is not always available for roots due to the surficial structure of the root plate or extremely cold water temperature (close to 0ºC), which can hardly be utilized by trees (Churakova (Sidorova) et al., 2016). Thus, Siberian trees are highly susceptible to drought, induced by dry and warm air during July and therefore the stable carbon isotopes can be sensitive indicators of such conditions. After volcanic eruptions, however, low light intensity due to dust veils induce low temperatures and reduced VPD, the driver for evapotranspiration. Under such conditions drought stress is unlikely to occur. However, the transition phases with changes from cool and moist to warm and dry conditions are more critical when drought is more likely to occur.

In our study, higher $\delta^{13}C$ values in tree-ring cellulose indicate increasing drought conditions as a consequence of reduced precipitation for two years after the CE 1815 volcanic eruption at TAY site. No further extreme hydro-climatic anomalies occurred at Siberian sites in the aftermath of the Pinatubo eruption.

4.5. Synthetized interpretation from the multi-parameter tree-ring proxies

Our analysis demonstrates the added value of a tree-ring derived multi-proxy approach to better capture the climatic variability after large volcanic eruptions. Besides the well-documented effects of temperature derived from TRW and MXD, CWT, stable carbon and oxygen isotopes in tree-ring cellulose provide important and complementary information about moisture and sunshine duration changes (an indirect proxy for leaf temperature effective for air-to-leaf VPD) after stratospheric volcanic eruptions.

Deleted: Continuous p
Deleted: ,
Deleted: in addition, is
Deleted: ing
Deleted:
Deleted: ,
Deleted: 1257
Deleted: all three
Deleted: s

Our results reveal a complex behavior of the Siberian climatic system to the stratospheric volcanic eruptions of the Common Era. The CE 535 and CE 1257 Samalas eruptions caused substantial cooling – very likely induced by dust veils (Churakova (Sidorova) et al., 2014; Guillet et al., 2017; Helama et al., 2018) – as well as humid conditions at the high-latitude sites. Conversely, only local climate responses were observed after the CE 1641 Parker, 1815 Tambora, and 1991 Pinatubo eruptions. Similar site-dependent impacts referred to the coldest summers of the last millennium in the Northern Hemisphere based on TRW and MXD reconstructions (Schneider et al., 2015; Stoffel et al., 2015; Wilson et al., 2016; Guillet et al., 2017). This absence of widespread and intense cooling or reduction of precipitation over vast regions of Siberia may result from the location and strength of the volcanic eruption, atmospheric transmissivity as well as from the modulation of radiative forcing effects by regional climate variability. These results are consistent with other regional studies, which interpreted the spatial-temporal heterogeneity of tree responses to past volcanic events (Wiles et al., 2014; Esper et al., 2017; Barinov et al., 2018) in terms of regional climate peculiarities.

5. Conclusions

In this study, we demonstrate that the consequences of large volcanic eruptions on climate are rather complex between sites and among events. The different locations and magnitudes of eruptions, but also regional climate variability, may certainly explain some of this heterogeneity. We show that each tree-ring and isotope proxy alone cannot provide the full information of the volcanic impact on climate but that they, when combined, contribute to the formation of the full picture by adding to a single, specific factor, which is critical for a comprehensive description of climate dynamics induced by volcanism and the inclusion of these phenomena in global climate models.

Deleted: In detail, o

Deleted: Similar site-dependent impacts were found in CE 1453, 1458 and 1601 (Fig. S1), frequently referred to as the coldest summers of the last millennium in the Northern Hemisphere based on TRW and MXD reconstructions (Schneider et al., 2015; Stoffel et al., 2015; Wilson et al., 2016; Guillet et al., 2017).

Deleted: spatio

Deleted: it

Deleted: s

The analyses with a larger number of samples in the investigations of Siberian and other Northern Hemispheric sites will indeed provide higher certainty in terms of data interpretation of climatic dynamics of these boreal regions. However, the multi-proxy approach as applied in our study provides a strong set of complementary information to the research field, as it allows the refinement of the interpretations and thus improves our understanding of the heterogeneity of climatic signals after CE stratospheric volcanic eruptions, as recorded in multiple tree-ring and stable isotope parameters.

Deleted: T

Author contribution: TRW analysis was performed at V.N. Sukachev Institute of Forest SB RAS by O.V. Churakova (Sidorova), D.V. Ovchinnikov, V.S. Myglan and O.V. Naumova. CWT analysis was carried out at the V. N. Sukachev Institute of Forest SB RAS, Krasnoyarsk, Russia by M. Fonti and at the University of Arizona by I. Panyushkina. Stable isotope analysis was conducted at the Paul Scherrer Institute (PSI), by O. V. Churakova (Sidorova), M. Saurer, and R. Siegwolf. MXD measurements were realized with a DENDRO Walesh 2003 densitometer at WSL and at the V.N. Sukachev Institute of Forest SB RAS, Krasnoyarsk, Russia by O. V. Churakova (Sidorova) and A. V. Kirdyanov. Samples from YAK and TAY were collected by M. M. Naurzbaev. All authors contributed significantly to the data analysis and paper writing.

Acknowledgements: This work was supported by Marie Curie International Incoming Fellowship [EU_ISOTREC 235122], Re-Integration Marie Curie Fellowship [909122] and UFZ scholarship [2006], RFBR [09-05-98015_r_sibir_a] granted to Olga V. Churakova (Sidorova); SNSF M. Saurer [200021_121838/1]; Era.Net RUSPlus project granted to M. Stoffel [SNF IZRPZ0_164735] and RFBR [№ 16-55-76012 Era_a] granted to E.A. Vaganov; project granted to Vladimir S. Myglan RNF, Russian Scientific Fond [№ 15-14-30011]; Alexander V. Kirdyanov was supported by the Ministry of Education and Science of the Russian Federation [#5.3508.2017/4.6] and RSF [#14-14-00295]; Scientific School [3297.2014.4] granted to Eugene A. Vaganov; and US National Science Foundation (NSF) grants [#9413327, #970966, #0308525] to Malcolm K. Hughes and US CRDF grant # RC1-279, to Malcolm K. Hughes and Eugene A. Vaganov. We thank Tatjana Boettger for her support and access to the stable isotope facilities within UFZ Haale/Saale scholarship 2006; Anne Verstege, Daniel Nievergelt for their help with sample preparation for the MXD and Paolo Cherubini for providing lab access at the Swiss Federal Institute for Forest, Snow and Landscape Research (WSL).

We thank two anonymous reviewers and handling Editor Juerg Luterbacher for their constructive comments on this manuscript.

Figure legend

Fig. 1. Location of the study sites (stars) and known volcanos from the tropics (black dots) considered in this study (a). Annual tree-ring width index (light lines) and smoothed by 51-year Hamming window (bold lines) from the northeastern Yakutia (YAK - **blue**, b) (Hughes et al., 1999; Sidorova and Naurzbaev 2002; Sidorova 2003), eastern Taimyr (TAY - **green**, c) (Naurzbaev et al., 2002), and Russian Altai (ALT - **red**, d) (Myglan et al., 2009). Photos show the larch stnads at YAK, TAY (M.M. Naurzbaev) and ALT (V.S. Myglan) sites.

Fig. 2. Normalized (z-score) individual tree-ring index chronologies (TRW, **black**), maximum latewood density (MXD, **purple**), cell wall thickness (CWT, **green**), $\delta^{13}C$ (**red**) and $\delta^{18}O$ (**blue**) in tree-ring cellulose chronologies from northeastern Yakutia (YAK), eastern Taimyr (TAY) and Altai (ALT) for the specific periods 520-560, 1242-1286, 1625-1660, 1790-1835, 1950-2000 before and after the eruptions CE 535, 540, 1257, 1640, 1815 and 1991 are presented. Vertical lines show year of the eruptions.

Fig. 3. Superposed epoch analysis (SEA) of $\delta^{18}O$, $\delta^{13}C$, CWT, TRW, and MXD chronologies for the Yakutia (YAK), Taimyr (TAY), and Altai (ALT) sites, summarizing negative anomalies 15 years before and 20 years after the volcanic eruptions in CE 535, 540, 1257, 1640, 1815, and 1991. Statistically negative anomalies are marked with a red star (**p<0.05*).

Fig. 4. Significant correlation coefficients between tree-ring parameters: TRW, MXD, CWT, $\delta^{13}C$ and $\delta^{18}O$ versus weather station data: temperature (T, red), precipitation (P, blue), vapor pressure deficit (VPD, green), and sunshine duration (S, yellow) from September of the previous year to August of the current year for three study sites were calculated. Table 2 lists stations and periods used in the analysis.

Deleted: Map with the locations of the study sites (stars) and volcanic eruptions (black dots) considered in this study (a). Annual tree-ring width index (light lines) and smoothed by 51-year Hamming window (bold lines) chronologies from northeastern Yakutia (YAK - **blue**, b) (Hughes *et al.,* 1999; Sidorova 2003), eastern Taimyr (TAY - **green**, c) (Naurzbaev *et al.,* 2002), and Russian Altai (ALT - **red**, d) (Myglan *et al.,* 2009) were constructed based on larch trees (Photos: V. Myglan – ALT, M. M. Naurzbaev – YAK, TAY). ¶
¶
Fig. 2.

Deleted: Normalized (z-score) individual tree-ring index chronologies (TRWi, **black**), maximum latewood density (MXD, **purple**), cell wall thickness (CWT, **green**), $\delta^{13}C$ (**red**) and $\delta^{18}O$ (**blue**) in tree-ring cellulose chronologies from YAK, TAY and ALT for the specific periods 10 years before and after the eruptions CE 535, 1257, 1640, 1815 and 1991 are presented. Vertical lines showed year of the eruptions.

Deleted: Superposed epoch analysis of $\delta^{18}O$, $\delta^{13}C$, CWT, TRW and MXD chronologies for the Yakutia (YAK), Taimyr (TAY), and Altai (ALT) sites, summarizing anomalies of the volcanic eruptions in CE 535, 540, 1257, 1640, 1815, and 1991.

Fig. 5. Responses of larch trees from Yakutia (YAK), Taimyr (TAY) and Altai (ALT) to volcanic eruptions (Table 1). Squares, rhombs, circles, and triangles indicate the years following each eruption that can be considered as very extreme (negative values < 5th percentile of the PDFs, intensive color), extreme (negative values >5th, <10th percentile of the PDFs, light color) and non-extreme (>10th percentile of the PDFs, white color). July temperature changes are presented with squares. Summer vapor pressure deficit (VPD) variability is shown with circles. July precipitations are presented with rhombs, and July sunshine duration is shown as triangles.

Table 1. List of stratospheric volcanic eruptions used in the study.

Table 2. Tree-ring sites in northeastern Yakutia (YAK), eastern Taimyr (TAY), and Altai (ALT) and weather stations used in the study. Monthly air temperature (T, °C), precipitation (P, mm), sunshine duration (S, h/month) and vapor pressure deficit (VPD, kPa) data were downloaded from the meteorological database: http://aisori.meteo.ru/ClimateR.

Fig. S1. Probability density function (Pdf) computed for each of the tree-ring parameter for northeastern Yakutia (YAK), eastern Taimyr (TAY) and Russian Altai (ALT). Tree-ring parameters (TRWi - black, MXD – purple, CWT – green, δ^{18}O - blue and δ^{13}C - red) in bold lines represent the probability density function. Dotted lines represent the anomalies (z-score) observed for the first and second years following the 535, 540, 1257, 1640, 1815 and 1991 volcanic eruptions for each tree-ring parameter.

Deleted: Response of larch trees from Siberia to the CE volcanic eruptions (Table 1) with percentile of distribution considered as very extreme (< 5th, intensive color), extreme (>5th, <10th, light color) and non-extreme (>10th, white color). July temperature changes presented as a square from **heavy blue** (cold) to **light blue** (moderate). Summer vapor pressure deficit (VPD) variabilities are shown as a circle from **purple** (low), light purple (moderate decrease) to **orange** (increase, developing to dry air). July precipitation presented as a rhomb from **heavy turquoise** (wet), **light blue** (moderate) to **orange** (dry). Low July sunshine duration shown as black triangle, while high – as yellow.¶

Deleted: List of stratospheric volcanic eruptions used in the study.

Deleted: Summary of tree-ring sites in northeastern Yakutia (YAK), eastern Taimyr (TAY) and Altai (ALT), and weather stations used in the study. Monthly air temperature (T, °C), precipitation (P, mm), sunshine duration (S, h/month) and vapor pressure deficit (VPD, kPa) data were used from available meteorological database http://aisori.meteo.ru/ClimateR.

References

Abaimov, A.P., Bondarev, A.I., Yzrzanova, O.V., Shitova, S.A.: Polar forests of Krasnoyarsk region. Nauka Press, Novosibirsk. 208 p, 1997.

Battipaglia, G., Cherubini, P., Saurer, M., Siegwolf, R.T.W., Strumia, S., Cotrufo, M.F.: Volcanic explosive eruptions of the Vesuvio decrease tree-ring growth but not photosynthetic rates in the surrounding forests. Global Change Biology. 13, 1-16, 2007.

Barinov, V.V., Myglan, V.S., Taynik, A.V., Ojdupaa, O.Ch., Agatova, A.R., Churakova (Sidorova) O.V. Extreme climatic events in Altai-Sayan region as indicator of major volcanic eruptions. Geophysical processes and biosphere. 17, 45-61, 2018. doi: 10.21455/GPB2018.3-3.

Boettger T., Haupt, M., Knöller, K., Weise, S., Waterhouse, G.S. … Schleser, G.H.: Wood cellulose preparation methods and mass spectrometric analyses of $\delta^{13}C$, $\delta^{18}O$, and non ex-changeable $\delta^{2}H$ values in cellulose, sugar, and starch: An inter-laboratory comparison, Anal. Chem. 79, 4603–4612, doi:10.1021/ac0700023, 2007.

Deleted: Beerling, D.J., Woodward, F.I.: Ecophysiological responses of plants to global environmental change since the last glacial maximum. New Phytologist. 125, 641–648, 1994.¶

Boike, J., Kattenstroth, B., Abramova, K., Bornemann, N., Cherverova, A., Fedorova, I., Fröb, K., Grigoriev, M., Grüber, M., Kutzbach, L., Langer, M., Minke, M., Muster, S., Piel, K., Pfeiffer, E.-M., Stoff, G., Westermann, S., Wischnewski, K., Wille, C., Hubberten, H.-W.: Baseline characteristics of climate, permafrost and land cover from a new permafrost observatory in the Lena Rive Delta, Siberia (1998-2011). Biogeosciences. 10, 2105-2128, 2013.

Briffa, K.R., Jones, P.D., Schweingruber, F.H., Osborn, T.J.: Influence of volcanic eruptions on Northern Hemisphere summer temperature over the past 600 years. Nature. 393, 450–455, 1998.

Bryukhanova, M.V., Fonti, P., Kirdyanov, A.V., Siegwolf, R., Saurer, M., Pochebyt, N.P., Churakova (Sidorova), O.V., Prokushkin, A.S.: The response of $\delta^{13}C$, $\delta^{18}O$ and cell anatomy of *Larix gmelinii* tree rings to differing soil active layer depths. Dendrochronologia. 34, 51-59, 2015.

Büntgen, U., Myglan, V.S., Ljungqvist, F.C., McCormick, M., Di Cosmo, N., Sigl M., ….Kirdyanov, A.V.: Cooling and societal change during the Late Antique Little Ice Age from 536 to around 660 AD. Nature Geoscience. 9, 231-236, 2016.

Castagneri, D., Fonti, P., von Arx, G., Carrer, M.: How does climate influence xylem morphogenesis over the growing season? Insights from long-term intra-ring anatomy in *Picea abies*. Annals of Botany 19:1011-1020, doi:10.1093/aob/mcw274, 2017.

Cernusak, L., Ubierna, N., Winter, K., Holtum, J.A.M., Marshall, J.D., Farquhar, G.D.: Environmental and physiological determinants of carbon isotope discrimination in terrestrial Plants. Transley Review New Phytologist. 200, 950-965, 2013.

Cernusak, L., Barbour, M., Arndt, S., Cheesman, A., English, N., Field, T., Helliker, B., Holloway-Phillips, M., Holtum, J., Kahmen, A., Mcnerney F, Munksgaard N, Simonin K, Song X, Stuart-Williams H, West J and Farquhar G.: Stable isotopes in leaf water of terrestrial plants. Plant, Cell & Environment. 39 (5), 1087-1102, 2016.

Churakova (Sidorova), O.V., Bryukhanova, M., Saurer, M., Boettger, T., Naurzbaev, M., Myglan, V.S., Vaganov, E.A., Hughes, M.K., Siegwolf, R.T.W.: A cluster of stratospheric volcanic eruptions in the AD 530s recorded in Siberian tree rings. Global and Planetary Change. 122, 140-150., 2014.

Churakova (Sidorova), O.V., Shashkin, A.V., Siegwolf, R., Spahni, R., Launois, T., Saurer M., Bryukhanova, M.V., Benkova, A.V., Kupzova, A.V., Vaganov, E.A., Peylin, P., Masson-Delmotte, V., Roden, J.: Application of eco-physiological models to the climatic interpretation of $\delta^{13}C$ and $\delta^{18}O$ measured in Siberian larch tree-rings. Dendrochronologa, doi:10.1016/j.dendro.2015.12.008, 2016.

Cook, E., Briffa, K., Shiyatov, S., Mazepa, V.: Tree-ring standardization and growth trend estimation. In: Methods of dendrochronology: applications in the environmental sciences, Eds: Cook, E.R., Kairiukstis, L.A. 104-123, 1990.

Cook, E.R., Krusic, P.J.: A Tree-Ring Standardization Program Based on Detrending and Autoregressive Time Series Modeling, with Interactive Graphics (ARSTAN). (Ed. by E.R., Cook and P.J., Krusic), 2008.

Craig, H.: Isotopic variations in meteoric waters. Science. 133, 1702– 1703, 1961.

Crowley, T.J., Unterman, M.B.: Technical details concerning development of a 1200 yr. proxy index for global volcanism. Earth Syst. Sci. Data. 5, 187-197, 2013.

Cuny, H.E., Rathgeber, C.B.K., Frank, D., Fonti, P., Fournier, M.: Kinetics of tracheid development explain conifer tree-ring structure. New Phytologist, 203, 1231–1241, 2014.

D'Arrigo, R.D., Jacoby, G.C., Frank, D., Pederson, N.D., Cook, E., Buckly, B.M., Nachin, B., Mijidorj, R., Dugarjav, C.: 1738-years of Mongolian temperature variability inferred from a tree-ring width chronology of Siberian pine. Geophisycal Research Letters. Vol. 28 (3), 543-546, 2001.

Dansgaard, W.: Stable isotopes in precipitation. Tellus. 16, 436–468, 1964.

Dawson, T.E., Mambelli, S., Plamboeck, A.H., Templer, P.H., Tu, K.P.: Stable isotopes in plant ecology Ann. Review of Ecology and Systematics. 33, 507-559, 2004.

Dongmann, G., Förstel, H., Wagener, K.: ^{18}O-rich oxygen from land photosynthesis. Nature New Biol. 240, 127–128, 1972.

Eschbach, W., Nogler, P., Schär, E., Schweingruber, F.H.: Technical advances in the radiodensitometrical determination of wood density. Dendrochronologia. 13, 155–168, 2015.

Esper, J., St. George, S., Anchukaitis, K., D'Arrigo, R., Ljungqvist, F., Luterbacher, J., Schneider, L., Stoffel, M., Wilson, R., Büntgen, U.: Large-scale, millennial-length temperature reconstructions from tree-rings. Dendrochronologia. 50, 81–90, 2018.

Esper, J., Büntgen, U., Hartl-Meier, C., Oppenheimer, C., Schneider, L.: Northern Hemisphere temperature anomalies during 1450s period of ambiguous volcanic forcing. Bull. Volcanology. 79, 41, 2017.

Farquhar, G. D.: Eds. Stable Isotopes and Plant Carbon-Water Relations. Academic Press, San Diego. 47–70, 1982.

Farquhar, G.D., Ehleringer, J.R., Hubick, K.T.: Annu. Rev. Plant Physiol. Plant Mol. Biol. 40, 503 p, 1989.

Farquhar, G.D., Lloyd, J.: Carbon and oxygen isotope effects in the exchange of carbon dioxide between terrestrial plants and the atmosphere. In: Ehleringer, J.R., Hall, A.E., Farquhar, G.D. (Eds) Stable Isotopes and Plant Carbon-Water Relations. Academic Press, San Diego, 47–70, 1993.

Fonti, P., Bryukhanova, M.V., Myglan, V.S., Kirdyanov, A.V., Naumova, O.V., Vaganov, E.A.: Temperature-induced responses of xylem structure of *Larix sibirica* (Pinaceae) from Russian Altay. American Journal of Botany. 100 (7), 1-12, 2013.

Francey, R.J., Allison, C.E., Etheridge D.M., Trudinger, C.M., Langenfelds, R.L., Michel, E., Steele, L.P.: A 1000-year high precision record of $\delta^{13}C$ in atmospheric CO_2. Tellus. Ser. B (51), 170-193, 1999.

Fritts, H.C.: Tree-rings and climate. London. New York; San Francisco: Acad. Press. 567 p, 1976.

Furst, G.G.: Methods of Anatomical and Histochemical Research of Plant Tissue. Nauka, Moscow. 156 p, 1979.

Gao, C., Robock, A., Ammann, C.: Volcanic forcing of climate over the past 1500 years: An improved ice core-based index for climate models. J. Geophys. Res. Atmos. 113:D23111. doi:10.1029/2008jd010239, 2008.

Gennaretti, F., Huard, D., Naulier, M., Savard, M., Bégin, C., Arseneault, D., Guiot, J.: Bayesian multiproxy temperature reconstruction with black spruce ring widths and stable isotopes from the northern Quebec taiga. Clym. Dyn. doi: 10.1007/s00382-017-3565-5, 2017.

Gillett, N.P., Weaver, A.J., Zwiers, F.W. Wehner, M.F.: Detection of volcanic influence on global precipitation. Geophysical Research Letters, 31 (12), doi:10.1029/2004GL020044 R, 2004.

Groisman, P.Ya.: Possible regional climate consequences of the Pinatubo eruption. Geophys. Res. Lett., 19, 1603–1606, 1992.

Gu, L., Baldocchi, D.D., Wofsy, S.C., Munger, J.W., Michalsky, J.J., Urbanski, S.P., Boden, T.A.: Response of a deciduous forest to the Mount Pinatubo eruption: Enhanced photosynthesis, Science. 299 (5615), 2035–2038, 2003.

Guillet, S., Corona, C., Stoffel, M., Khodri M,, Lavigne F., Ortega, P.,….Oppenheimer, C.: Climate response to the 1257 Samalas eruption revealed by proxy records. Nature geoscience, doi:10.1038/ngeo2875, 2017.

Hansen, J., Sato, M., Ruedy, R., Lacis, A., Asamoah, K., Borenstein S,, ….Wilson, H.: A Pinatubo climate modeling investigation. In The Mount Pinatubo Eruption: Effects on the Atmosphere and Climate, NATO ASI Series Vol. I 42. G. Fiocco, D. Fua, and G. Visconti, Eds. Springer-Verlag, 233-272, 1996.

Harrington, C.R.: The Year without a summer? World climate in 1816. Ottawa: Canadian Museum of Nature, ISBN 0660130637, 1992.

Helama, S., Arppe, L., Uusitalo, J., Holopainen, J., Mäkelä, H.M., Mäkinen, H., Mielikäinen, K., Nöjd, P., Sutinen, R., Taavitsainen, J.-P., Timonen, M., Oinonen, M.: Volcanic dust veils from sixth century tree-ring isotopes linked to reduced irradiance, primary production and human health. Scientific reports 8, 1339, doi:10.1038/s41598-018-19760-w, 2018.

Hughes, M.K., Vaganov, E.A., Shiyatov, S.G., Touchan, R. & Funkhouser, G.: Twentieth-century summer warmth in northern Yakutia in a 600-year context. The Holocene. 9(5), 603-608, 1999.

Iles, C.E., Hegerl, G.C.: The global precipitation response to volcanic eruptions in the CMIP5 models. Environ. Res. Lett. 9, doi:10.1088/1748-9326/9/10/104012, 2014.

Joseph, R., Zeng, N.: Seasonally modulated tropical drought induced by volcanic aerosol. J. Climate, 24, 2045–2060, 2011.

Kirdyanov, A.V., Treydte, K.S., Nikolaev, A., Helle, G., Schleser, G.H.: Climate signals in tree-ring width, wood density and $\delta^{13}C$ from larches in Eastern Siberia (Russia) Chemical Geology, 252, 31-41, 2008. doi:10.1016/j.chemgeo.2008.01.023

Körner, Ch.: Paradigm shift in plant growth control. Curr. Opinion Plant Biol. 25, 107-114, 2015.

Lavigne, F., Degeai, J.-P., Komorowski, J.-C., Guillet, S., Robert, V., Lahitte, P., Oppenheimer, C., Stoffel, M., Vidal, C.M., Suro, I.P., Wassmer, P., Hajdas, I., Hadmoko, D.S., Belizal, E.: Source of the great A.D. 1257 mystery eruption unveiled, Samalas volcano, Rinjani Volcanic Complex, Indonesia. Proc Natl Acad Sci 110, 16742–16747, doi:10.1073/pnas.1307520110, 2013.

Lenz, O., Schär, E., Schweingruber F.H.: Methodische Probleme bei der radiographisch-densitometrischen Bestimmung der Dichte und der Jahrrinbreiten von Holz. Holzforschung, 30, 114-123, 1976.

Loader, N.J., Robertson, I., Barker, A.C., Switsur, V.R., Waterhouse, J.S.: Improved technique for the batch processing of small whole wood samples to alpha-cellulose. Chemical Geology. 136, 313-317, 1997.

Loader, N.J., Young, G.H.F., Grudd, H., McCarroll.: Stable carbon isotopes from Torneträsk, norther Sweden provide a millennial length reconstruction of summer sunshine and its relationship to Arctic circulation. Quaternary Science Reviews. 62, 97-113, 2013.

McCarroll, D., Loader, N.J.: Stable isotopes in tree rings. Quaternary Science Review. 23, 771-801, 2004.

Meronen, H., Henriksson, S.V., Räisänen, P., Laaksonen, A.: Climate effects of northern hemisphere volcanic eruptions in an Earth System Model. Atmospheric Research, 114-115: 107-118, 2012.

Munro, M.A.R., Brown, P.M., Hughes, M.K., Garcia, E.M.R.: Image analysis of tracheid dimensions for dendrochronological use. Radiocarbon, Eds. by M.D. Dean, J. Swetnam T), pp. 843-851. Tucson, Arizona, 1996.

Myglan, V.S., Oidupaa, O. Ch., Kirdyanov, A.V., Vaganov, E.A.: 1929-year tree-ring chronology for Altai-Sayan region (Western Tuva). Journal of archeology, ethnography and anthropology of Eurasia. 4 (36), 25-31, 2008.

Naurzbaev, M.M., Vaganov, E.A., Sidorova, O.V., Schweingruber, F.H.: Summer temperatures in eastern Taimyr inferred from a 2427-year late-Holocene tree-ring chronology and earlier floating series. The Holocene. 12(6), 727-736, 2002.

Deleted: Lehmann, M.M., Goldsmith, G.T., Schmid, L., Gessler, A., Saurer, M., Siegwolf, R.T.W.: The effect of ^{18}O-labelled water vapour on the oxygen isotope ratio of water and assimilates in plants at high humidity. New Phytologist. 217, 1, 105-116. doi: 10.1111/nph.14788, 2018.¶

Panofsky, H.A., Brier, G.W.: Some applications of statistics to meteorology. University Park, PA. Mineral industries extension services, college of mineral industries, Pennsylvania State University, 224 p, 1958.

Panyushkina, I.P., Hughes, M.K., Vaganov, E.A., Munro, M.A.R.: Summer temperature in northern Yakutia since AD 1642 reconstructed from radial dimensions of larch tracheids. Canadian Journal of Forest Research. 33, 1-10, 2003.

Peng, Y., Shen, C., Wang, W.-C., Xu, Y.: Response of summer precipitation over Eastern China to large volcanic eruptions. Journal of Climate. 23, 818-824, 2009.

R Core Team.: R: A Language and Environment for Statistical Computing. Vienna, Austria, 2016.

Robock, A.: Volcanic eruptions and climate. Reviews of Geophysics. 38(2), 191-219, 2000.

Robock, A., Liu, Y.: The volcanic signal in Goddard Institute for Space Studies three-imensional model simulations. J. Climate. 7, 44-55, 1994.

Roden, J.S., Siegwolf, R: Is the dual isotope conceptual model fully operational? Tree Physiology. 32, 1179-1182, 2012.

Saurer, M., Kirdyanov, A.V., Prokushkin, A.S., Rinne K.T., Siegwolf, R.T.W.: The impact of an inverse climate–isotope relationship in soil water on the oxygen-isotope composition of *Larix gmelinii* in Siberia. New Phytologist. 109, 3, 955-964, 2016.

Saurer, M., Robertson, I., Siegwolf, R., Leuenberger, M.: Oxygen isotope analysis of cellulose: an interlaboratory comparison. Analytical cemistry, 70, 2074-2080, 1998.

Saurer, M., Kirdyanov, A. V., Prokushkin, A. S., Rinne, K. T., Siegwolf, R.T.W.: The impact of an inverse climate-isotope relationship in soil water on the oxygen-isotope composition of *Larix gmelinii* in Siberia. New Phytologist. 209(3), 955-964, 2016.

Scheidegger, Y., Saurer, M., Bahn, M., Siegwolf, R.: Linking stable oxygen and carbon isotopes with stomatal conductance and photosynthetic capacity: a conceptual model. Oecologia. 125, 350–357. doi: 10.1007/s004420000466, 2000.

Schneider, L., Smerdon, J.E., Büntgen, U., Wilson, R.J.S., Myglan, V.S., Kirdyanov, A.V., Esper, J.: Revising mid-latitude summer temperatures back to A.D. 600 based on a wood density network. Geophys. Res. Lett. 42, GL063956, doi:10.1002/2015gl063956, 2015.

Schweingruber, F.H.: Tree rings and environment dendroecology. Paul Haupt Publ Bern, Stuttgart, Vienna 1996. pp. 609, 1996.

Sidorova, O.V., Naurzbaev, M.M.: Response of Larix cajanderi to climatic changes at the upper timberline and in the Indigirka River valley. Lesovedenie (in Russian). 2, 73-75, 2002.

Sidorova, O.V.: Long-term climatic changes and the larch radial growth on the northern Middle Siberia and the Northeastern Yakutia in the Late Holocene. Abs. PHD Diss, V.N. Sukachev Institute of Forest, Krasnoyarsk, 2003.

Sidorova, O.V., Naurzbaev, M.M., Vaganov, E.A.: Response of tree-ring chronologies growing on the Northern Eurasia to powerful volcanic eruptions. Problems of ecological monitoring and ecosystem modeling, XX, 60-72, 2005.

Sidorova, O.V., Saurer, M., Myglan, V.S., Eichler, A., Schwikowski, M., Kirdyanov, A.V., Bryukhanova, M.V., Gerasimova, O.V., Kalugin, I., Daryin, A., Siegwolf, R.:. A multi-proxy approach for revealing recent climatic changes in the Russian Altai. Climate Dynamics, 38 (1-2), 175–188, 2011.

Sidorova, O.V., Siegwolf, R., Myglan, V.S., Loader, N.J., Helle, G., Saurer, M.: The application of tree-rings and stable isotopes for reconstructions of climate conditions in the Altai-Sayan Mountain region. Climatic Changes, doi: 10.1007/s10584-013-0805-5, 2012.

Sidorova, O.V., Siegwolf, R., Saurer, M., Naurzbaev, M., Shashkin, A.V., Vaganov, E.A.: Spatial patterns of climatic changes in the Eurasian north reflected in Siberian larch tree-ring parameters and stable isotopes. Global Change Biology, doi: 10.1111/j.1365-2486.2009.02008.x, 16, 1003-1018, 2010.

Sidorova, O.V., Siegwolf, R.T.W., Saurer, M., Naurzbaev, M.M., Vaganov, E.A.: Isotopic composition ($\delta^{13}C$, $\delta^{18}O$) in Siberian tree-ring chronology. Geophysical research Biogeosciences. 113, 1-13, 2008.

Sigl, M., Winstrup, M., McConnell, J.R.: Timing and climate forcing of volcanic eruptions for the past 2500 years. Nature. 523, 543-549. doi:10.1038/nature14565, 2015.

Sprenger, M., Tetzlaff, D., Buttle, J. M., Laudon, H., Leistert, H., Mitchell, C., Snelgrove, J., Weiler, M., Soulsby, C.: Measuring and modelling stable isotopes of mobile and bulk soil water, Vadose Zone Journal, https://doi.org/10.2136/vzj2017.08.0149, 20, 2017.

Sternberg, L.S.O.: Oxygen stable isotope ratios of tree-ring cellulose: The next phase of understanding. New Phytologist. 181 (3), 553-562, 2009.

Stirzaker, D.: Elementary Probability density functions. Cambridge. Sec. Ed. 538 p, 2003.

Stoffel, M., Khodri, M., Corona, C., Guillet, S., Poulain, V., Bekki, S., Guiot, J., Luckman, B.H., Oppenheimer, C., Lebas, N., Beniston, M., Masson-Delmotte, V.: Estimates of volcanic-induced cooling in the Northern Hemisphere over the past 1,500 years. Nature Geoscience. 8, 784–788, 2015.

Stothers, R.B.: Climatic and Demographic Consequences of the Massive Volcanic Eruption of 1258. Climatic Change. 45, 361-374, 2000.

Stothers, R.B.: Mystery cloud of AD 536. Nature. 307, 344-345, doi:10.1038/307344a0, 1984.

Sugimoto, A., Yanagisawa, N., Fujita, N., Maximov, T.C.: Importance of permafrost as a source of water for plants in east Siberian taiga. Ecological Research. 17 (4), 493-503, 2002.

Toohey, M., Sigl, M.: Volcanic stratospheric sulphur injections and aerosol optical depth from 500 BCE to 1900 CE. Earth System Science Data. doi:10.5194/essd-9-809-2017, 2017.

Vargas, A. I., Schaffer, B, Yuhong, L. Sternberg, L.S.: Testing plant use of mobile vs immobile soil water sources using stable isotope experiments. New Phytologist. 215, 582–594, doi: 10.1111/nph.14616, 2017.

Vaganov, E.A., Hughes, M.K., Kirdyanov, A.K., Schweingruber, F.H., Silkin, P.P.: Influence of snowfall and melt timing on tree growth in subarctic Eurasia. Nature. 400, 149-151, 1999.

Vaganov, E.A., Hughes, M.K., Shashkin, A.V.: Growth dynamics of conifer tree rings. Springer Verlag, Berlin., pp. 353, 2006.

Wegmann, M., Brönnimann, S., Bhend, J., Franke, J., Folini, D., Wild, M., Luterbacher, J.: Volcanic influence on European summer precipitation through monsoons: Possible cause for “years without summer”. AMS, doi.org/10.1175/JCLI-D-13-00524.1, 2014.

Wigley, T.M.L., Briffa, K.R., Jones, P.D.: On the Average Value of Correlated Time Series, with Applications in Dendroclimatology and Hydrometeorology. Journal of Climate and Applied Meteorology. 23 (2), 201-213, doi:10.1175/15200450(1984)023.0201, 1984.

Wiles, G.C., D’Arrigo, R.D., Barclay, D., Wilson, R.S., Jarvis, S.K., Vargo, L., Frank, D.: Surface air temperature variability reconstructed with tree rings for the Gulf of Alaska over the past 1200 years. The Holocene. 6, 10.1177/0959683613516815, 2014.

Wilson, R.J.S., Anchukaitis, K., Briffa, K. et al.: Last millennium Northern Hemisphere summer temperatures from tree rings. Part I: the long-term context. Quaternary Science Review. 134, 1–18, 2016.

Zielinski, G.A., Mayewski, P.A., Meeker, L.D., Whitlow, S., Twickler, M.S., Morrison, M., Meese, D.A., Gow A.J., Alley, R.B.: Record of volcanism since 7000 BC from the GISP2 Greenland ice core implications for the volcano-climate system. Science. 264 (5161), 948-952, 1994.

Zielinski, G.A.: Use of paleo-records in determining variability within the volcanism-climate system. Quaternary Science Reviews. 19, 417-438, 2000.

Page 18: [1] Deleted Olga Churakova 1/18/2019 2:06:00 PM

YAK 535 540 1257 1640
1815 1991

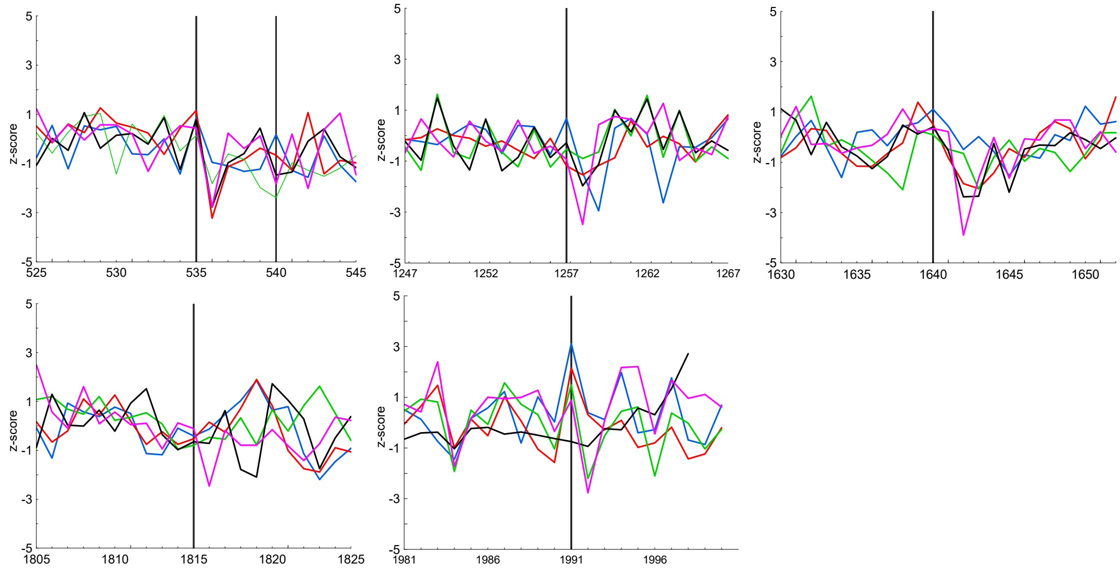

TAY

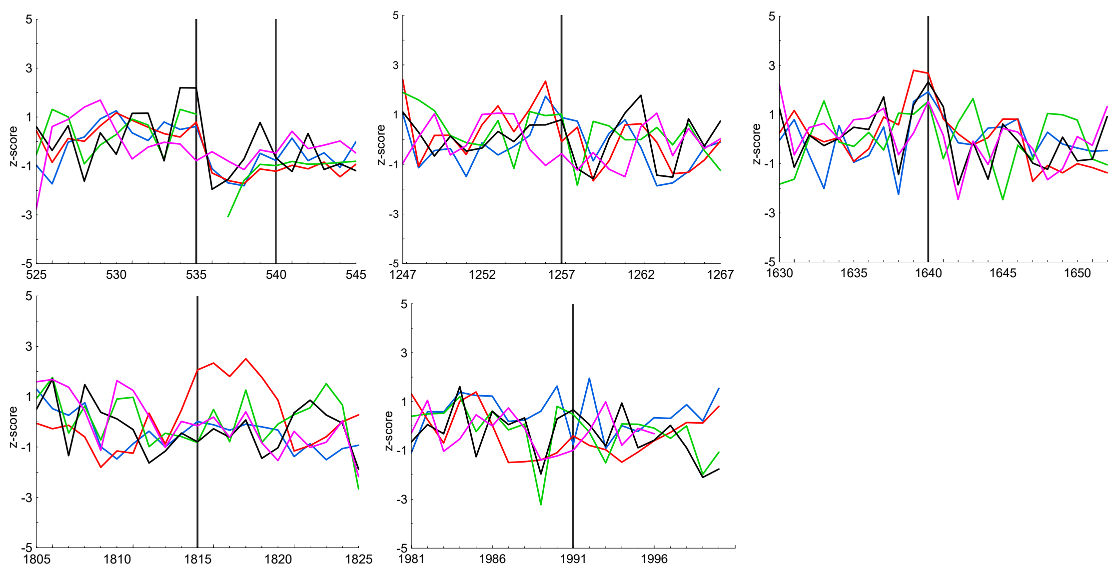

ALT

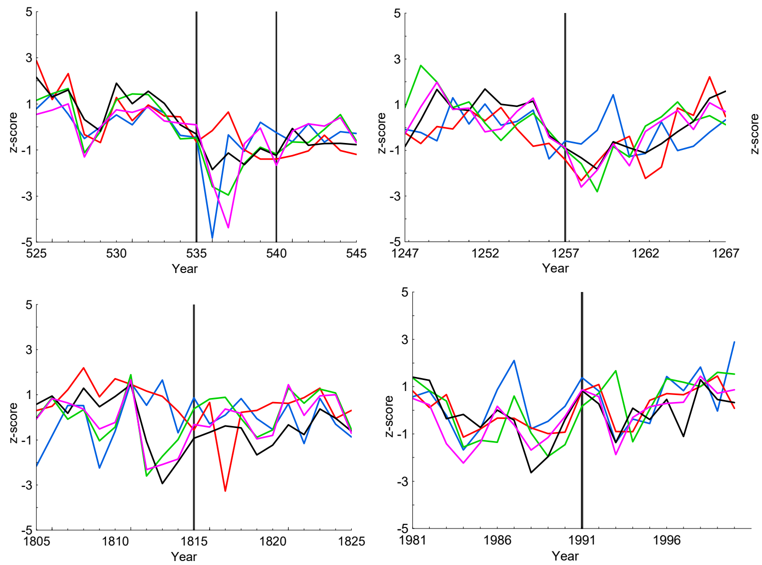

Fig. 2. Normalized (z-score) individual tree-ring index chronologies (TRWi, **black**), maximum latewood density (MXD, **purple**), cell wall thickness (CWT, **green**), $\delta^{13}C$ (**red**) and $\delta^{18}O$ (**blue**) in tree-ring cellulose chronologies from YAK, TAY and ALT for the specific periods 10 years before and after the eruptions CE 535, 1257, 1640, 1815 and 1991 are presented. Vertical lines showed year of the eruptions.

Page 22: [2] Deleted **Olga Churakova** **1/18/2019 2:11:00 PM**

YAK TAY ALT

$\delta^{18}O$

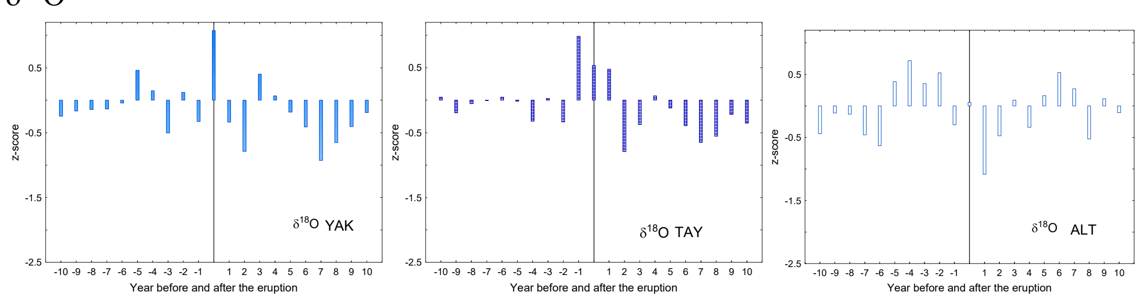

$\delta^{13}C$

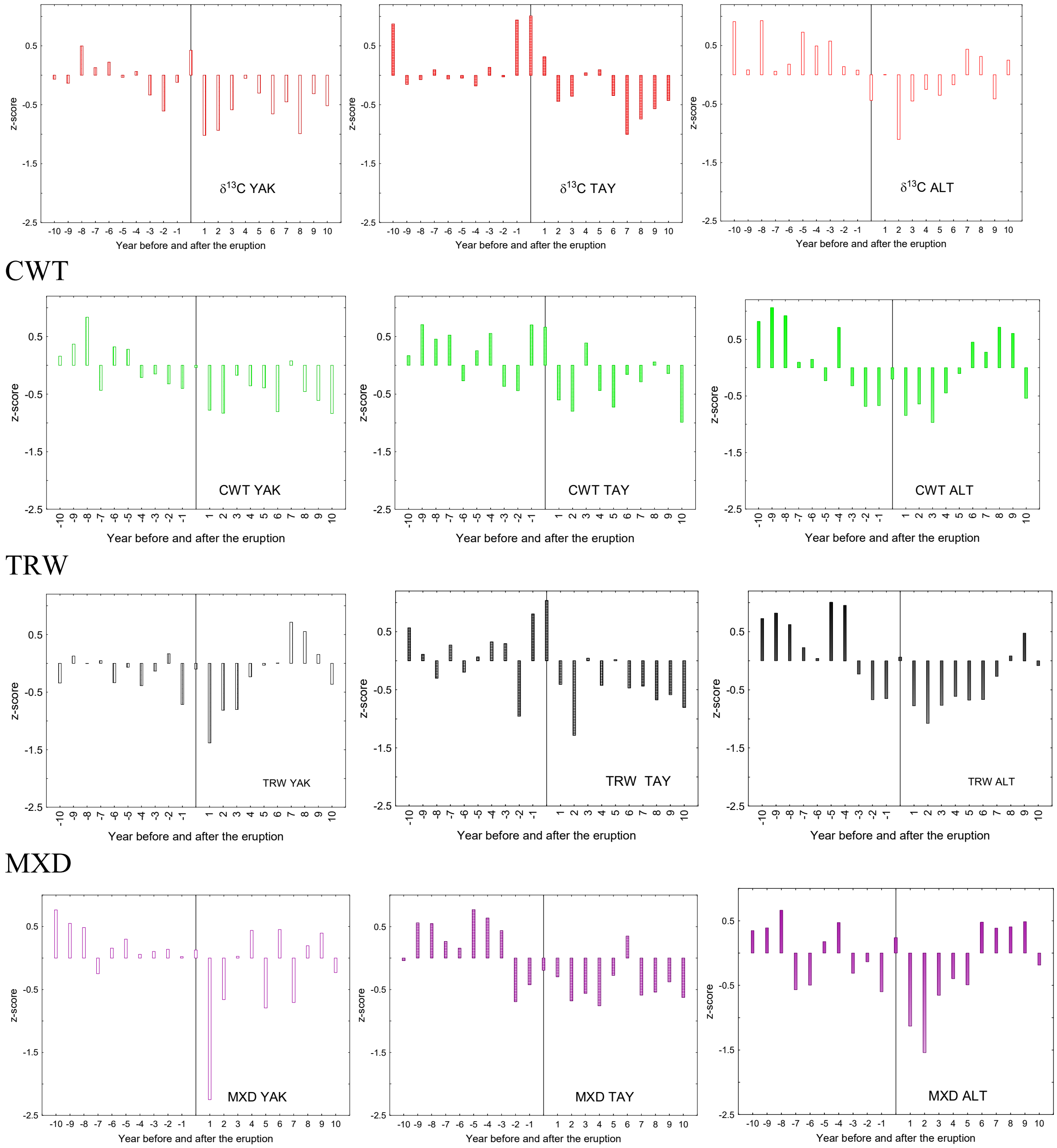

Fig. 3. Superposed epoch analysis of $\delta^{18}O$, $\delta^{13}C$, CWT, TRW and MXD chronologies for the Yakutia (YAK), Taimyr (TAY), and Altai (ALT) sites, summarizing anomalies of the volcanic eruptions in CE 535, 540, 1257, 1640, 1815, and 1991.